論文 / 著書情報
Article / Book Information

題目(和文)	
Title(English)	Construction of engineered extracellular matrix proteins for regulation of cellular functions
著者(和文)	SuttinontChawapun
Author(English)	Chawapun Suttinont
出典(和文)	学位:博士(工学), 学位授与機関:東京工業大学, 報告番号:甲第10814号, 授与年月日:2018年3月26日, 学位の種別:課程博士, 審査員:小畠 英理,粂 昭苑,白木 伸明,堤 浩,三重 正和
Citation(English)	Degree:Doctor (Engineering), Conferring organization: Tokyo Institute of Technology, Report number:甲第10814号, Conferred date:2018/3/26, Degree Type:Course doctor, Examiner:,,,,
学位種別(和文)	博士論文
Type(English)	Doctoral Thesis

Construction of engineered extracellular matrix proteins for regulation of cellular functions

Graduate School of Biological Information

Tokyo Institute of Technology

Suttinont Chawapun

Advisor Prof. Kobatake Eiry

Contents

Chapter 1: General Introduction

1. Introduction

In the present, tissue engineering has been developing to achieve novel material suitable for treatment. The effective process to derive functional and practical tissue engineering is imitating nature of the niche-like cellular microenvironment which consisted of cells interact with other cells, extracellular matrix (ECM), and signaling system. This triad factor in cell niche interplay and control cell microenvironment[1].Thus, biomimetic materials are designed to create a natural niche-like cellular microenvironment and introduce various advantages in tissue engineering (Fig 1).

One challenge in regenerative central nervous system (CNS) is to overcome the limit in regeneration after injury in adult[2]. Many patients suffer from brain degenerative disease such as Parkinson's disease, Alzheimer's disease, however, there are currently no clinical treatment for damaged brain. Some researches demonstrated that some regenerative neuron remains in CNS, but the non-permissive environment disrupted regeneration[3]. Understanding of factors which influence neurite outgrowth is critical for development of therapeutics to promote CNS regeneration. Taken together, creating biomaterial which enhance permissive environment in CNS regeneration can be useful for understanding more in brain function, promoting neural regeneration, and modulating disease processes.

Therefore, the aim of this thesis is to generate multi-functional ECMs providing proper environments to differentiate neural-lineage cell for neural regeneration. Briefly to achieve this proposed, the well-known neural cell-cell CAM, N-cadherin-derived sequence was fused to ECMs and characterized for their capability to mimic N-cadherin in the neural differentiation. Another neural CAMs, laminin-derived sequence was fused to ECMs and later the function was characterized as substrate in astrocyte differentiation. Furthermore, bFGF were tethered to the ECM proteins for induction of proliferation and differentiation of cells without addition of any soluble growth factors. These all together are expected to create multi-functional ECMs which function as neural-like environment in nervous system generation.

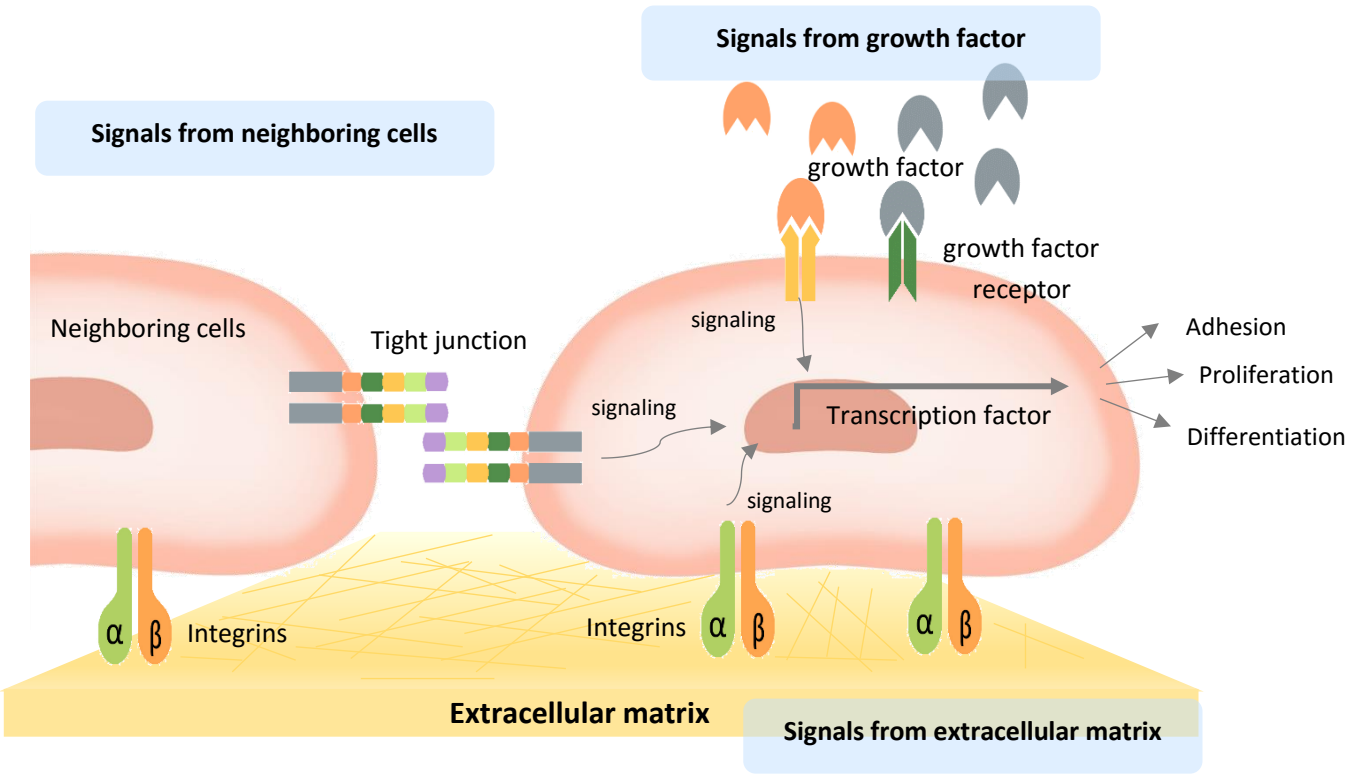

Figure 1: The cell interactions, cell-to-cell, cell-to-extracellular matrix, and cell-to-signaling factor, in cellular microenvironment.

Tissue engineering in central nervous system regeneration

Nervous system is subdivided into the central nervous system (CNS) and peripheral nervous system (PNS). The CNS consisted of the brain and spinal cord, whereas the PNS is outside CNS and functions to innervate muscle tissue for motor control when receive input from the environment[4]. Neurons are the main functional element in nervous system and another important cellular component in CNS is glial cells. The CNS composed of 4 types of glial cells: (i) astrocytes, (ii) oligodendrocytes, (iii) ependyma, and (iv) microglial cells. Astrocytes are most abundant cell types in CNS and play important roles in brain development[5].

The critical point when brain injury occurs is the regeneration of injured central nervous system (CNS) had extremely limited regenerative potential[6, 7]. Surprisingly in the recent study, the

capability to regrow in CNS was shown. This finding demonstrated that some regenerative neuron remains in CNS, but the non-permissive environment disrupted regeneration. The discovery of neural stem cells (NSCs) persist in the adult ventricular subventricular zone (SVZ) on the walls of lateral ventricles and the dentate gyrus in the hippocampus[8]. The finding reveals that neurons are generated throughout life. Therefore, the construction of synthetic biomaterial creating permissive environment can induce the potential of endogenous NSCs to regenerate in brain injury.

The effective process to derive practical tissue engineering is mimicking niche-like microenvironment, which consisted of cells, extracellular matrix, and signaling molecules, that are brought into play through induce intracellular signaling. Here, the crucial interplay among cell, ECM, and signaling molecules for neural regeneration are explained.

1.1 Cell-extracellular matrix interaction

The extracellular matrix (ECM) is a non-cellular component present within all tissues and organs, and it determines the tissue's physical properties such as morphogenesis, differentiation and homeostasis[9]. The ECM is composed of macromolecules and produced locally by cells and in different tissues is adapted to particular functional requirement. ECM interact with cells via cell surface receptors binding and transmit signal across the cell membrane to cytoplasm. These signals initiate the expression of specific genes which affect cell function. In biomaterial field, it is often mimic characteristics of natural extracellular matrix to achieve desired cellular response[10]. Synthetic biomaterials have been developing to over come some problem from natural source and introduce novel materials for clinal application[11]. The deigned ECM must have the following functions[12];

(i) Cell binding ability to materials which can contribute to cell migration, proliferation, differentiation

(ii) Suitable mechanical properties (elasticity, rigidity) are required variously depend on cell types.

(iii) ECM need to have biocompatibility and bioactivities which induce non-immunogenic responses.

(iv) Biodegradability after injury site are repaired

Following these requirements, our laboratory use Elastin-like polypeptides (ELPs) as the structural unit for designed biomaterials and fusion of CAMs for cell binding activity.

1.1.1 Elastin-like polypeptides (ELPs)

Elastin-like polypeptides (ELPs) are attractive for tissue engineering applications due to their various properties and highly customizable. ELPs are tropoelastin-derived repetitive artificial polypeptide which composed of pentapeptide VPGXG repeats exhibit an inverse temperature phase transition[13]. $(VPGXG)_n$ is the common use ELPs where X, can be any amino acid other than proline, and n represents the number of repetitive sequence[14].

In addition, ELPs can fuse with other non-ELP sequence without losing their function such as viscoelasticity, hence other functional sequence such as cell adhesion molecule (CAMs) or bioactive peptide sequence can be fused to either end or between ELPs. The addition of other functional sequence can introduce complex functional ELPs[13].These advantages of straightforward synthesis, minimal cost, and ligand modification cannot readily be achieved when using full-length native matrix proteins to functionalize material surface.

In my study, 12 repeats of Ala-Pro-Gly-Val-Gly-Val (APGVGV) motif (E) is used as a stable structural unit which have hydrophobic adsorption property. Synthetic ELPs often lack of cell attachment ability, hence the modification of ELPs with cell adhesion molecules (CAMs) or bioactive sequence are required.

1.1.2 Cell adhesion molecules (CAMs)

Cell adhesion molecule (CAMS) are proteins located on the cell surface that mediate cell to cell or cell to extracellular matrix interaction, which also have ability to transmit signal across the cell membrane and directly activating intracellular signaling[15].

CAMs can mainly divided into 4 groups;

(i) Cadherins

(ii) The integrin family

(iii) Selectin

(iv) Immunoglobin (Ig) superfamily of CAMs

In this study, CAMs-binding sequence, mainly binding to cadherins and integrin family, which have ability to mediate signaling associated with a neurite outgrowth response were focused on this research.

(i) Cadherins

Cadherins are a family of glycoproteins located on the cell surface involved in Ca^{2+}-dependent cell-to-cell or cell-to-ECM interaction[16, 17]. Cadherins can be divided into various cadherin-subtype. In here, N-cadherin and E-cadherin in classical cadherin subtype which interplay in CNS development were focused on this research[18].

N-cadherin and E-cadherin are in type I of classical cadherin and structure of both cadherin consists of a unique cytoplasmic domain and 5 cadherin EC domains (EC1-EC5) in their extracellular region (Fig 2). In the N-terminal cadherin repeat (EC1) domain, it contains a cell adhesion recognition motif (HAV). N-cadherin and E-cadherin appear to be very similar at the high-resolution structural level, and a similar Ca^{2+} regulating mechanism; however, they are totally different in function. E-cadherin and N-cadherin have an interplay function in embryonic and brain development. The expression of E-cadherin is found in embryonic development. However, when neural differentiation begins, E-cadherin expression is replaced by N-cadherin. According to various stem cells research suggested that undifferentiated iPS cells binds to E-cadherin, on the other hand N-cadherin is detected after neural differentiation[19, 20].

N-cadherin mediates adhesion and has a role in neurite outgrowth. This function of N-cadherin mediated via down-regulation of Rho-ROCK signaling, resulting in stimulation of neurite outgrowth and expression of neural marker. RhoA is quanosin triphophase (GTPase) and active form of RhoA induce effector protein ROCK signal. The cross-talk between RhoA and Rac1 could be demonstrated that active form of RhoA induce ROCK signaling which phosphorylates myosin light chain (MLC) phosphatase, resulting in cessation of neurite growth. In contrast of Rac1, active Rac signals to a serine-threonine kinase (PAK1) signal that inhibit MLC kinase, resulting in antagonistic effects from active RhoA[21, 22]. Hence, N-cadherin exerts a neuritogenic effect in regulation of proliferation and differentiation of neural progenitor cells during development[23, 24, 25].

(ii) Integrin family

Integrin are heterodimeric transmembrane receptors consisting of α and β subunits and the pairing of these subunits dictates specificity for ligand. Integrins bind non-covalently to plasma membrane of cells and extracellular matrix proteins such as laminin, fibronectin, and many other molecules. Most of integrins-binding peptide bind to more than one integrin ligand and induce broad specificity[26, 27]. Various integrin-binding peptides was synthesized and used in biomaterial construction for enhance cell binding activity via integrin receptors[28].

Some examples of well-known integrin-binding sequence are explained in following;

- **Fibronectin-derived sequence (RGD)**

The tripeptide Arginine-Glycine-Aspartic acid (RGD), well known integrin mediated cell binding peptide, influences and regulates cell migration, proliferation, and differentiation. The RGD was found in fibronectin which bound to $\alpha_5\beta_1$ fibronectin receptor ligand, however, another protein which assembled the fibronectin receptor could also be bound to other receptors such as found in laminin, vitronectin, and collagens[29]. RGD peptide can bind to multiple integrins such as; $\alpha_5\beta_1$, $\alpha 8\beta 1$, $\alpha_V\beta_{(1, 3, 5, 6, 8)}$, and $\alpha_{IIb}\beta_3$[30]. Various researches use RGD sequence because of important roles in cell adhesion, proliferation, migration, and differentiation[31, 32] and also have ability in promoting neurites extension[33].

- **Laminin-derived sequence (IKVAV, YIGSR)**

Laminin is large protein composed of three subunits, an α chain, a β chain and a γ chain. Many neural research showed that laminin enhances neurite outgrowth and migration. Ajioka *et al*. succeeded in using of laminin-coating porous sponge for enhancement of neuroblast migration into the injured cerebral cortex[34]. Moreover, other research studies also confirmed the neurite outgrowth and migration properties of laminin[35, 36]. Therefore, laminin plays important functions in induction of neural differentiation and promotion of neural regeneration. However, the bioavailability of laminin is limited according batch-batch composition variation and cause in irreproducible result. Thus, the application of synthetic peptide mimic natural extracellular matrix offers several advantages for biomaterials[30].

Laminin-derived sequence, which have ability to promote neurite outgrowth, have been screened. Two laminin-derived sequences Ile-Lys-Val-Ala-Val (IKVAV), and another pentapeptide Try-Ile-Gly-Ser-Arg (YIGSR), were found in active region of the α chain and in cysteine-rich region of the B1 chain short arm, respectively. Whereas, Arg-Asn-Ile-Ala-Glu-Ile-Lys-Asp-Ile (RNIAEIIKD) was found in γ chain[37, 38, 39]. Recently, a short IKVAV sequence was conjugated to polyethylene glycol (PEG)-hydrogels and succeeded in enhance NSC attachment, proliferation, and directed NSC differentiation into neurons[40]. YIGSR and RNIAEIIKD were also evaluated their functions in neurite outgrowth and shown their abilities[41,42].

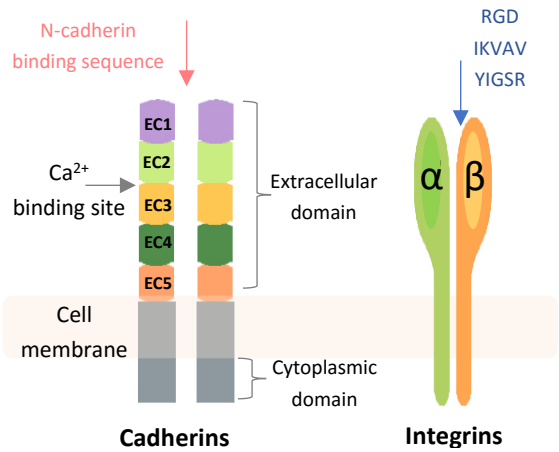

Figure 2: Schematic drawing of CAMs; N-cadherin binding sequence can bind to cadherins (left), and laminin-derived sequence can bind to integrins (right).

Different types of ECM interactions trigger cell responsiveness via diverse sensing mechanisms and downstream signaling pathways. Nevertheless, the outcome, stem cell renewal or differentiation, may be the same.

1.2 Cell-growth factor interaction

Growth factors are also important for regulation of cellular processes complexed with the ECM, and they are indispensable for tissue engineering. Specific signal-transduction pathways in the CNS control the differentiation of stem cell to generate neural progenitor and glial progenitor cells, subsequently to grow mature cells, neurons, oligodendrocytes, and astrocytes, in brain. Thus, specific cell type is controlled by specific signal-transduction[43] for example basic fibroblast growth factor (bFGF) cause the neural progenitor population to proliferate[44]. Epidermal growth factor (EGF) cooperate with ciliary neurotrophic factor (CNTF) force glial progenitors towards astrocytic differentiation.

Hence, proper growth factor has to be selected for creating targeted cell niche. However, soluble growth factor which added to cell culture system is difficult to control their concentration due to diffusion, cell uptake, and degradation[45]. Therefore, a strategy to immobilize growth factors to ECMs has been developed.

2.1 Strategies for immobilization of growth factors to ECMs

Strategies of tethering growth factors to ECMs have been developed by chemically or genetically methods. For examples in chemically immobilization method, Radisic *et al*. succeeded chemical-covalently immobilized vascular endothelial growth factor (VEGF) onto three-dimensional porous collagen scaffold for enhanced proliferation[46]. In our laboratory, growth factors were immobilized to ECMs using genetically engineering method. In those studies, growth factors were tethered to ECMs non-covalently by fusing helical peptides which forms coiled-coil structure to growth factors (bFGF, EGF, VEGF) and ECMs, respectively[47].

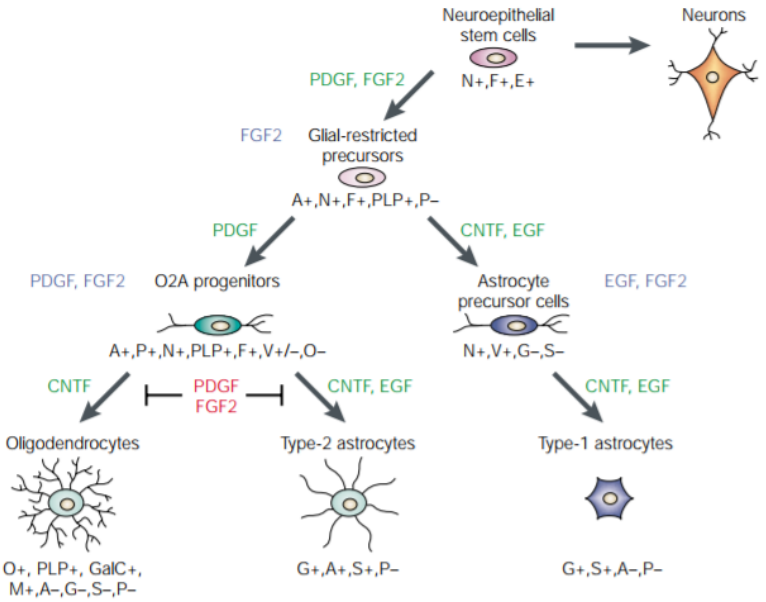

Figure 3: Cellular differentiation in the CNS. Growth factor that induce proliferation and maintain cell at a given stage are indicated in blue, whereas, those that promote the progression of differentiation are in green. Growth factor that inhibit differentiated progression are in red[43].

1.3 Cell-cell interaction

Cell-cell interaction is the direct interaction between cell and its neighboring cell that play a key role in multiple organization in tissue[48]. Cell-cell interaction in stem cells occurs through cell adhesion molecules and gap junctions[49].

In the CNS, not only neural cells play important roles in brain development, but also astrocyte cells. Astrocytes play important roles in maintaining optimal environment for the normal development and function of neurons including[50, 51];

- Support the neural synapse formation during development, which is the main function of neuron, and maintain synapse homeostasis.
- Supply energy in the form of lactate to neurons
- Form blood-brain barrier (BBB) which restricts the exchange of molecules between blood and brain
- Play direct communication to neurons via neuroactive molecules, …

To understand the mechanism in neurological disease or neural regeneration, the construction of biomaterial creating niche-like environment that can co-culturing both neurons and astrocytes have been concerned. This will open new possibilities to be a useful tool for understanding of neurodegenerative disease.

1.4 Objective

The main purpose of this study is to construct multi-functional biomimetic material for creating permissive environment for neural-lineage differentiation.

To achieve the above objective, experiments were designed with the following specific objectives:

1. Develop a method to immobilize bFGF to designed ECM using electrostatic interaction between the basic domain of bFGF and the acidic domain of D20 in ERE-D20
2. Characterize E-/N-cadherin binding peptides (SWELYYPLRANL) ability to induce neural differentiation from mouse iPS cells
3. Develop artificial ECM composed of various laminin-derived sequence (IKVAV and YIGSR) as potential substrate in astrocyte differentiation

This study should shed light on the usefulness of multi-functional ECM for neural-lineage differentiation. This would also lead to useful information for understanding more in CNS function and promoting neural regeneration.

1.5 Reference

1. Lanza, R., Langer, R., and Vacanti, J. P. Principles of tissue engineering. Academic press, 2011.
2. Chandrasekaran, A., Avci, H. X., Leist, M., Kobolak, J., and ´ Dinnyes, A. ´ Astrocyte differentiation of human pluripotent stem cells: new tools for neurological disorder research. Frontiers in cellular neuroscience 10 (2016).
3. Richardson, P., McGuinness, U., and Aguayo, A. Axons from cns neurones regenerate into pns grafts. Nature 284, 5753 (1980), 264–265
4. Hollinger, J. O. An introduction to biomaterials. CRC press, 2011.
5. Sofroniew, M. V., and Vinters, H. V. Astrocytes: biology and pathology. Acta neuropathologica 119, 1 (2010), 7–35.
6. Huebner, E. A., and Strittmatter, S. M. Axon regeneration in the peripheral and central nervous systems. In Cell Biology of the Axon. Springer, 2009, pp. 305–360.
7. Horner, P. J., and Gage, F. H. Regenerating the damaged central nervous system. Nature 407, 6807 (2000), 963–970.
8. Tong, C. K., Chen, J., Cebrian-Silla, A., Mirzadeh, Z., ´ Obernier, K., Guinto, C. D., Tecott, L. H., Garc´ıa-Verdugo, J. M., Kriegstein, A., and Alvarez-Buylla, A. Axonal control of the adult neural stem cell niche. Cell stem cell 14, 4 (2014), 500–511.]
9. Frantz, C., Stewart, K. M., and Weaver, V. M. The extracellular matrix at a glance. J Cell Sci 123, 24 (2010), 4195–4200.
10. Kim, Y., Ko, H., Kwon, I. K., and Shin, K. Extracellular matrix revisited: Roles in tissue engineering. International neurourology journal 20, Suppl 1 (2016), S23.
11. Chan, B., and Leong, K. Scaffolding in tissue engineering: general approaches and tissue-specific considerations. European spine journal 17, 4 (2008), 467–479.
12. Kim, B.-S., and Mooney, D. J. Development of biocompatible synthetic extracellular matrices for tissue engineering. Trends in biotechnology 16, 5 (1998), 224–230.

13. MacEwan, S. R., and Chilkoti, A. Elastin-like polypeptides: Biomedical applications of tunable biopolymers. Peptide Science 94, 1 (2010), 60–77.
14. Girotti, A., Reguera, J., Rodr´ıguez-Cabello, J. C., Arias, F. J., Alonso, M., and Testera, A. M. Design and bioproduction of a recombinant multi (bio) functional elastin-like protein polymer containing cell adhesion sequences for tissue engineering purposes. Journal of Materials Science: Materials in Medicine 15, 4 (2004), 479–484.
15. Joddar, B., and Ito, Y. Artificial niche substrates for embryonic and induced pluripotent stem cell cultures. Journal of biotechnology 168, 2 (2013), 218–228.
16. Tepass, U., Truong, K., Godt, D., Ikura, M., and Peifer, M. Cadherins in embryonic and neural morphogenesis. Nature Reviews Molecular Cell Biology 1, 2 (2000), 91–100.
17. Hirano, S., and Takeichi, M. Cadherins in brain morphogenesis and wiring. Physiological Reviews 92, 2 (2012), 597–634.
18. Hirano, S., and Takeichi, M. Cadherins in brain morphogenesis and wiring. Physiological Reviews 92, 2 (2012), 597–634.
19. Haque, A., Yue, X.-S., Motazedian, A., Tagawa, Y.-i., and Akaike, T. Characterization and neural differentiation of mouse embryonic and induced pluripotent stem cells on cadherin-based substrata. Biomaterials 33, 20 (2012), 5094–5106.
20. Stocker, A. M., and Chenn, A. Differential expression of alphae-catenin and alpha-n-catenin in the developing cerebral cortex. Brain research 1073 (2006), 151–158.
21. Niederost, B., Oertle, T., Fritsche, J., McKinney, R. A., and ¨ Bandtlow, C. E. Nogo-a and myelin-associated glycoprotein mediate neurite growth inhibition by antagonistic regulation of rhoa and rac1. Journal of Neuroscience 22, 23 (2002), 10368–10376.
22. Fournier, A. E., Takizawa, B. T., and Strittmatter, S. M. Rho kinase inhibition enhances axonal regeneration in the injured cns. Journal of Neuroscience 23, 4 (2003), 1416–1423.
23. Matsunaga, M., Hatta, K., and Takeichi, M. Role of n-cadherin cell adhesion molecules in the histogenesis of neural retina. Neuron 1, 4 (1988), 289–295.

24. Hansen, S., Berezin, V., and Bock, E. Signaling mechanisms of neurite outgrowth induced by the cell adhesion molecules ncam and ncadherin. Cellular and molecular life sciences 65, 23 (2008), 3809–3821.
25. Bixby, J. L., and Zhang, R. Purified n-cadherin is a potent substrate for the rapid induction of neurite outgrowth. The Journal of Cell Biology 110, 4 (1990), 1253–1260.
26. Albelda, S. M., and Buck, C. A. Integrins and other cell adhesion molecules. The FASEB Journal 4, 11 (1990), 2868–2880.
27. Hynes, R. O. Integrins: a family of cell surface receptors. Cell 48, 4 (1987), 549–554.
28. Schense, J. C., Bloch, J., Aebischer, P., and Hubbell, J. A. Enzymatic incorporation of bioactive peptides into fibrin matrices enhances neurite extension. Nature biotechnology 18, 4 (2000), 415–419.
29. Ruoslahti, E., and Pierschbacher, M. D. New perspectives in cell adhesion: Rgd and integrins. Science 238, 4826 (1987), 491–498.
30. Bellis, S. L. Advantages of rgd peptides for directing cell association with biomaterials. Biomaterials 32, 18 (2011), 4205–4210.
31. Adnan, N., Mie, M., Haque, A., Hossain, S., Mashimo, Y., Akaike, T., and Kobatake, E. Construction of a defined biomimetic matrix for long-term maintenance of mouse induced pluripotent stem cells. Bioconjugate chemistry 27, 7 (2016), 1599–1605.
32. Elloumi, I., Kobayashi, R., Funabashi, H., Mie, M., and Kobatake, E. Construction of epidermal growth factor fusion protein with cell adhesive activity. Biomaterials 27, 18 (2006), 3451–3458.
33. Cui, F., Tian, W., Hou, S., Xu, Q., and Lee, I.-S. Hyaluronic acid hydrogel immobilized with rgd peptides for brain tissue engineering. Journal of Materials Science: Materials in Medicine 17, 12 (2006), 1393– 1401.
34. Ajioka, I., Jinnou, H., Okada, K., Sawada, M., Saitoh, S., and Sawamoto, K. Enhancement of neuroblast migration into the injured cerebral cortex using laminin-containing porous sponge. Tissue Engineering Part A 21, 1-2 (2014), 193–201.

35. Laura, M., Leipzig, N. D., and Shoichet, M. S. Promoting neuron adhesion and growth. Materials today 11, 5 (2008), 36–43.
36. Hall, P. E., Lathia, J. D., Caldwell, M. A., et al. Laminin enhances the growth of human neural stem cells in defined culture media. BMC neuroscience 9, 1 (2008), 71.
37. Sephel, G., Tashiro, K., Sasaki, M., Greatorex, D., Martin, G., Yamada, Y., and Kleinman, H. Laminin a chain synthetic peptide which supports neurite outgrowth. Biochemical and biophysical research communications 162, 2 (1989), 821–829.
38. Sephel, G., Tashiro, K., Sasaki, M., Greatorex, D., Martin, G., Yamada, Y., and Kleinman, H. Laminin a chain synthetic peptide which supports neurite outgrowth. Biochemical and biophysical research communications 162, 2 (1989), 821–829.
39. Graf, J., Iwamoto, Y., Sasaki, M., Martin, G. R., Kleinman, H. K., Robey, F. A., and Yamada, Y. Identification of an amino acid sequence in laminin mediating cell attachment, chemotaxis, and receptor binding. Cell 48, 6 (1987), 989–996.
40.] Li, X., Liu, X., Josey, B., Chou, C. J., Tan, Y., Zhang, N., and Wen, X. Short laminin peptide for improved neural stem cell growth. Stem cells translational medicine 3, 5 (2014), 662–670.
41. Masuda, T., Sakuma, C., Kobayashi, K., Kikuchi, K., Soda, E., Shiga, T., Kobayashi, K., and Yaginuma, H. Laminin peptide yigsr and its receptor regulate sensory axonal response to the chemoattractive guidance cue in the chick embryo. Journal of neuroscience research 87, 2 (2009), 353–359.
42. Schense, J. C., Bloch, J., Aebischer, P., and Hubbell, J. A. Enzymatic incorporation of bioactive peptides into fibrin matrices enhances neurite extension. Nature biotechnology 18, 4 (2000), 415–419.
43. Holland, E. C. Gliomagenesis: genetic alterations and mouse models. Nature Reviews Genetics 2, 2 (2001), 120–129.
44. Bizen, N., Inoue, T., Shimizu, T., Tabu, K., Kagawa, T., and Taga, T. A growth-promoting signaling component cyclin d1 in neural stem cells has antiastrogliogenic function to execute self-renewal. Stem Cells 32, 6 (2014), 1602–1615.

45. Ito, Y. Covalently immobilized biosignal molecule materials for tissue engineering. Soft matter 4, 1 (2008), 46–56.
46. Chiu, L. L., and Radisic, M. Scaffolds with covalently immobilized vegf and angiopoietin-1 for vascularization of engineered tissues. Biomaterials 31, 2 (2010), 226–241.
47. Assal, Y., Mie, M., and Kobatake, E. The promotion of angiogenesis by growth factors integrated with ecm proteins through coiled-coil structures. Biomaterials 34, 13 (2013), 3315–3323.
48. Cooper, G. The cell: A molecular approach, 2nd edn. the cell: A molecular approach. sunderland, ma, 2000
49. Miyatani, S., Shimamura, K., Hatta, M., Nagafuchi, A., Nose, A., Matsunaga, M., Hatta, K., and Takeichi, M. Neural cadherin: role in selective cell-cell adhesion. Science 245, 4918 (1989), 631–635.
50. Chandrasekaran, A., Avci, H. X., Leist, M., Kobolak, J., and ´ Dinnyes, A. ´ Astrocyte differentiation of human pluripotent stem cells: new tools for neurological disorder research. Frontiers in cellular neuroscience 10 (2016).
51. Crompton, L. A., Cordero-Llana, O., and Caldwell, M. A. Astrocytes in a dish: Using pluripotent stem cells to model neurodegenerative and neurodevelopmental disorders. Brain Pathology 27, 4 (2017), 530–544.

Chapter 2: Development of bFGF-tethered ECM for Tissue Engineering using Electrostatic Interaction

2.1 Introduction

In the present, various tissue engineering materials have been researching because they offer potential in consistent and rapid treatment, and improving the quality of life at a more affordable price. The effective process to derive functional and practical tissue engineering is imitating nature of the cells. Biological tissues consist of the cells, the extracellular matrix (ECM), and the signaling system (e.g., growth factors, cytokines), which interplay and control cell microenvironments, known as 'niches'[1]. The ECM is non-cellular component present within all tissues and organs, and it determines the tissue's physical properties such as morphogenesis, differentiation and homeogenesis[2].

ECMs material alone may be limited the function in tissue engineering, hence enriched with signaling molecule such as growth factors could enhance potential of material. Growth factors are also important for regulating of cellular processes complexed with the ECM, and they are indispensable for tissue engineering[3]. Several techniques for construction ECM-growth factor complexes have been investigated to increase the local concentration of growth factors and enhance activity of growth factor in longer period. In many cases, growth factors are immobilized to ECMs or embedded in hydrogel for delivery has been developed for stable releasing of growth factors to cells.

A mitogenic growth factor, basic fibroblast growth factor (bFGF) is well used growth factor for tissue engineering because of their wide variety for cellular functions[4]. However, the half-life of bFGF *in vivo* is short and also rapidly degraded when injected inside the body[5]. Additionally, when soluble growth factors are added to the cells, it is difficult to control their local concentration due to cell uptake, diffusion, and degradation[6]. To overcome this disadvantage, a strategy to immobilize growth factors to ECMs has been promoted.

Recently, there is a range of available strategies for conjugating growth factors with different substrate[7, 8, 9]. In our previous study, growth factors were noncovalently immobilized on genetically engineered ECMs[10, 11]. The coiled-coil peptides were fused to both bFGF and ECMs for immobilization of growth factor to ECMs. New strategies are continuously emerging but the need for developing and optimized system still exists. Yamamoto *et al.* reported that bFGF has a highly basic amino acid domain with isoelectric point (IEP) of 9.6 allowing it to directly interact electrostatically with the acidic region of

another protein (IEP of 5.0)[12]. Therefore, we focused to use the property of basic region of bFGF for tethering to our designed ECMs via acidic domain.

For tethering of bFGF to our design ECM, a polyaspartic acid domain which consisted of 5 repeats of 4 aspartic acids and a serine, DDDDS (D20), was introduced to our designed artificial ECM, ERE. As reported by Suzuki *et. al*, the fusion protein encoding D20 can form a complex with a cationic polymer, polyethylenimine, by electrostatic interaction because the aspartic acid-rich domain is negatively charged under physiological conditions[13, 14]. Here, ERE which constructed previously in our lab[15] was used as our designed ECMs and fusion with D20. ERE which consisted of elastin-like polypeptide (E), 12 repeats of Ala-Pro-Gly-Val-Gla-Val (APGVGV) motif derived from elastin, as a structural unit and cell adhesive RGD sequence[16] as an active functional unit. The repeated APGVGV sequence (E12) have a highly hydrophobic property allowing this designed protein, ERE-D20, adsorb well onto the hydrophobic surface of the plate[17].

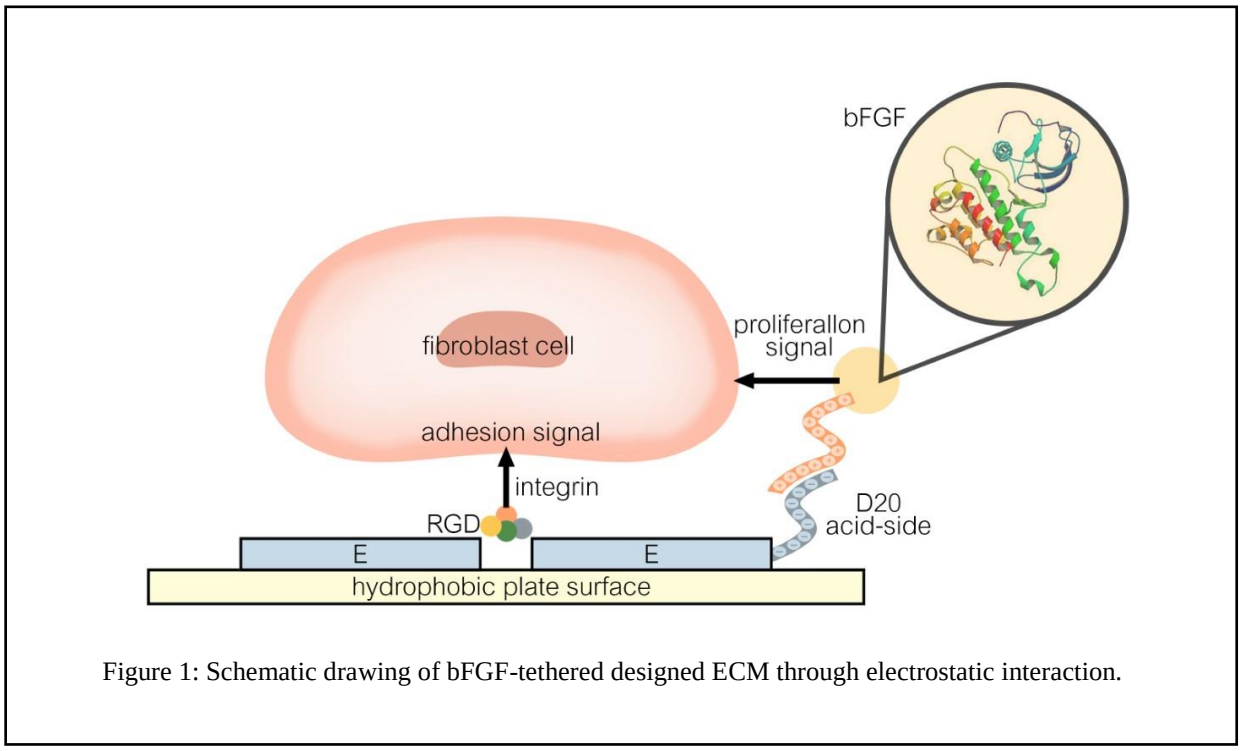

Figure 1: Schematic drawing of bFGF-tethered designed ECM through electrostatic interaction.

In this study, bFGF-tethered ECM was developed to be alternative method in construct efficient multi-functional ECMs which is a promising approach in tissue engineering. It was expected that bFGF could be tethered to D20 domain fused to ERE (ERE-D20) by electrostatic interaction between the basic domain of bFGF and the acidic domain of D20 in ERE-D20 (Fig. 1). Therefore, the capability in electrostatic interaction between bFGF and ERE-D20 was investigated. In addition to evaluated cell adhesion activity of ERE-D20, even fusion with D20 domain. Finally, the effect of immobilized bFGF to ERE-D20 on cell proliferation activity was evaluated compared to soluble bFGF adding in cell culture medium.

2.2. Materials and Methods

2.2.1 Plasmid construction

The plasmid pET32c-NHis-ERE constructed in our laboratory was digested with Nco I and Bgl II to obtain the ERE gene fragment[18]. The plasmid pET32c-NHis-C2D20 encoded 5 repeats of 4 aspartic acids and a serine, DDDDS (constructed as previously described)[14]. The plasmid was digested with Nco I and Bgl II followed by insertion of the ERE gene fragment. The resulting plasmid for expression of ERE-D20 protein in *E.coli* was named pET32c-NHis-ERE-D20.

2.2.2 Protein expression and purification

In this chapter, 3 types of plasmid were used, pET32c-NHis-E12, pET32c-NHis-ERE[17], and pET32c-NHis-ERE-D20 for expression of E12, ERE, and ERE-D20, respectively. These 3 types of plasmid were introduced into *E.coli* BL21 (DE3) competent cells by heat shock. Transformed *E.coli* cells were cultured in Luria-Bertani (LB) media with ampicillin at 37°C. 1mM Isopropylthio-β-D-galactoside (IPTG) was added after O.D. reached at 0.6 for induction of protein expression. After culture overnight at 30°C, cells were harvested by centrifugation and re-suspended in BugBuster Reagent (Novagen) in the presence of Benzonase nuclease (Sigma-Aldrich). Re-suspended cells were rotated at 4°C for 30 min followed by centrifugation. The supernatant was applied to His-Select Nickel Affinity Gel (Sigma-Aldrich) followed by rotation at 4°C for 1 h. After washing with phosphate buffer (50 mM sodium phosphate, 300 mM NaCl, pH 8.0), proteins were eluted by phosphate buffer with 100 mM imidazole. The eluted protein

solution was dialyzed using Slide-A-Lyzer Dialysis Cassettes (Pierce) against phosphate buffer saline (PBS) to remove imidazole. The purified protein was analyzed by 15% sodium dodecyl sulfate polyacrylamide gel electrophoresis (SDS-PAGE) and the protein concentration was measured using a BCA assay kit (Pierce).

2.2.3 C3H10T1/2 cell culture

The murine fibroblast cell line C3H10T 1/2 cells, obtained from Riken Cell Bank, was cultured in Dulbecco's modified Eagle's medium (DMEM) with 10% fetal bovine serum (FBS) and antibiotics (100 U/ml penicillin, 100 µg/ml streptomycin). Culture medium was changed every 2 days.

2.2.4 Adsorption of constructed protein on hydrophobic surface of plates.

These 3 types of protein, E12, ERE, and, ERE-D20, consisted of E12 motif which had a highly hydrophobic property allowing these designed proteins adsorb onto the hydrophobic surface of the plate. From this property, these proteins could be absorbed onto hydrophobic plate surface and could be detected the saturated concentration of absorption by ELISA using anti-polyhistidine antibody. Solution of proteins were added to 96-well suspension culture plate (Sumilon, MS-8096R) in varied concentration and incubated for 2h at 37°C. Plates were washed with PBS-T (PBS including 0.05% Tween 20) followed by blocking with Blocking One (Nacalai Tesque, Inc.) overnight at 4°C. After washing with PBS-T, anti-polyhistidine antibody (Sigma-Aldrich) was added to the plate and incubated for 1 h at 37°C. After washing with PBS-T again, anti-mouse IgG peroxidase conjugate (Sigma-Aldrich) was added and incubated for 1 h at 37°C. After washing with PBS-T, TMB peroxidase substrate (KPL, Inc.) was added to the plate. Finally, 1 M HCl was added to stop the reaction and the absorbance at 450 nm was measured by a microplate reader.

2.2.5 Cell adhesive ability of ERE-D20 on hydrophobic surface

Plates were prepared by added 1000 nM ERE or ERE-D20 on 24-well suspension culture plate (Iwaki). Then, plates were washed 3 times before added cells. 8000 cells of C3H10T1/2 cells suspended in Fibrolife Serum-Free Medium were added to the wells and cultured for 4h. After washing with PBS,

attached cells were evaluated using cell counting-kit 8 (Dojindo) and the absorbance at 450 nm was measured by a microplate reader.

2.2.6 Cell adhesion activity (RGD competition assay)

Cells were incubated with various soluble RGD peptide (Calbiochem) concentration (0, 1, 10, 20, 30 μM) at 37°C for 15 min before seeded on ERE and ERE-D20 coated 24-well hydrophobic plate (Iwaki) and cultured for 4h. After washing with PBS, attached cells were evaluated with a cell counting-kit 8 (Dojindo).

2.2.7 Tethering of bFGF to ERE-D20 through electrostatic interaction

The interaction between ERE-D20 and bFGF was determined by ELISA using anti-bFGF antibody. First, ERE and ERE-D20 were coated on 96-well suspension culture plates (Sumilon, MS-8096R) and incubated for 2 h at 37°C. Then, wells were washed with PBS-T followed by blocking with Blocking One at 4°C, overnight. After washing with PBS-T, 100 nM bFGF was added and incubate for 1 h at 37°C. Next wells were washed three times with PBS-T before a solution of 1/1000 diluted rabbit anti-bFGF antibody (Sigma-Aldrich) was added and incubated for 1 h at 37°C. Wells were washed again with PBS-T, a solution of 1/1000 diluted anti-rabbit IgG-HRP (Jackson ImmunoResearch Inc.) was added and incubated for 1 h at 37°C. After washing with PBS-T, TMB peroxidase substrate was added to the wells and later 1M HCl was added to stop the reaction. The absorbance at 450 nm was measured by a microplate reader (Fig 7A). The ability of various concentrations of recombinant bFGF tethered to ERE-D20 was also tested. First, 1000 nM of ERE-D20 was coated on 96-well suspension plates (Sumilon, MS-8096R). After blocking with Blocking One overnight, various concentrations of bFGF (0-10 μM) was added and incubated for 1 h at 37°C. The detection assay was same as above.

2.2.8 Cell proliferation on bFGF-tethered ERE-D20

1000 nM of ERE-D20 was added onto a 24-well hydrophobic plate (Iwaki) for coating by incubated 2 h at 37°C. After washing with PBS, 100 nM of recombinant bFGF (Sigma-Aldrich) was added to the wells and the plate was incubate for 2 h at 37°C. After washing with PBS, C3H10T1/2 cells suspended in Fibrolife Fibroblast Serum-Free Medium (Lifeline cell technology) without recombinant

bFGF were added 8,000 cells/well and cultured. For negative control, non-coated and E12-coated plate were used, while ERE- and fibronectin-coated plate were used as positive control. Cells was cultured on negative and positive control plate using soluble bFGF-added medium. During culture, media were changed every 2 days. The number of growth cells on day 1 and day 5 was evaluated using Cell Counting Kit-8 (Dojindo molecular technologies, Inc.) and the absorbance at 450 nm was measured by microplate reader. Additionally, from this experiment, the condition which bFGF was added and incubated on ERE-D20 coated hydrophobic plate for 1 h at 37°C before tested was designated as "**ERE-D20/bFGF**" condition.

2.2.9 Evaluation of immobilized-bFGF induce cell proliferation using FGFR inhibitor

A high affinity inhibitor for FGFR1, PD 173074, was used to detect whether cell proliferation was promoted by immobilized-bFGF. Cells were incubated with or without 75 nM of FGFR1 inhibitor, PD 173074, before transferred to ERE-D20/bFGF-coated hydrophobic plate (Iwaki). Cells were cultured in Fibrolife Fibroblast Serum-Free Medium (Lifeline cell technology) without recombinant bFGF and medium was changed every 2 days. The number of cells on day 2 and day 4 was evaluated using Cell Counting Kit-8.

2.2.10 Statistical Analysis

Values are given as mean value ± standard deviation. Statistical analysis was performed by independent two-sample *t*-test with equal valiances. Values of $P < 0.05$ were considered to be statistically significant.

2.3. Result and discussion

2.3.1 Design and expression of ERE-D20 protein

In this experiment, three different plasmids; pET32c-NHis-E12, pET32c-NHis-ERE, and pET32c-NHis-ERE-D20 were used and for expression of proteins named as E12, ERE, and ERE-D20, respectively. The plasmids, pET32c-NHis-E12 and pET32c-NHis-ERE were constructed previously in our laboratory[10]. The plasmid, pET32c-NHis-ERE$(DDDDS)_5$ for expression of designed extracellular matrix ERE-D20 was genetically engineered from pET32c-NHis-ERE plasmid by insertion of gene fragment encoding 5 repeats of 4 aspartic acids and serine. The aspartic rich tail in $(DDDDS)_5$ was negatively charged oligo peptide tail in physiological condition which expected to tethering with basic rich domain of bFGF via electrostatic interaction (ERE-D20).

To express E12, ERE, and ERE-D20 proteins, *E.coli* BL21 (DE3) was used as a host strain. Protein expression was induced by addition 1 mM IPTG and cultured overnight at 30°C.

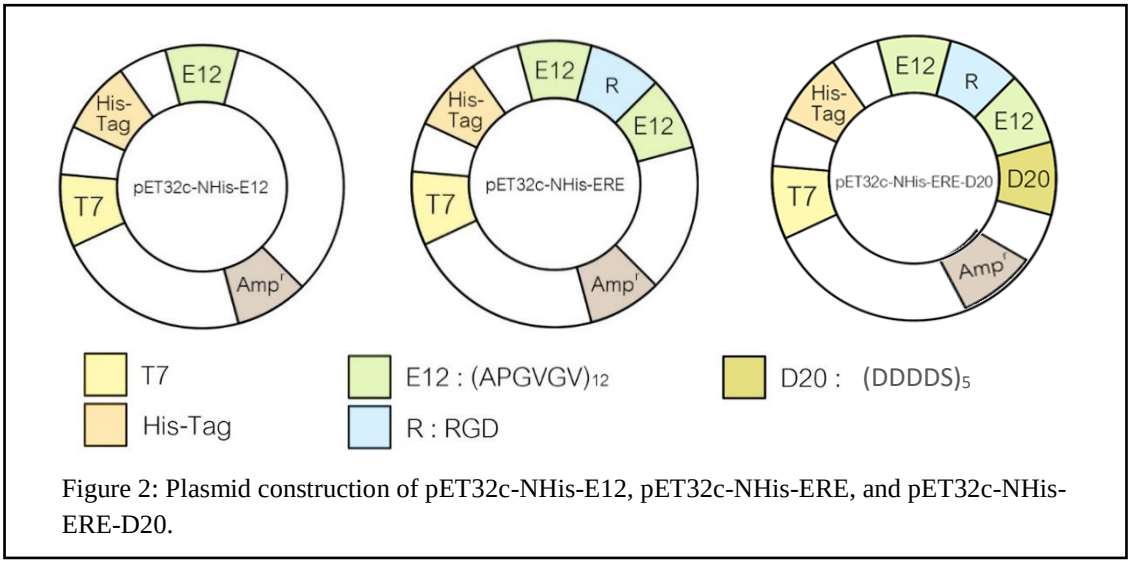

Figure 2: Plasmid construction of pET32c-NHis-E12, pET32c-NHis-ERE, and pET32c-NHis-ERE-D20.

Expressed proteins were collected and purified from soluble fraction by nickel affinity gel using His-Tag. The size of designed proteins was confirmed by SDS-PAGE (15% acrylamide) (Fig 3). The molecular mass of E12, ERE, and ERE-D20 was 8.2 kDa, 15.3 kDa, and 18.3 kDa, respectively. Although, the band of ERE in SDS-PAGE slightly larger than the expected molecular size from its calculated molecular weight. This behavior has been previously reported for ELP-fused proteins due to the

physicochemical characteristics of ELPs[19]. However, the band of ERE-D20 appeared at nearly the expected molecular size. It is suggested that the physicochemical characteristics of the ELPs were cancelled by the negatively charged D20 domain.

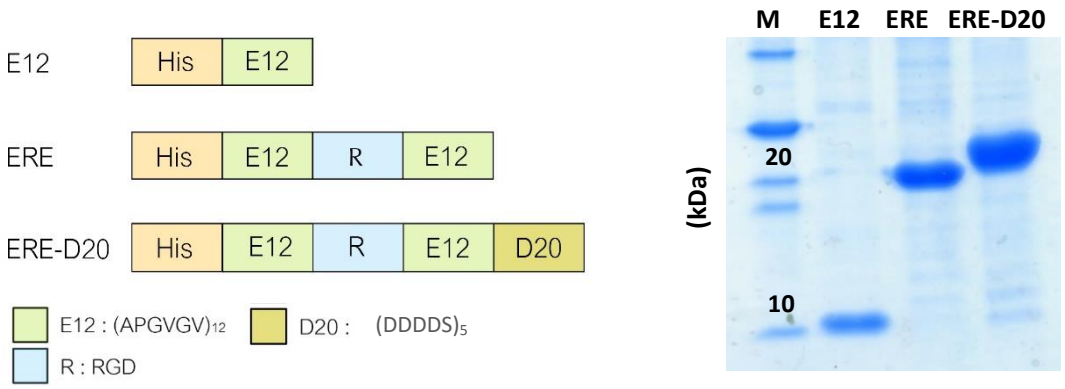

Figure 3: Protein expression and purification. SDS-PAGE analysis of purified proteins was used to confirmed the size of targeted proteins: E12 (8.2 kDa), ERE (15.3 kDa), ERE-D20 (18.3 kDa).

2.3.2 Adsorption of constructed protein on hydrophobic surface of plates.

These three-type of proteins, E12, ERE, ERE-D20 consisted of E12 motif which had a highly hydrophobic property allowing these proteins absorbed on hydrophobic surface[17]. Including His-tag at C-terminal of proteins, the saturated concentration of each protein adsorbed on hydrophobic surface was evaluated by ELISA using anti-polyhistidine antibody (Fig. 4). First, various concentration of E12, ERE, and ERE-D20 (from 0 nM to 1250 nM) was coated onto 96-well hydrophobic plate and adsorbed proteins were detected with an anti-polyhistidine antibody. The saturated concentrations of E12, ERE, and ERE-D20 proteins adsorbed on hydrophobic plate surface were around 1000 nM. As shown in this result, the adsorption of ERE-D20 was slightly lower than ERE. It would be caused by the hydrophilicity of D20 domain. However, it was shown that ERE-D20 maintained the ability to adsorb onto the hydrophobic surface, even after fusion with D20.

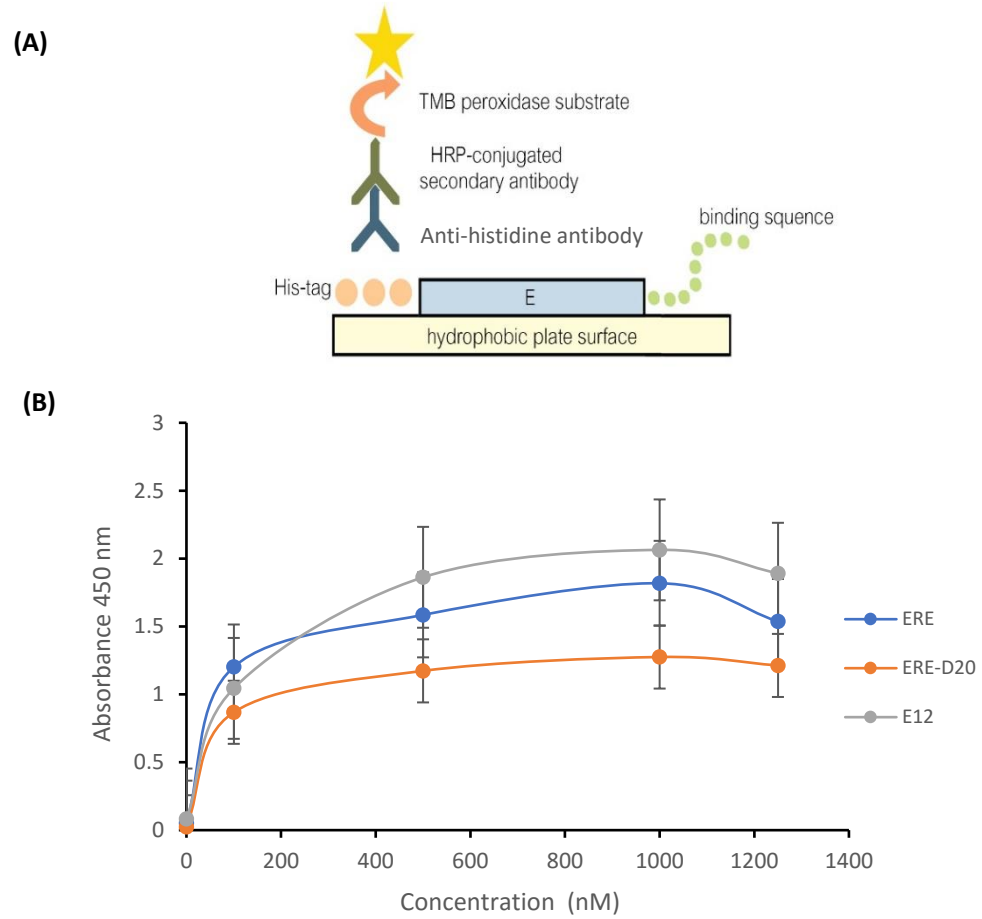

Figure 4: Adsorption of E12, ERE, and ERE-D20 on the hydrophobic surface of the plates. (A) Schematic drawing of the detection of adsorbed-protein on hydrophobic plate by ELISA. (B) Various concentration of designed protein was coated on the hydrophobic plate surface and saturated adsorption of proteins were detected by ELISA assay. Errors bars showed the standard deviation of three independent measurements.

2.3.3 Cell adhesion activity of ERE-D20

RGD sequence was fused to our designed biomaterial as cell adhesive binding site. Therefore, to test whether RGD sequence in ERE and also ERE-D20 could be functioned even fused with ELPs, RGD competition assay was performed. A various soluble RGD peptides (GRGDSP) were mixed with 10T1/2 cells suspension in Fibrolife Serum-Free Medium for 15 min before transfer cells to ERE and ERE-D20 coated hydrophobic plate surface. After transferred and cultured for 4 h, attached cells were evaluated using cell counting-kit 8 and the absorbance at 450 nm was measured by microplate reader. The result showed in figure 5 that the cell adhesion on both ERE and ERE-D20 coated plate was inhibited by the addition of soluble RGD peptide and the attachment of cells were decreasing depending on the RGD

concentrations. This result suggested that RGD motif which fused in our designed materials, were effective for cell adhesion.

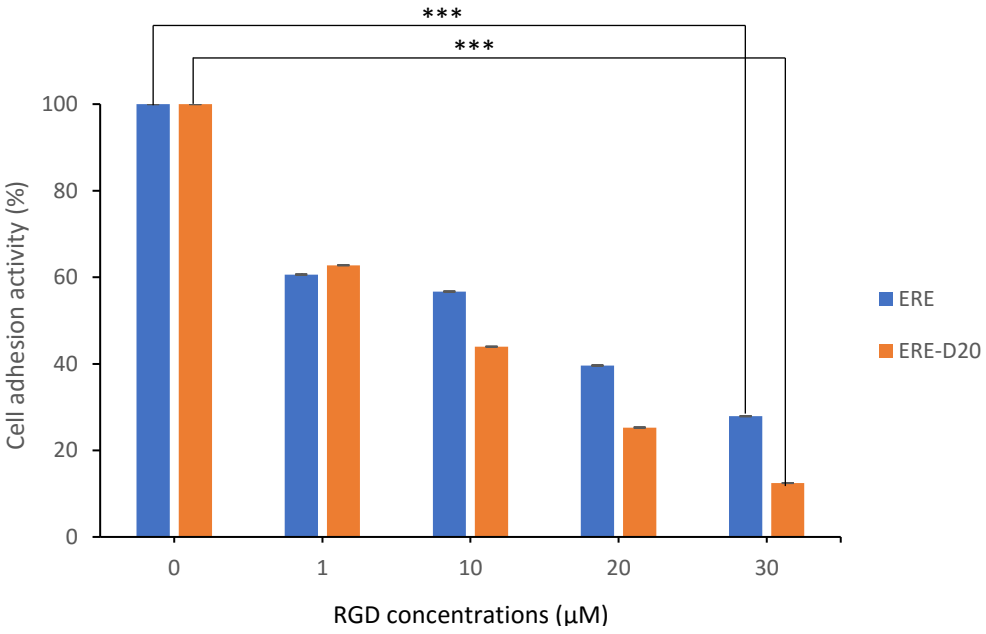

Figure 5: Inhibition effect of RGD on cell adhesive activity. Various concentration of RGD was added and incubated with cells before transferred cells to ERE and ERE-D20 coated plate. Adhesive cells were detected using CCK-8 assay. Statistically significant differences were indicated for $P < 0.005$ (***).

2.3.4 Cell adhesion ability of ERE-D20 on hydrophobic surface

In our designed protein, ERE-D20, RGD sequence hold cell adhesion activity which could bind to integrin receptor of cell membrane and from above experiment (2.3.3) also shown that RGD maintained their ability, even fusion with D20. However, D20 was negatively charged domain and generally cell membrane was highly charge negatively[20]. Therefore, the effect of D20 on cell adhesion activity had to be evaluated. Cells were seeded onto E12, ERE, ERE-D20, bFGF-tethered ERE-D20 (ERE-D20/bFGF,) coated hydrophobic plate. Non-coated well was used as negative control and 'RGD' sequence was originated from fibronectin, so fibronectin was used as positive control. After cultured for 4 h, attached cells were detected by observed via light microscope (fig. 6B) and live cells which attached on the well were detected by cell counting-kit 8 (Fig. 6A). The absorbance at 450 nm was measured using microplate reader. Cells seeded on non-coated well could not attached and also on E12-coated well which means the

function of E12 part in designed protein did not support cell binding activity. In contrast to cells seeded on ERE, ERE-D20, ERE-D20/bFGF, and fibronectin showed cells were attached on the surface. Cells adhered on ERE-D20 showed no significant difference to cell adhered on fibronectin. Therefore, these results proved that ERE-D20 maintained cell adhesion activity, even after fusion with D20 domain. Additionally, cells seeded on bFGF-tethered ERE-D20 showed similar cell adhesion activity as ERE-D20 alone, so bFGF-tethered toERE-D20 was not cell binding obstacle.

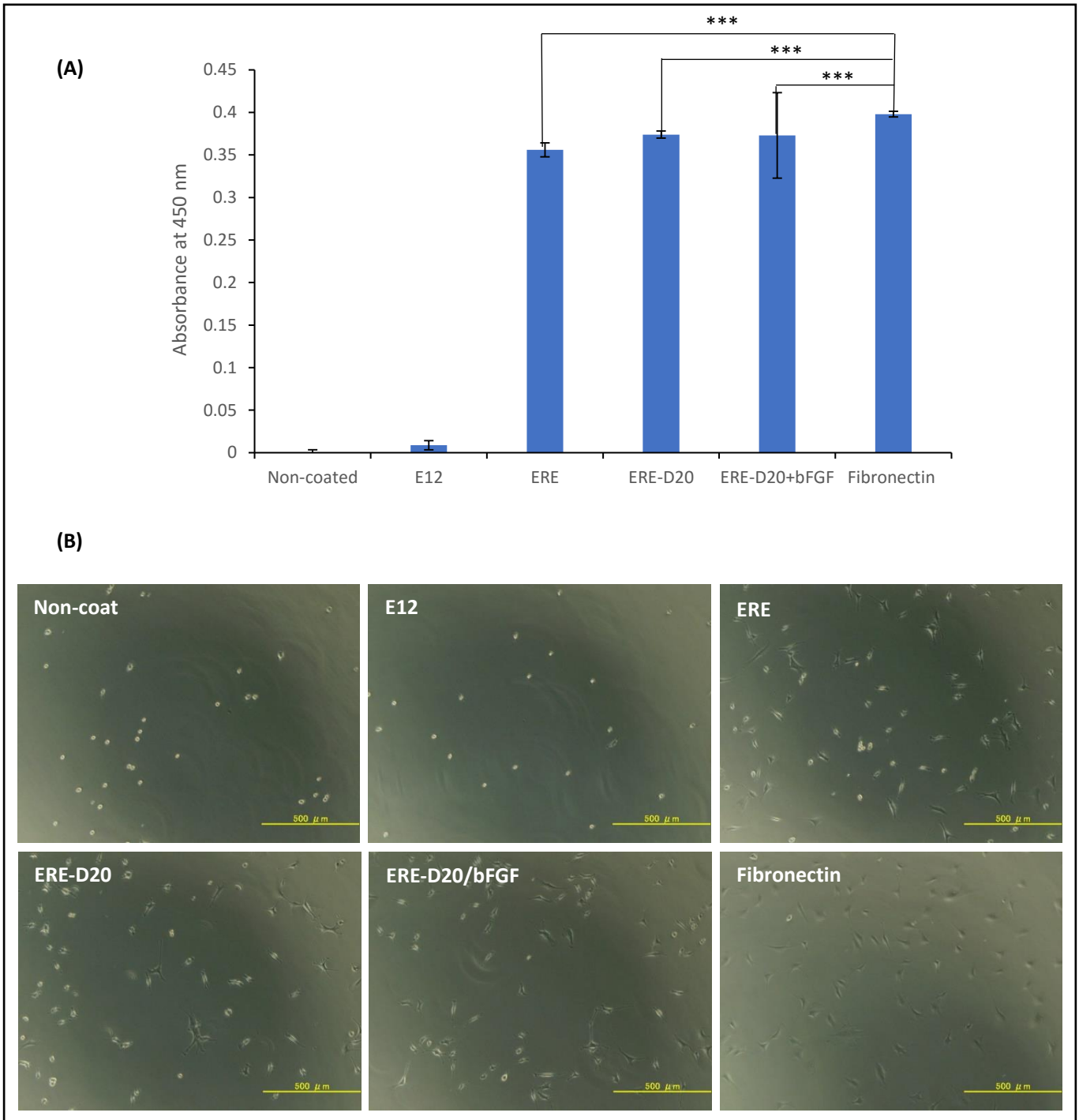

Figure 6: Cell adhesive activity of ERE-D20. (A) Evaluation of cell adhesion on various material after incubation for 4h using CCK-8 assay. (B) Bright-field images of cell adhesion on various protein-coated surface at 4 h after seeded cells. Scale bar = 500μm. Statistically significant differences were indicated for $P < 0.005$ (***).

2.3.5 Tethering of bFGF to ERE-D20 through electrostatic

The interaction between ERE-D20 and bFGF was evaluated by ELISA using anti-bFGF antibody. First, to determine whether D20 domain would be interacted with bFGF. ERE and ERE-D20 were coated on 96-well hydrophobic plate surface followed by addition of bFGF. After washing with PBS, remaining bFGF-tethered on material was detected using anti-bFGF antibody (Fig. 7, A). As shown in Figure 7, B, the absorbance measuried from bFGF-tethered ERE-D20 showed significant difference from ERE. It meant bFGF was tethered to D20 domain of ERE-D20, whereas could not be tethered to ERE alone. This result confirmed that bFGF bind to the D20 domain. Then, we evaluated the binding of varied bFGF concentrations. Various concentration of bFGF (from 0 µM to 10 µM) was added onto 1000 nM ERE-D20 coated hydrophobic plate surface. After washing with PBS, the remaining bFGF-tethered to ERE-D20 was detected using ELISA. The result in figure 7, C showed that the tethered bFGF increased in a concentration-dependent manner and saturated at 2500 nM. However, 2500 nM of bFGF was excessive concentration for active cell proliferation, so we decided to use 100 nM bFGF tethered to ERE-D20 in cell proliferation assay.

Corresponding to study from Suzuki *et al*. which reported the fusion protein encoding D20 was shown to form complex with polyethylenimine by electrostatic interaction[13]. The calculated isoelectric point of ERE-D20 and bFGF are approximately 3.9 and 9.6, respectively. Therefore, ERE-D20 should be able to tether bFGF through electrostatic interaction under physiological condition. These results proved that bFGF was tethered to ERE-D20 through electrostatic interaction between the basic domain of bFGF and D20 of ERE-D20.

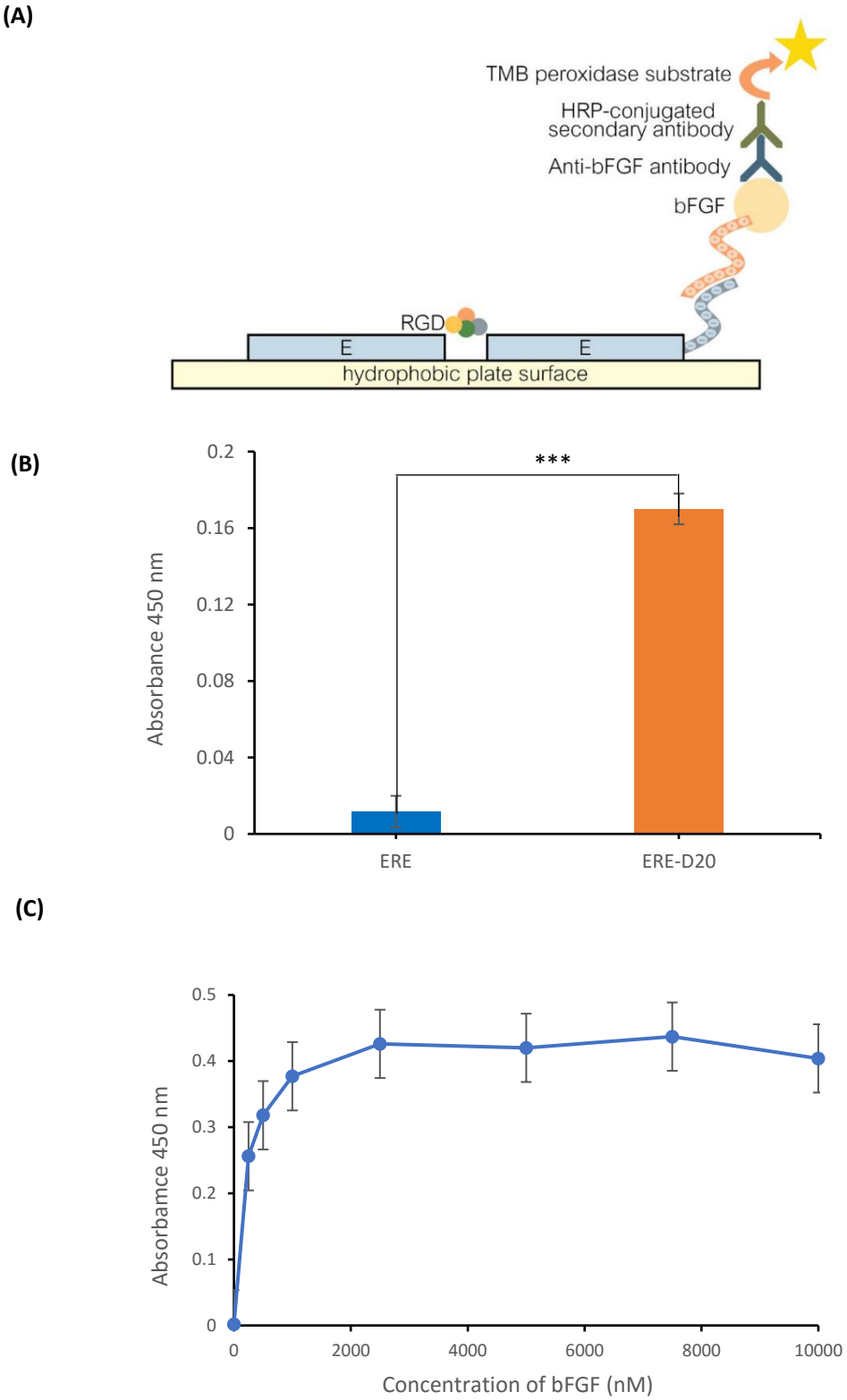

Figure 7: Evaluation of bFGF tethered to ERE-D20. (A) Schematic drawing of bFGF-tethered ERE-D20 through electrostatic interaction was detected by ELISA using anti-bFGF antibody. (B) Specific binding between basic domain of bFGF and negatively charged of D20 in ERE-D20. (C) Various concentrations of bFGF tethered to ERE-D20 (1000 nM). Error bars show the standard deviations of three independent measurements. Statistically significant differences were indicated for $P < 0.005$ (***).

2.3.6 Cell proliferation on bFGF-tethered ERE-D20

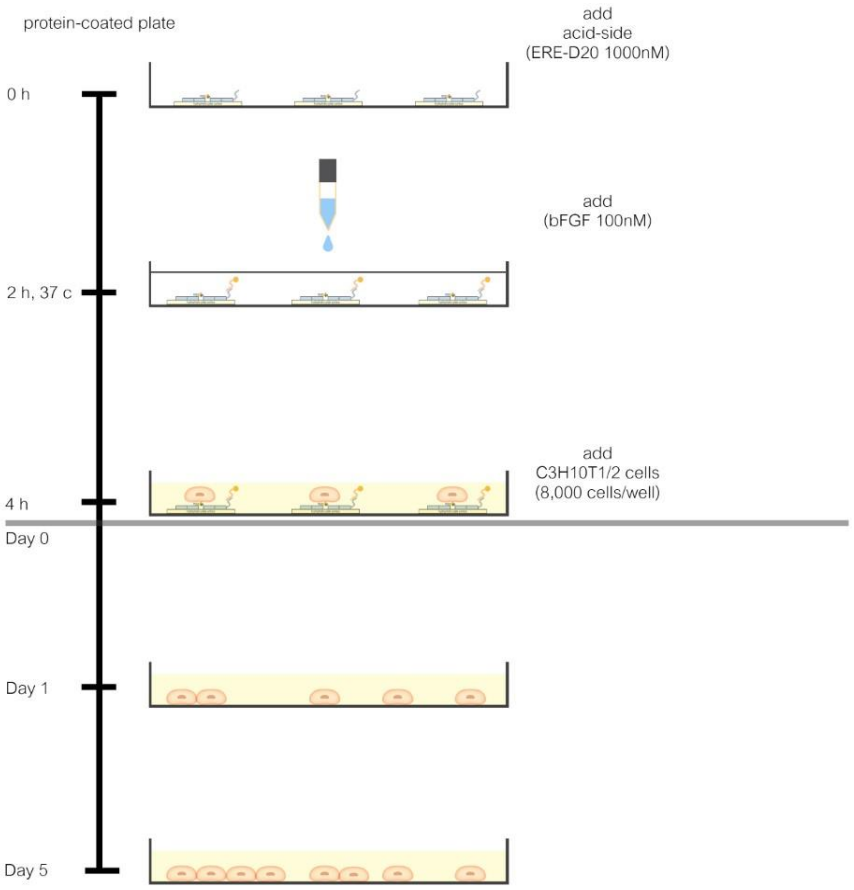

Figure 8: Cell proliferation assay. Cells were cultured on ERE-D20/bFGF coated hydrophobic plate in Fibrolife Serum-free Medium. Cell proliferation was detected using CCK-8 assay at day 1 and day 5.

To determine whether bFGF-tethered on ERE-D20 had any effect on 10T1/2 cells proliferation in Fibrolife Serum-free Medium condition. The cell proliferation assay was showed in Fig. 8. First, the surface of 24-well hydrophobic plate was coated with ERE-D20 following incubated with bFGF (ERE-D20/bFGF) or without bFGF (only ERE-D20 coated well). After washing with PBS, 10T1/2 cells were seed onto the plate and cultured in Fibrolife Serum-free Medium without addition of soluble bFGF in medium. Non-coated wells were used as negative control. Cell proliferative activities were evaluated at 1 day and 5 days after seed cells using cell counting-kit 8 assay. As shown in Fig 9, there was significant differences of cell numbers between ERE-D20 and ERE-D20/bFGF. Cells cultured onto ERE-D20 coated

plate without tethered bFGF were attached on the well surface, but cell growth was scarcely observed after 5 days of culture. In contrast to ERE-D20 coated plate with tethered bFGF, cells were well attached on the well surface and significant proliferation was observed at day 5 of culture. These significant differences were caused immobilized bFGF, which tethered to ERE-D20 via electrostatic interaction.

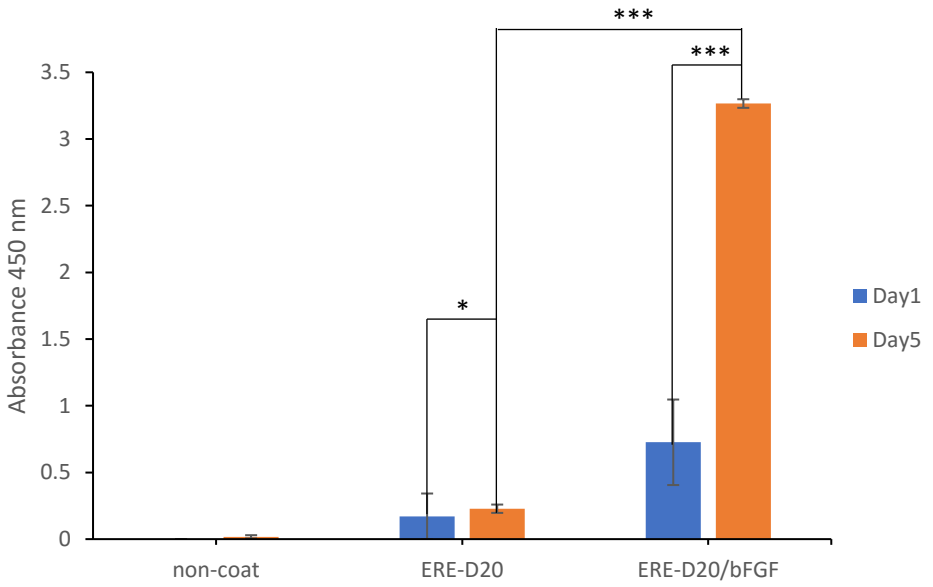

Figure 9: Induction of cell proliferation activities by cultured 10T1/2 cells on bFGF-tethered ERE-D20. Cells were cultured on ERE-D20 with or without tethered bFGF for 1 day and 5 days. Error bars show the standard deviations of three independent measurements. Statistically significant differences were indicated for $P < 0.05$ (*) and $P < 0.005$ (***).

After evaluation of cell proliferation on bFGF-tethered ERE-D20, the different effect between immobilized bFGF and soluble bFGF on cell proliferation was determined. This experiment was evaluated whether bFGF-tethered ERE-D20 (immobilized form) played the same or better effect on cell proliferation as free form bFGF (soluble bFGF added in the medium). Cells were seeded onto the wells of 24-well suspension culture plates coated with E12, ERE, ERE-D20/bFGF (bFGF-tethered to ERE-D20 before seeded cells), and gelatin. Cells seeded on non-coated, E12, ERE, and gelatin, were cultured with external soluble bFGF added in medium. However, cells seeded onto ERE-D20/bFGF was cultured in medium without addition of soluble bFGF. The results of cell growth on various materials were evaluated at day 1 and day 5 using cell counting-kit 8. As shown in Figure 10, the result of cell growth on ERE-D20/bFGF without addition of soluble bFGF in medium showed the no significant differences to cells cultured in soluble bFGF-added medium on gelatin coated-plate. However, the growth of cells cultured on ERE-

D20/bFGF showed significant difference to cells cultured on ERE in medium with soluble bFGF. From these results, cells cultured on bFGF-tethered ERE-D20 were underwent proliferation without addition of soluble bFGF and slightly better than addition of soluble bFGF in medium condition.

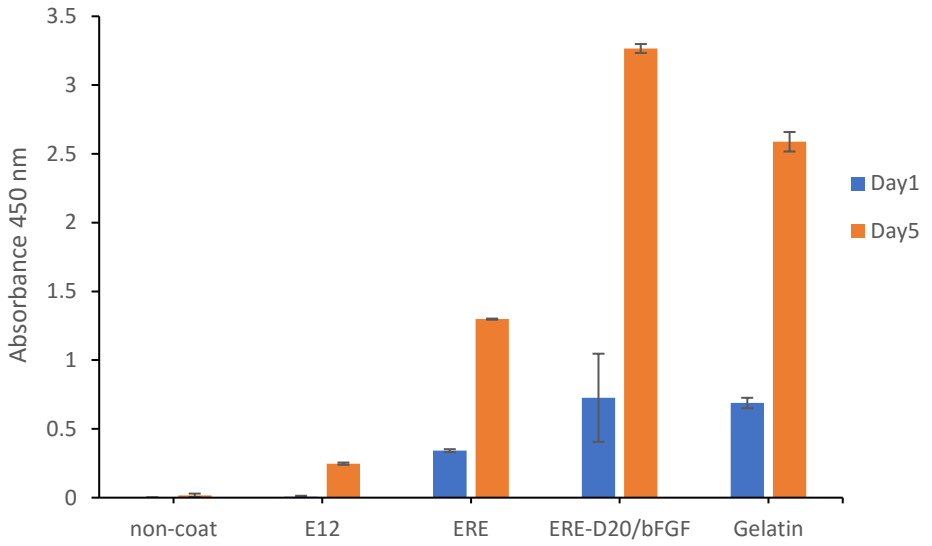

Figure 10: Cell proliferation activity of bFGF-tethered ERE-D20 without addition of soluble bFGF compared with soluble bFGF-added medium. 10T 1/2 cells were cultured on various materials and gelatin used as positive control. Soluble bFGF was added in Fibrolife media except ERE-D20/bFGF-coated plate. Cell proliferation was evaluated using CCK-8 at day 1 and day 5 after treated cells. Error bars show the standard deviation of three independent measurements.

Next, cell growth on ERE-D20 was compared to culture on fibronectin because RGD, cell binding sequence which fused into ERE-D20, was originated from sequence in fibronectin. Cell proliferation assay was done in the same way as previous experiment. Cells seeded on fibronectin coated plate were cultured in medium with soluble bFGF, whereas cells seeded on ERE-D20 were cultured in medium without soluble bFGF. The cell proliferative result was detected using cell counting kit-8 at day 5 after seeded cells and the result showed in figure 11, A. Cells cultured on bFGF-tethered ERE-D20 without addition of soluble bFGF showed similar number of cell growth compared to cells cultured on fibronectin with addition of soluble bFGF. Corresponding to the cell counting-kit 8 assay, bright-field images (Fig. 11, B) also showed the similar morphology of cells cultured in both conditions. It was suggested that immobilized form of bFGF could enhance cell proliferation and retain their activities for longer period without addition of external bFGF.

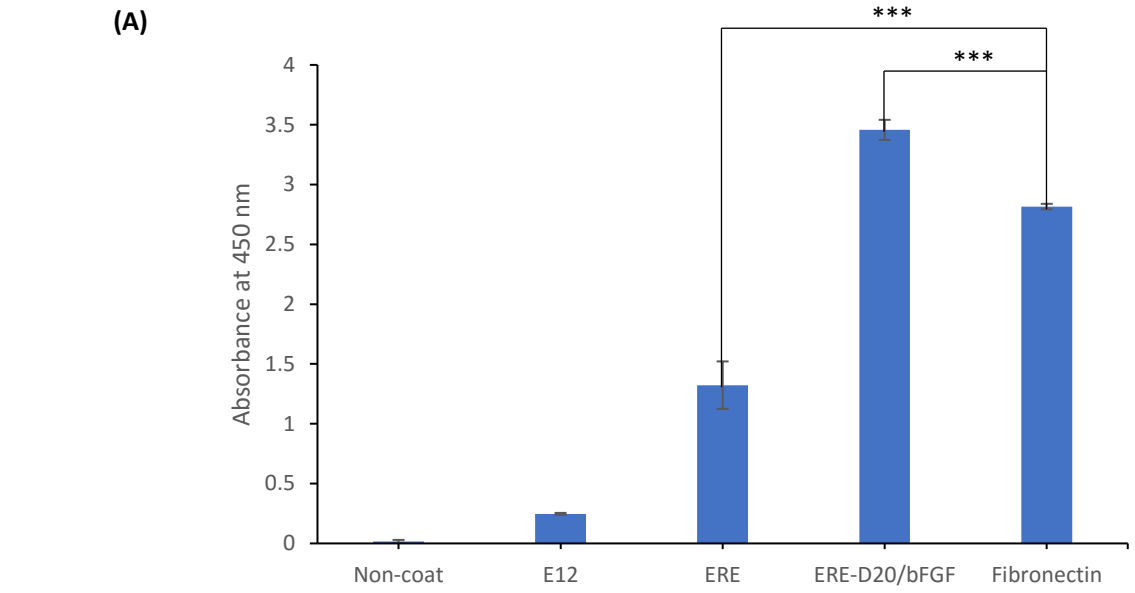

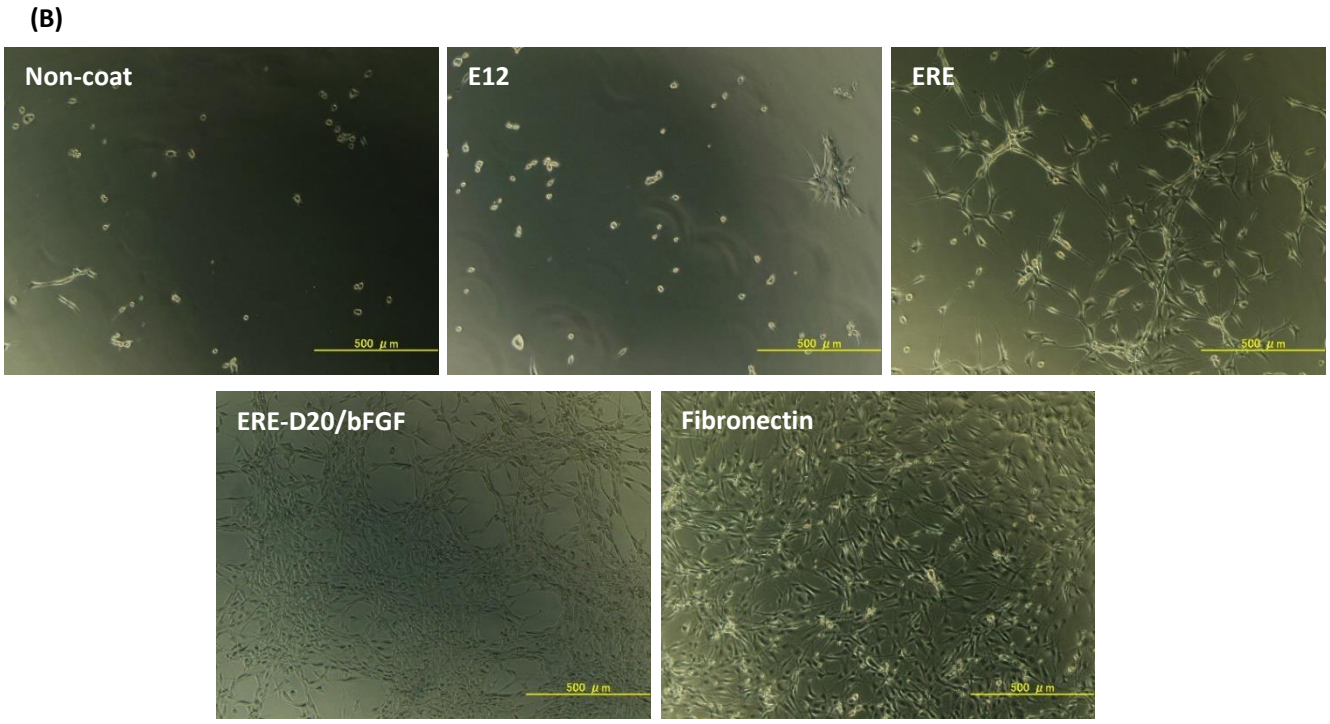

Figure 11: Cell proliferation activities of bFGF-tethered ERE-D20 compared to fibronectin. Soluble bFGF was added in Fibrolife media except ERE-D20/bFGF-coated plate. (A) cell proliferation was evaluated using CCK-8 at day 5 after seeded cells. Error bars show the standard deviation of three independent measurements. (B) Representative images of 10T1/2 cells cultured on various protein-coated hydrophobic surface. was Scale bar 500 μm. Statistically significant differences were indicated for $P < 0.005$ (***).

2.3.7 Evaluation of immobilized-bFGF induce cell proliferation using FGFR inhibitor

Finally, whether the immobilized bFGF enhanced the cell growth on ERE-D20/bFGF was evaluated by using an inhibitor, PD173074, binds to FGF-receptor1 (FGFR1) with high affinity[21]. Cells were mixed with PD173074 for 15 min before seeding of cells onto ERE-D20/bFGF. Cells cultured on ERE-D20/bFGF without treatment of FGFR inhibitor were used as control. Cell number was evaluated at day 2 and day 4 using cell counting kit-8. As shown in figure 12, when cells were treated with FGFR inhibitor before seeding onto ERE-D20/bFGF, cells could not grow well as same as cells without FGFR inhibitor treatment. From this result suggested that bFGF which tethered to ERE-D20 enhanced 10T1/2 cells proliferation. Furthermore, to confirm whether immobilized-bFGF could promote cell proliferation via the same signaling pathway as soluble bFGF, activation of MEK/ERK and JNK signaling pathways should be evaluated with or without FGFR1 inhibitor using western blot analysis.

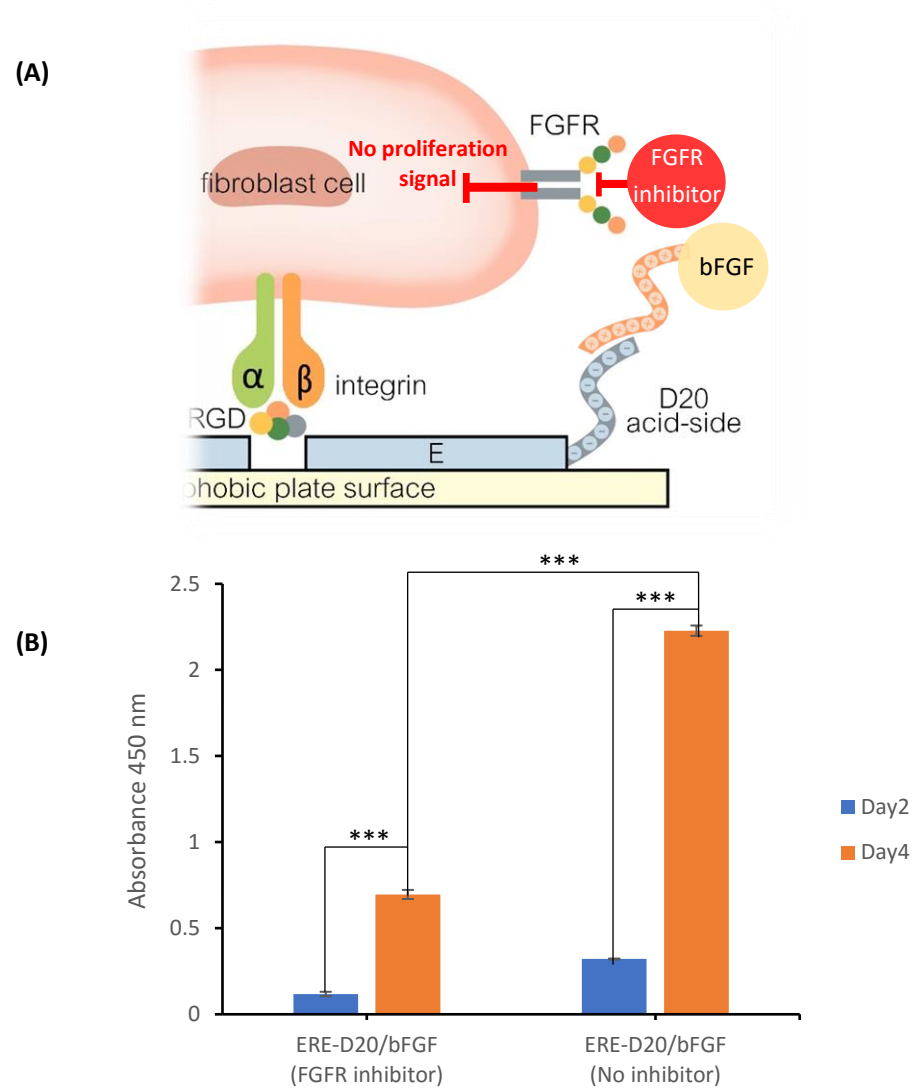

Figure 12: The different in number of cell proliferation. (A) Schematic drawing of the experiment evaluated bFGF-tethered ERE-D20 in cell proliferation effect using FGFR inhibitor. (B) Cells were mixed with or without FGFR inhibitor before seeded on ERE-D20/bFGF and cell proliferation was detected using CCK-8 assay. Error bars show the standard deviations of three independent measurements. Statistically significant differences were indicated for $P < 0.005$ (***).

In addition to answer the mechanism of immobilized bFGF induced signaling pathway, whether bind to the FGF receptor on cell membrane for active signaling pathway and endocytosis into cytoplasm or retain binding FGF receptor and stimulate the signal continuously. Fluorescently labeled targeted growth factor can be used for example, Rhodamine Red™-X, succinimidyl Ester have to be mixed with bFGF before used. Therefore, fluorescently labeled-bFGF can be tracing in real time and showed the predictable release characteristics. Furthermore, the bFGF released period have to be investigated.

2.4 Conclusion

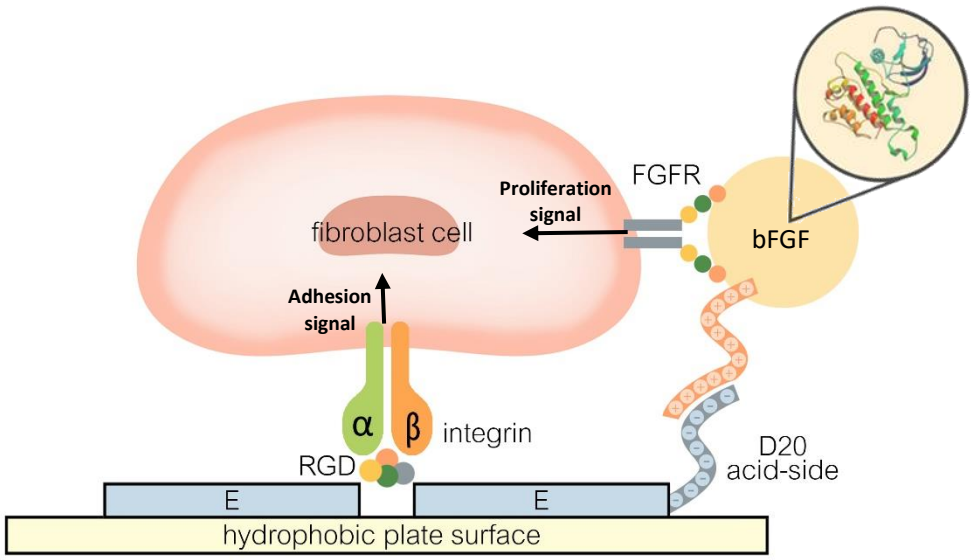

Figure 13: Schematic drawing of bFGF-tethered design ECM, ERE-20, through electrostatic interaction. Cell adhesion activity occurs via the interaction of RGD (R) sequence to integrin receptor on cell surface. bFGF-tethered ERE-D20 also remain its ability to induce fibroblast cell proliferation via FGF receptor.

In this study, it was shown that bFGF could be tethered to the designed extracellular matrix (ERE-D20) via electrostatic interaction between the basic domain of bFGF and the acidic domain of ERE-D20. Cell cultured on bFGF-tethered ERE-D20 were well attached on ERE-D20 and underwent proliferation without addition of soluble bFGF. From these data, the tethering of bFGF to our design extracellular matrix ERE-D20 via electrostatic interaction showed the alternative method to construct efficient multi-functional ECMs which was simple, efficient, and easy-to-use because these method does not need modification of growth factors. This immobilizing method could be applied to delivery of growth factors in tissue engineering.

2.5 Reference

1. Lanza, R., Langer, R., and Vacanti, J. P. Principles of tissue engineering. Academic press, 2011.
2. Kim, B.-S., and Mooney, D. J. Development of biocompatible synthetic extracellular matrices for tissue engineering. Trends in biotechnology 16, 5 (1998), 224–230.
3. Hajimiri, M., Shahverdi, S., Kamalinia, G., and Dinarvand, R. Growth factor conjugation: strategies and applications. Journal of biomedical materials research Part A 103, 2 (2015), 819–838.
4. Eswarakumar, V., Lax, I., and Schlessinger, J. Cellular signaling by fibroblast growth factor receptors. Cytokine & growth factor reviews 16, 2 (2005), 139–149.
5. Edelman, E. R., Mathiowitz, E., Langer, R., and Klagsbrun, M. Controlled and modulated release of basic fibroblast growth factor. Biomaterials 12, 7 (1991), 619–626.
6. Ito, Y. Covalently immobilized biosignal molecule materials for tissue engineering. Soft matter 4, 1 (2008), 46–56.
7. Chiu, L. L., and Radisic, M. Scaffolds with covalently immobilized vegf and angiopoietin-1 for vascularization of engineered tissues. Biomaterials 31, 2 (2010), 226–241.
8. Mammadov, R., Mammadov, B., Guler, M. O., and Tekinay, A. B. Growth factor binding on heparin mimetic peptide nanofibers. Biomacromolecules 13, 10 (2012), 3311–3319.
9. Elloumi, I., Kobayashi, R., Funabashi, H., Mie, M., and Kobatake, E. Construction of epidermal growth factor fusion protein with cell adhesive activity. Biomaterials 27, 18 (2006), 3451–3458.
10. Kobatake, E., Takahashi, R., and Mie, M. Construction of a bfgf tethered extracellular matrix using a coiled-coil helical interaction. Bioconjugate chemistry 22, 10 (2011), 2038–2042.
11. Assal, Y., Mie, M., and Kobatake, E. The promotion of angiogenesis by growth factors integrated with ecm proteins through coiled-coil structures. Biomaterials 34, 13 (2013), 3315–3323.
12. Yamamoto, M., Ikeda, Y., Tabata, Y. Controlled release of growth factors based on biodegradation of gelatin hydrogel. J Biomater Sci Polym Ed 12, 1(2001), 77-88.
13. Suzuki, M., Takayanagi, A., and Shimizu, N. Targeted gene delivery using humanized single-chain antibody with negatively charged oligopeptide tail. Cancer science 95, 5 (2004), 424–429.

14. Bae, J., Mie, M., and Kobatake, E. Targeted gene delivery via pei complexed with an antibody. Applied biochemistry and biotechnology 168, 8 (2012), 2184–2190.
15. Elloumi, I., Kobayashi, R., Funabashi, H., Mie, M., and Kobatake, E. Construction of epidermal growth factor fusion protein with cell adhesive activity. Biomaterials 27, 18 (2006), 3451–3458.
16. D'Souza, S. E., Ginsberg, M. H., and Plow, E. F. Arginyl-glycylaspartic acid (rgd): a cell adhesion motif. Trends in biochemical sciences 16 (1991), 246–250.
17. Kobatake, E., Onoda, K., Yanagida, Y., and Aizawa, M. Design and gene engineering synthesis of an extremely thermostable protein with biological activity. Biomacromolecules 1, 3 (2000), 382–386.
18. Kobatake, E., Takahashi, R., and Mie, M. Construction of a bfgftethered extracellular matrix using a coiled-coil helical interaction. Bioconjugate chemistry 22, 10 (2011), 2038–2042.
19. McPherson, D. T., Xu, J., and Urry, D. W. Product purification by reversible phase transition followingescherichia coliexpression of genes encoding up to 251 repeats of the elastomeric pentapeptide gvgvp. Protein expression and purification 7, 1 (1996), 51–57.
20. Cevc, G. Membrane electrostatics. Biochimica et Biophysica Acta (BBA)-Reviews on Biomembranes 1031, 3 (1990), 311–382.
21. Skaper, S. D., Kee, W. J., Facci, L., Macdonald, G., Doherty, P., and Walsh, F. S. The fgfr1 inhibitor pd 173074 selectively and potently antagonizes fgf-2 neurotrophic and neurotropic effects. Journal of neurochemistry 75, 4 (2000), 1520–1527.

Chapter 3: Construction of Biomimetic ECM for Neural Differentiation from Mouse Induced Pluripotent Stem Cells

3.1 Introduction

In the previous knowledge, the regeneration of injured central nervous system (CNS) had extremely limited regenerative potential, while differ from peripheral nervous system (PNS) in adult mammalian. PNS can regenerate and allow substantial functional recovery[1, 2]. Surprisingly in the recent study, the capability to regrow in CNS was shown. This finding demonstrated that some regenerative neuron remains in CNS, but the non-permissive environment disrupted regeneration[3]. The inhibitors that limit CNS regeneration had been shown to activate Rho family of small GTPase which interplayed between activation of RhoA and suppression of Rac1[4, 5] following by induction of neurite retraction. Many researches were confirmed the antagonistic effects of RhoA/Rac1 in neural differentiation and shown the notion that interfering RhoA activation and stimulated Rac1 activation enhance neural differentiation[6, 7.] Therefore, the discoveries of molecules which inactivates RhoA and activates Rac1 could be interesting targets for supporting CNS regeneration.

E-/N-cadherin binding sequence (SWEYYPLRANL), called as 'CBP' in our experiment, was interesting target due to the functions of N-cadherin in neural differentiation. N-cadherin is a Ca^{2+}-dependent cell-cell adhesion molecules which found mostly during neural development in ventricular zone of cortex. Absence of N-cadherin effects on the neural development in entire cortex[8]. As reported by Haque and colleagues[9] that N-cadherin substrate mediated down-regulation of Rho-ROCK signaling, resulting in stimulation of neurite outgrowth and expression of neural marker. Taken together, N-cadherin exerts a neuritogenic effect in CNS development. In addition to neuritogenic effect, N- cadherin play a role in selective adhesion. The possibility that N-cadherin was involved in neural recognition mechanism because N-cadherin played a key role in neural attachment to other cells and found expressing in various neural tissue[10, 11]. E-/N-cadherin binding sequence (SWEYYPLRANL, CBP), was found by Devemy *et al.*[12] had the properties to binding both E- and N-cadherin/Fc chimeric proteins. Both E- and N-cadherin existed in type I cadherin, thus similar in structure and could form heterotypic intercellular junctions[13]. However, the binding to E-cadherin/Fc chimeric protein was shown lesser affinity than the N-cadherin/Fc chimeric protein. Therefore, CBP sequence was hypothesized to have both cell adhesive function and induction of neural differentiation similar to N-cadherin.

In this study, E-/N- cadherin binding peptide-based biomimetic ECMs were constructed and characterized for their capability to mimic N-cadherin in the neural differentiation. The designed ECM protein, ERE-CBP, was constructed in our previous study[14] which consisted of elastin-derived unit (E), $(APGVGV)_{12}$, as a stable structural unit and tripeptide cell adhesive RGD (R) integrin-binding sequence, and E-/N- cadherin binding sequence, SWELYYPLRANL (CBP), as an active functional unit. Because of both RGD sequence and SWELYYPLRANL was detectable in enhancing neural outgrowth during embryogenesis development, therefore we hypothesized that RGD and N-cadherin binding sequence in our designed protein ERE-CBP could enhance neural differentiation[15, 11]. Other designed ECM proteins, ERE and E-CBP, were also used in this study to evaluate the effects of RGD and SWELYYPLRANL separately on neural differentiation.

In this study, the substrate properties of designed ECM protein, E-CBP, was shown the effect of cell adhesive activity on E13.5 mouse cortical cells. Then mouse iPS cells were used to confirmed cell adhesive activity and the ability to promoted specific neural differentiation lineage without exogenous neuro-inductive signals. Another benefit was that the synthesis of designed protein was relatively simple and inexpensive due to the expression from *Escherichia coli*. Therefore, this study explores the potentials of CBP peptide sequence (SWELYYPLRANL) for its 'N-cadherin mimicking properties'.

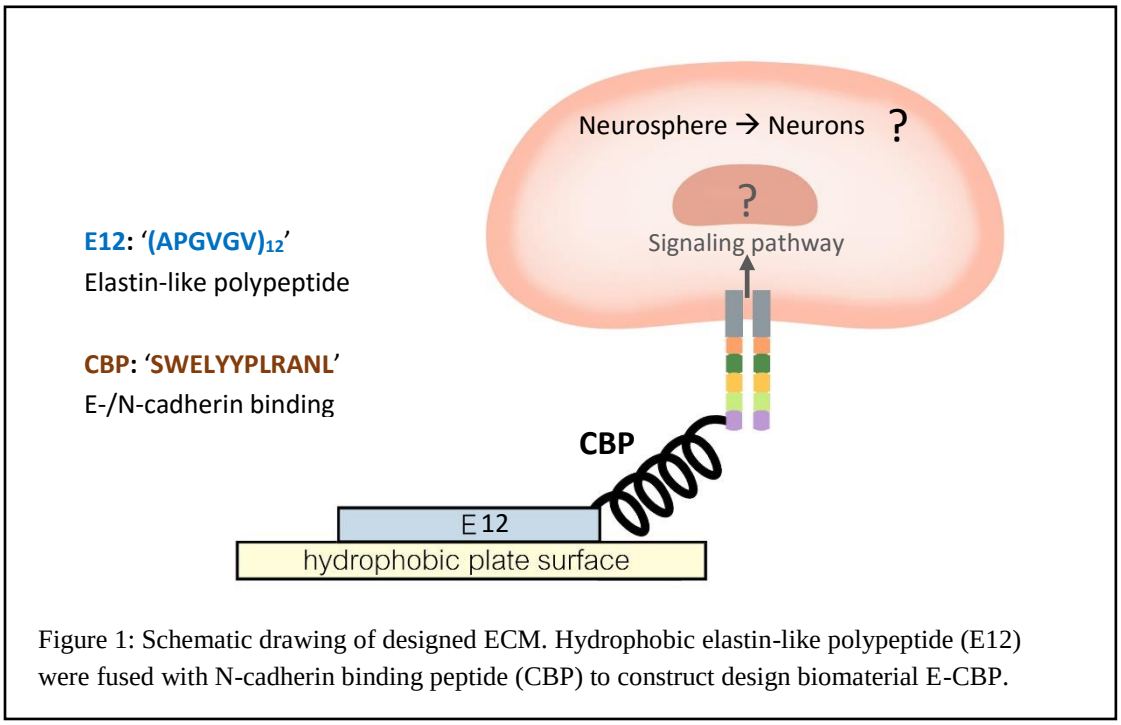

Figure 1: Schematic drawing of designed ECM. Hydrophobic elastin-like polypeptide (E12) were fused with N-cadherin binding peptide (CBP) to construct design biomaterial E-CBP.

3.2. Materials and Methods

3.2.1 Plasmid construction

Four different plasmids, pET32c-NHis-E12, pET32c-NHis-E12-RGD-E12, pET32c-NHis-E12-RGD-E12-CBP, and pET32c-NHis-E12-CBP, were used in this experiment. Each plasmids were constructed for designed ECM proteins, E12, ERE, ERE-DBP and E-CBP, respectively. Plasmid construction protocols for pET32c-NHis-E12 and pET32c-NHis12-RGD-E12 have been described elsewhere[16]. Here, to prepare pET32c-NHis-E12-RGD-E12-CBP, and pET32c-NHis-E12-CBP, the synthetic oligonucleotide encoding E-/N-cadherin common binding peptide (CBP) was introduced to the 3' end of E12 sequence in pET32c-NHis-E12 and pET32c-NHis-E12-RGD-E12, respectively, by digested with EcoR I (Takara) and Bgl II (Takara). Then CBP encoding DNA fragment containing BamH I and EcoR I sites were ligated with digested pET32c-NHis-E12-CBP and pET32c-NHis-E12-RGD-E12-CBP plasmids[14].

3.2.2 Protein expression and purification

The constructed four plasmids, pET32c-NHis-E12, pET32c-NHis-E12-R-E12, pET32c-NHis-E12-CBP, and pET32c-NHis-E12-R-E12-CBP were transfected into *E.coli* BL21(DE3) competent cells for expression of proteins. Transformed *E.coli* cells were cultured in Luria-Bertani (LB) medium containing 50 μg/ml ampicillin at 37°C until OD ~ 0.6. Protein expression was induced by addition of 1 mM isopropyl β-D-1-thiogalactopyranoside (IPTG). Cells were cultured overnight at 30°C and harvested by centrifugation and resuspended in BugBuster Reagent (Novagen) with Benzonase Nuclease (Sigma-Aldrich). After 30 min rotation at RT, the sample was separated between supernatant (soluble fraction) and inclusion bodies (insoluble fraction) by centrifugation. E12 and ERE proteins were collected from soluble fraction, ERE-CBP and E-CBP proteins were collected from insoluble fraction.

From soluble fraction: the supernatant was applied to His-Select Nickel Affinity Gel (Sigma-Aldrich) followed by incubation at 4°C for 1 h. After washing with phosphate buffer (50 mM sodium phosphate, 300 mM NaCl, pH 8.0), proteins were eluted by phosphate buffer with 100 mM imidazole. The resultant protein solution was dialyzed using Slide-A-Lyzer Dialysis Cassettes (Pierce) against phosphate-buffered saline (PBS).

From insoluble fraction: After centrifugation for separation between soluble and insoluble fraction, soluble fraction was discarded. Insoluble fraction was dissolved by addition of PBS with 8 M urea and rotated at 4°C for 1 h followed by, sonication for 20 min before addition to His-Select Nickel Affinity Gel (Sigma-Aldrich). After rotation at 4°C for 1 h, phosphate buffer with 4 M Urea was used for washing gel. Protein were eluted by 100 mM imidazole in phosphate buffer with 4 M Urea. The resultant protein solution was dialyzed using Slide-A-Lyzer Dialysis Cassettes (Pierce) against PBS with 2 M Urea for 2 h and PBS with 0.5 M Urea for 2 h sequentially to decrease the concentration of urea in protein solution. Finally, protein solution was dialysed with PBS overnight.

The purified protein was analyzed by 15% sodium dodecyl sulfate polyacrylamide gel electrophoresis (SDS-PAGE) and the protein concentration was measured using BCA assay kit (Pierce).

3.2.3 Adsorption of constructed protein on hydrophobic plates.

These four types of protein consisted of E12 motif which had a highly hydrophobic property allowing these targeted proteins adsorb onto the hydrophobic surface of the plate. From this property, these proteins were added to 96-well suspension culture plate (Sumilon, MS-8096R) in varied concentrations from 0 mM to 1000 mM and incubated for 1 h at 37°C. Plates were washed with PBS-0.05% Tween 20 (PBS-T) followed by addition of Blocking One reagent (Nacalai Tesque, Inc.) overnight at 4°C. After washing with PBS-T, anti-polyhistidine antibody (Sigma-Aldrich) was added to the plate and incubated for 1 h at 37°C followed by washing with PBS-T again. Then, anti-mouse IgG peroxidase conjugate (Sigma-Aldrich) was added and incubated for 1h at 37°C. After washing with PBS-T, TMB peroxidase substrate (KPL, Inc.) was added to the plate. Finally, 1M HCl was added to stop the reaction and the absorbance at 450 nm was measured by a microplate reader.

3.2.4 E13.5 cortical cell preparation and culture

Cortical cells were prepared from embryonic ICR mouse at E13.5 day. Cortex from 13.5 days of embryo mouse brain was dissected and washed in DEP-C water. Then cortex was transferred 1.5 ml tube and 50 µl trypsin was added and incubated at 37°C for 5-15 min (until cells were separated). Then, 50 µl of trypsin inhibitor was added followed by addition of 50 µl of DNase I. After incubation at 37°C for 5 min, explanted media (include serum) 750 µl was added and pipetting to separate cells. Then cells were

washed using 1% PBS. After washing, neural basal medium with 1% B27 supplement and pipetting to separate cells before using in experiment.

For adhesion and neural differentiation experiment: After E13.5 cortical cells were singly dissociated, cells were seeded at 10^6 cells per well on various protein-coated hydrophobic 24-well plate culturing with Neural differentiation medium; NDM (Neurobasal® medium (NB, Gibco), 1% B-27® supplement minus vitamin A (Gibco), and 1% GlutaMAX™ supplement (Gibco)). After transferred for 2 days, cell adhesive activity was evaluated using CCK-8 assay. For neural differentiation detection, cells were culture until day 10.

3.2.5 mouse iPS cell culture.

Standard mouse iPSC line APS0002-iPS-MEF-Ng-178B-5 was used in this experiment. The culture media for APS0002-iPS-MEF-Ng-178B-5 cell line was composed of DMEM (Wako) supplemented with 15% fetal bovine serum (Hyclone, Thermo Scientific), 1% nonessential amino acids (NEAA, Gibco), 0.1 mM 2-mercaptoethanol (Sigma), 1000 U/mL penicillin and 100 µg/mL streptomycin (Gibco), and 1000 U/mL Leukemia inhibitory factor (LIF) (Wako).

Mouse iPS cells were cultured on MMC treated STO cells, where the later was used as feeder layer. To prepared MMC treated STO cells, SNL76/7 (STO) cells were cultured on gelatin coated 10 dishes and when the confluency reached around 90%, 10 µg/mL of mitomycin C containing in DMEM medium was added to the plates. After treatment for 3-4 h, plates were washed with PBS and the MMC treated STO cells were trypsinized and collected. Therefore, before culturing miPS cells, MMC treated STO cells were prepared. MMC treated STO cells were cultured on gelatin treated 60 mm dish at a density 10^6 cells/plate. One day after MMC treated STO cells seeded, miPS 10^4 cells were added to the plates and the medium was changed to miPS cells culture medium. Cells were cultured in a humidified incubator with 5% CO_2 at 37°C for 3-4 days on feeder layer before further passage.

3.2.6 Induction of neural differentiation from miPS cells

miPS cells were cultured in suspension plate using basal differentiation medium (BDM) in the absence of antidifferentiation factors such as LIF and feeder layer cells to form Embryoid bodies (EBs).

EB is the multicellular three-dimension structure which mimic post-implantation embryonic tissues and has the ability to differentiate into all three germ layers; ectoderm, mesoderm, endoderm [17, 18]. Embryoid bodies (EBs) were formed by culturing miPS cells at $5x10^4$ cells/well in 6-well suspension culture plate using basal differentiation media (BDM). BDM was composed of Glassgow Minimum Essential Medium (GMEM, Wako), supplemented with 10% KSR (Gibco), 1 mM sodium pyruvate (Gibco), 1% nonessential amino acids (Gibco), 0.1 mM 2-mercaptoethanol (Sigma), 1000 U/mL penicillin and 100 µg/mL streptomycin (Gibco). Suspension plate was shaken with shaker in `T-motion' to control cell shape and size. BDM media was changed at day 3 of EBs formation.

After 5 days of EB formation, EBs was transferred to protein-coated non-treated 24-well plate (Iwaki). To prepare protein-coated surface, non-treated 24 well plate was coated with each protein, 1000 nM E12, 1000 nM ERE, 1000 nM ERE-CBP and 750 nM E-CBP, 250 µl/well and incubated at 37°C for 1h. After incubation, protein-coated wells were washed with PBS before addition of cells. EBs were transferred to protein-coated well (approximately 50 EBs per well) and cultured in Neural differentiation medium (NDM) which composed of Neurobasal® medium (NB, Gibco), 1% B-27® supplement minus vitamin A (Gibco), and 1% GlutaMAX™ supplement (Gibco). EBs were cultured for 10 days and medium was changed every 3 days.

3.2.7 Immunostaining

Cells were fixed with 4% paraformaldehyde for 15 min at room temperature and then washed with 1% PBS 3 times followed by incubation with PBS including 0.2% Triton X for 3 min. After washed with PBS 2 times, 1% bovine serum albumin (BSA) was added and incubated for 1h. Then primary antibody was added to samples. In this experiment, neuron-specific β-III tubulin antibody produced in mouse (R&D Systems) for immature neuron staining and monoclonal anti-MAP2 antibody produced in mouse (Sigma-Aldrich) for mature neuron staining were used as primary antibodies, respectively. Primary antibody was diluted in 1% BSA in 1:500 ratio and incubated for 1h. After washed with PBS 3 times, secondary antibody, Rabbit anti-mouse IgG Alexa Flour 568 (1:500, diluted in 1% BSA) and Hoechst 33258 solution (1:2000, diluted in 1% BSA) were added and incubated for 1h, then washed with PBS 2 times. Finally, samples were observed by using fluorescence microscopy.

3.2.8 Quantitative PCR Analysis.

Total RNA was prepared using the RNeasy Mini kit (Qiagen, Valencia, CA) according to the manufacturer's instructions. Using 2.5 μg of total RNA in 20 μl reaction, cDNA was synthesized by using SuperScript™ III Reverse Transcriptase (Thermo Fisher) primed with oligo-dT according to the manufacturers instruction. Quantitative real-time PCR was performed with the FastStart essential DNA green master (Roche), which consisted of FastStart Taq DNA polymerase and double-stranded DNA specific SYBR green I dye, for product detection using LightCycler® Nano instrument (Roche) and the data were analyzed by its software. Neuronal markers expression (Nestin, β-III tubulin, and MAP2) was normalized against GAPDH expression of same sample. All reactions were done in duplicate. The primers used in this experiment was listed in Table 1.

Table 1: List of primers using in quantitative PCR.

Primers		Sequence (5'-3')
GAPDH	Forward	ATCTTCTTGTGCAGTGCCAGCCSTCGTCCCG
	Reverse	AGTTGAGGTCAATGAAGGGGTCGTTGATGG
Nestin	Forward	GCTACATACAGGACTCTGCTG
	Reverse	AAACTCTAGACTCACTGGATTCT
β-III tubulin	Forward	AGCGATGAGCACGGCATAG
	Reverse	CAGGTTCCAAGTCCACCAGA
MAP2	Forward	TCAGACTTCCACCGAGCAG
	Reverse	AGGGGAAAGATCATGGCCC

3.2.9 Statistical Analysis. Values are given as mean value ± standard deviation. Statistical analysis was performed by independent two-sample *t*-test with equal valiances. Values of $P < 0.05$ were considered to be statistically significant.

3.3. Result and discussion

3.3.1 Design and expression of designed ECM proteins

Four different plasmids, pET32c-NHis-E12, pET32c-NHis-E12-RGD-E12, pET32c-NHis-E12-CBP, and pET32c-NHis-E12-R-E12-CBP, were used in this experiment (Fig 2) and expressed E12, ERE, E-CBP, and ERE-CBP proteins, respectively. These four plasmids were introduced into *E.coli* BL21(DE3) as a host strain for protein expression that was induced by addition of IPTG 1mM and culture overnight at 30°C.

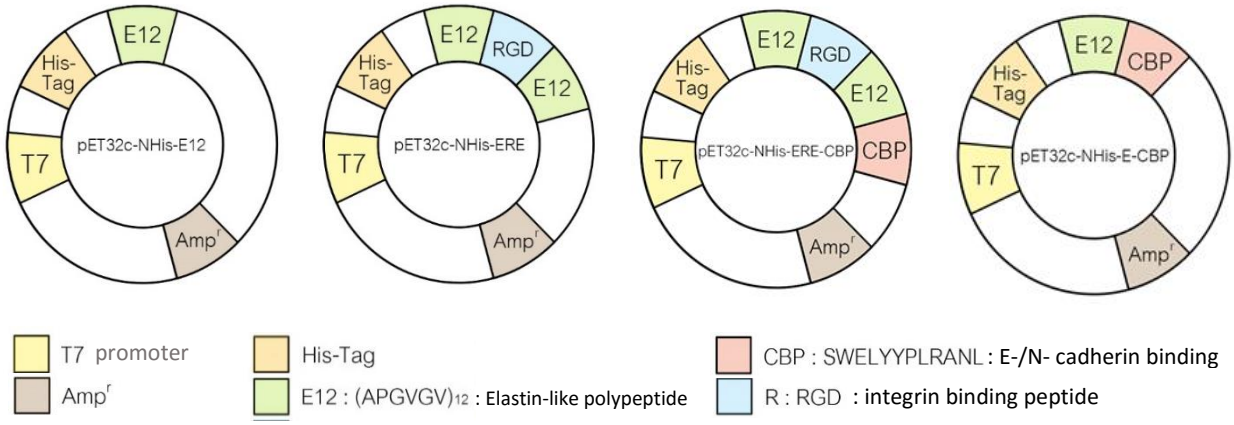

Figure 2: Plasmid construction of pET32c-NHis-E12, pET32c-NHis-E12-R-E12, pET32c-NHis-E12-RGD-E12-CBP, and pET32c-NHis-E12-CBP.

Expressed proteins were collected and purified by nickel affinity gel using His-Tag. E12 and ERE proteins were purified from soluble fraction, whereas ERE-CBP and E-CBP protein were purified from insoluble fraction. The size of designed proteins were confirmed by SDS-PAGE (15% acrylamide) (Fig 3). The sizes of E12, ERE, ERE-CBP, and E-CBP were 8.2 kDa, 15.3 kDa, 17 kDa, and 11 kDa respectively.

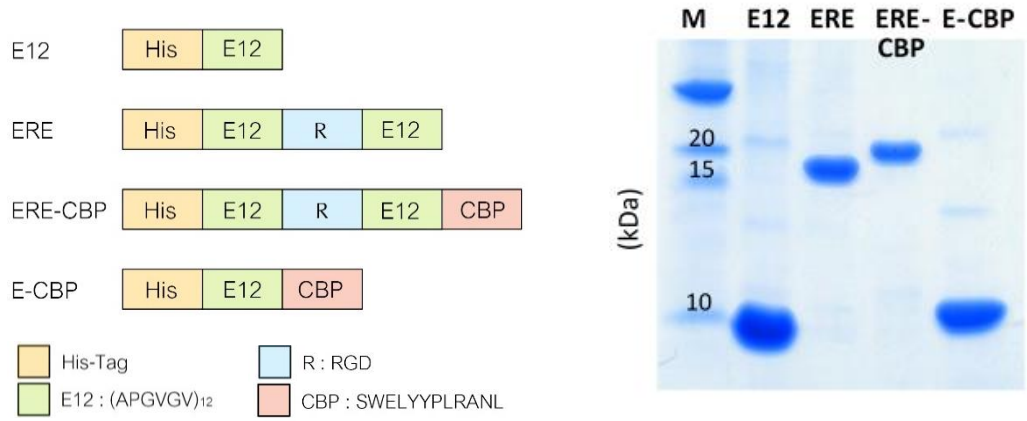

Figure 3: Protein expression and purification. SDS-PAGE analysis of purified proteins was used to confirmed the size of targeted proteins: E12 (8.2 kDa), ERE (15.3 kDa), ERE-CBP (17 kDa), and E-CBP (11 kDa). Lane M is molecular weight marker (kDa).

3.3.2 Absorption of constructed protein on the hydrophobic surface of the plate

The purpose of these ECMs construction due to testing the effect from functional parts in our design ECMs whether differentiated mouse iPS cells towards neural lineages *in vitro*. To received this purpose, these proteins were generated to be easily adsorbed on surface of hydrophobic plate. Therefore, targeted sequence could be easily tested.

These four-type of proteins, E12, ERE, ERE-CBP, and E-CBP consisted of E12 motif which has a highly hydrophobic property allowing these proteins absorbed on hydrophobic surface[16]. Including His-tag at C-terminal of proteins, the saturated-concentration of each protein absorbed on hydrophobic surface could be detected by ELISA using anti-polyhistidine antibody. The saturated concentration of each proteins was used for coating hydrophobic plate and tested the function of proteins. As shown in Fig 4, the saturation concentration of ERE-CBP and E-CBP proteins absorbed on hydrophobic plate surface were 1000 nM and 750 nM, respectively. These was almost same as the saturation concentration of E12 and ERE proteins shown in chapter 2. From these results, CBP peptide does not effect on the ability to adsorb onto the hydrophobic surface.

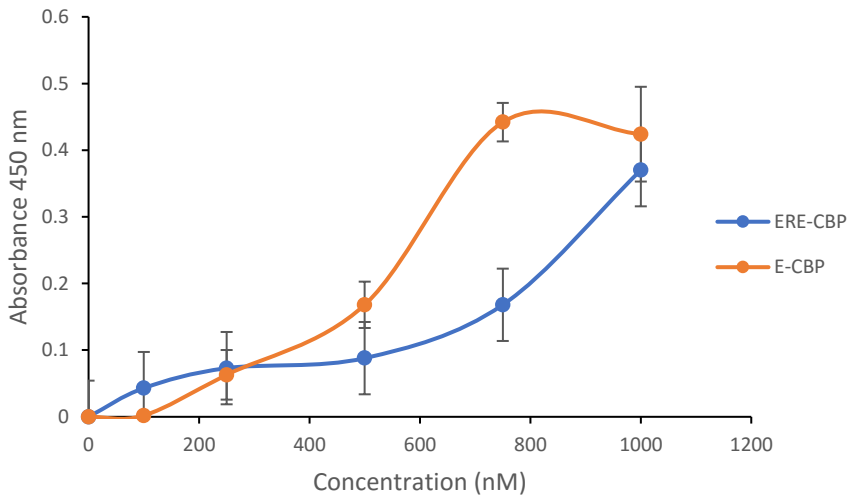

Figure 4: Adsorption of E12, ERE-CBP, and E-CBP on the hydrophobic surface of plate. Various concentration of proteins was coated and detected by ELISA.

3.3.3 Effects of designed ECM proteins on E13.5 mouse cortical cells

Dissociated E13.5 mouse cortical cells were used to test the effects of designed ECM proteins (ERE, ERE-CBP, and E-CBP) on cell adhesive and neural differentiation.

3.3.3.1 Cell adhesive activity of designed ECM proteins on E13.5 mouse cortical cells

E13.5 mouse cortical cells were seeded (10^6 cells per well) on various protein-coated hydrophobic 24-well plate (ERE, ERE-CBP, E-CBP were designed material, N-cadherin and laminin were used as positive control). Cell adhesive activities were evaluated after 2 days culture using cell counting kit-8 (CCK-8) assay. Briefly, the principle of CCK-8 assay is that dehydrogenase activities in living cells reduces tetrazolium salt contained in CCK-8 kit to give a yellow-color formazan dye which can be detected the absorbance at 450 nm via microplate reader. Therefore, the production of yellow-color formazan dye reflects the number of living cells.

From the result of cell adhesive activities on various materials (Fig 5) showed that cells could adhere on all designed protein-coated plates. Especially, cell adhesive activity on E-CBP showed similar

result as N-Cadherin. ERE showed similar cell adhesive activity as laminin. The RGD (R) part in ERE was derived from laminin. Surprisingly, only CBP sequence alone (E-CBP) was enough for E13.5 cortical cell binding. E-CBP showed almost same call adhesive activity on E13.5 cortical cell as N-cadherin.

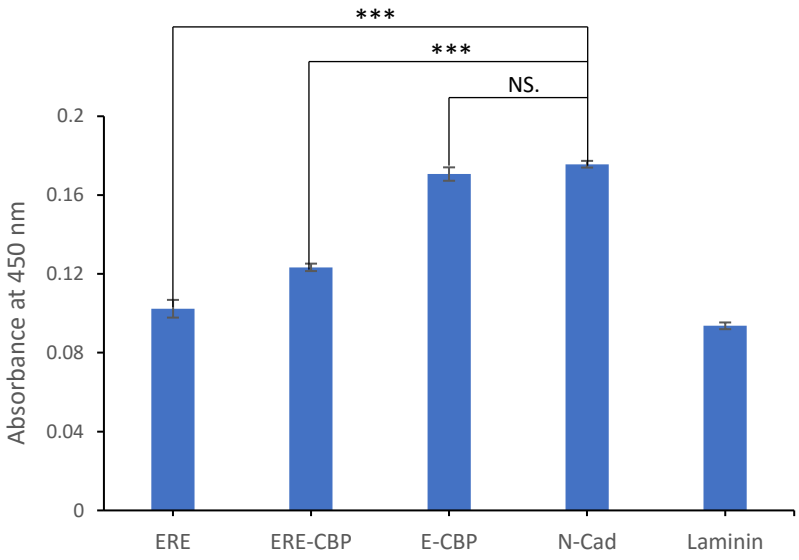

Figure 5: Cell adhesive activity of various materials on E13.5 mouse cortical cells. Cell adhesive activities were evaluated using CCK-8 assay at day2 after seeding cells. Statistically significant differences were indicated for $P < 0.005$ (***), not significant (NS).

3.3.3.2 The effects of designed-proteins on neural differentiation from E13.5 mouse cortical cells

Cortical cells from E13.5 mouse embryo was used to test whether designed material has the effect on neural differentiation as same as N-cadherin. E13.5 mouse cortical cells were seeded 10^6 cells per well on various protein-coated non-treated 24-well plate (ERE, ERE-CBP, E-CBP were designed material, N-cadherin and laminin were used as positive control). After 6 days culture, cell morphology was observed using bright field microscope. From bight-field images (Fig. 6A), cells cultured on ERE-CBP, E-CBP and positive control, N-cadherin, showed similar cell morphologies. They showed neural-like single cells spreading homogeneously. However, cells cultured on ERE-coated plate showed neurite outgrowth from aggregated cells. From the cell morphology image on ERE-coated plate, we could distinguish that cell-adhesive RGD sequence does not have strong cell-binding interaction with E13.5 cortical cells. It was

similar to previous cell result (3.3.3.1) that ERE cell adhesive activity was ~40% less than E-CBP and N-cadherin.

After 10 days culture, real time-PCR assay was performed to analyze neuronal-related RNA expression. The expression of Nestin, neural progenitor cells marker, and β-III tubulin, early neurons marker, were evaluated by real time-PCR. As shown in Fig. 6B, ERE-CBP and E-CBP had the effects on the expression of Nestin and β-III tubulin mRNAs from E13.5 cortical cells similar to N-cadherin, while the cells cultured on ERE expressed Nestin and β-III tubulin lower than cell cultured on N-cadherin.

By comparing the results among designed proteins in this study, E-CBP, which consisted of solely E-/N-cadherin cell-binding sequence, showed similar results in both cell adhesive activity and effects on neural differentiation as N-cadherin. In E13.5 cortical cells, the developing of postmitotic neurons was noticeable in cortical plate region. According to N-cadherin binding site, which expressed in neural cells, were highly detectable in E13.5 cortex, in contrast to decreasing in E-cadherin binding site, which usually occurs in embryonic cells and disappeared in neural differentiating, suggest that cells from E13.5 was differentiating to neural cells[19, 8]. From these facts, we could assume that E-CBP showed higher cell-binding activity and effects on neural differentiation than other designed proteins via N-cadherin binding site. Therefore, E-CBP was chosen as our effective designed protein in cell adhesive and neural-inductive properties on cortical cells. Whereas E-CBP showed the similar effect on E13.5 cortical cells as N-cadherin, it was difficult to conclude that E-CBP has effects on induction of neural differentiation because E13.5 cortical cells had already determined their cell fate by some key factors that regulate specific development stage[20, 21, 22]. Therefore, from these results E-CBP has the effect on cell adhesive activity as N-cadherin, but could not be distinguished that E-CBP has the neural-inductive activity on E13.5 cells.

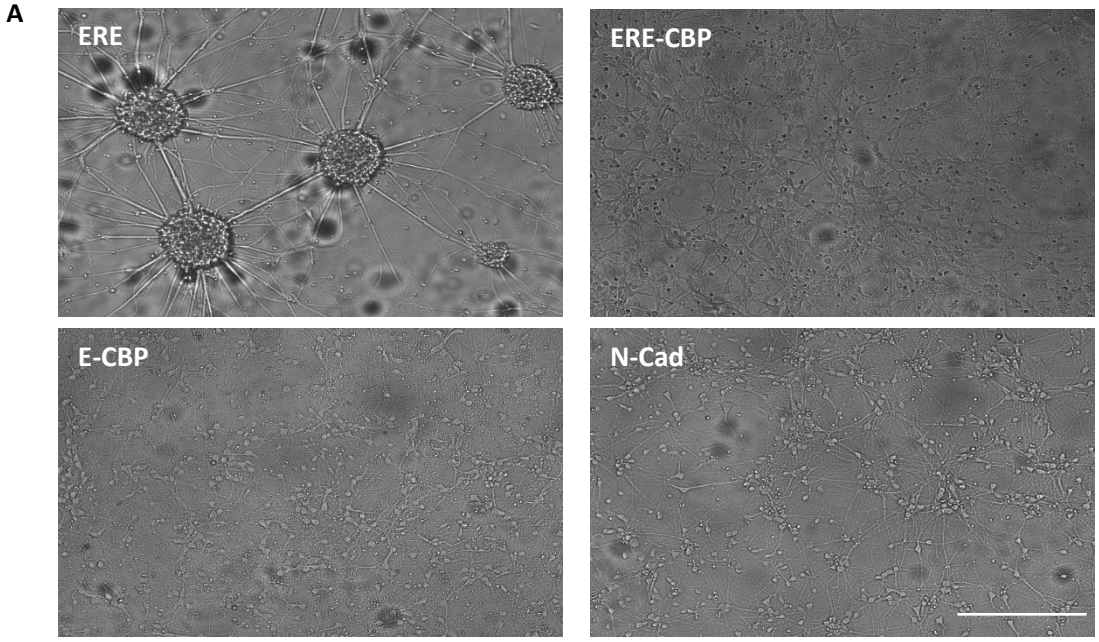

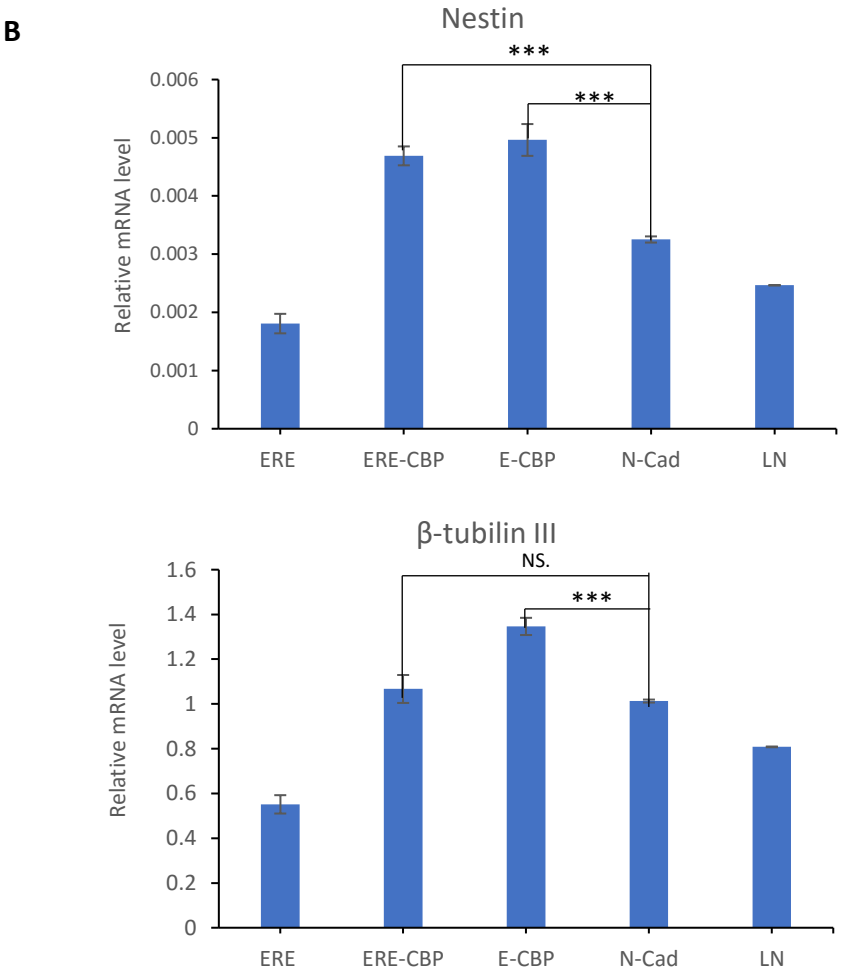

Figure 6: Neural differentiation analysis of E13.5 cortical cells. (A) Cell morphology was observed by light microscope at day 6 after cultured on protein-coated plate. Scale bar 500 μm. (B) Real-time PCR analysis of Nestin and β-III tubulin expression after cultured on designed protein-coated plate for 10 days. Statistically significant differences were indicated for $P < 0.005$ (***), not significant (NS).

To confirm neural-inductive effect of E-CBP, mouse iPS cells, pluripotent stem cells which could be differentiated to all cell in 3 germ layers depends on inductive factor, were used in next experiments to evaluate neural-inductive effects of E-CBP.

3.3.4 Neural Differentiation on E-CBP-coated plate from mouse iPS cells

For neural differentiation from miPS cells, embryoid bodies protocol was used to prepared neural progenitor cells because undifferentiated iPS cells have low affinity to N-cadherin. Experiment design was shown in Fig 7. Mouse iPS cells was cultured in suspension plate for formation of EBs before transfer on designed proteins-coated plate. After 5 days culture in suspension plate for EB formation, EBs were transferred onto protein-coated plate, E-CBP, E12 (as negative control), N-cadherin and laminin (as positive control). EBs were cultured in NDM medium without addition growth factors for 10 days. Finally, neural differentiation from EBs was evaluated by real-time PCR and immunostaining.

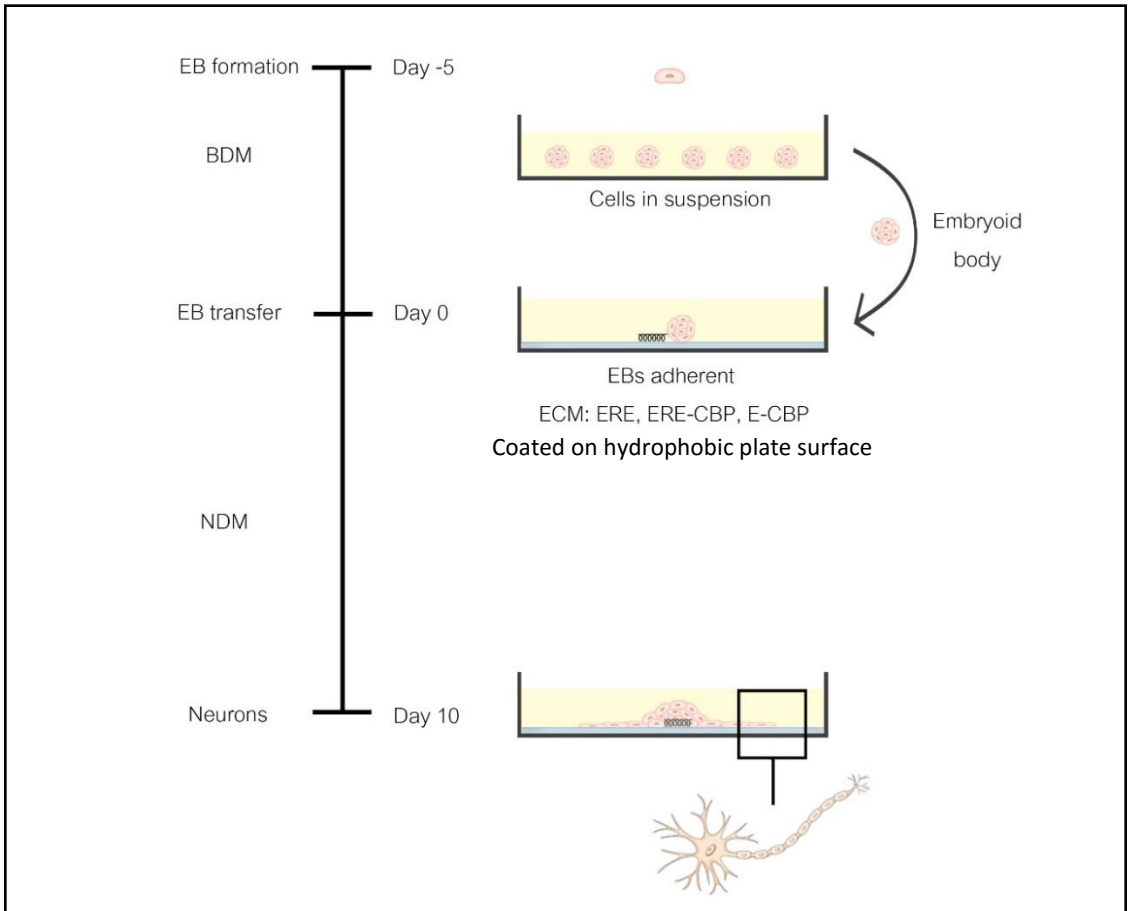

Figure 7: Neuronal differentiation protocol. EBs were forming by cultured in suspension plate and shaken plate in 'T-motion' for 5 days. Then transfer to protein-coated plate and culture for 10 days in NDM medium.

After 2 days EBs transfer onto protein-coated plate, the number of binding EBs were evaluated. To calculate the binding EBs ratio, the number of binding EBs and total EBs were counted respectively. EBs binding percentage on E12 coated plate which was used as negative control showed the lowest binding ratio. The ratio was 5 times smaller than positive control. Therefore, EBs could bind non-specifically on E12, but not significant. Compared to N-cadherin, E-CBP showed the almost same ratio of binding EBs (Fig 8), so EBs could bind well onto E-CBP as N-cadherin.

After 3 days EB transfer, EBs converted to neuron were analyzed as neurite outgrowth from EBs is one of the indicators for the initiation of differentiation. EBs which had neurite outgrowth was counted as converted EBs. Fig 9 showed the conversion ratio of EBs. The results showed no significant differences of EBs conversion ratio among E-CBP, N-cadherin, and laminin. The bright-field images (Fig. 9B) showed the similar morphology of neurite outgrowth from EBs even cultured on different materials. To confirm these observation, real-time PCR for evaluation of neural-related gene expression and immunostaining were performed.

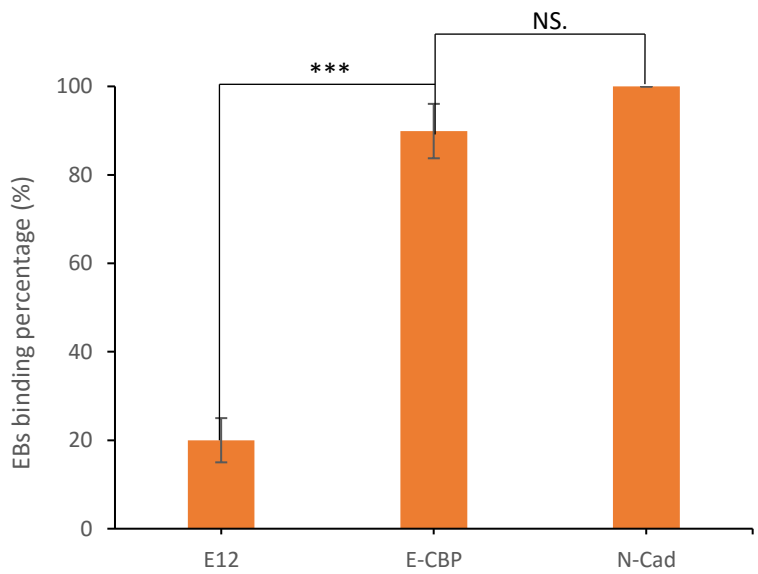

Figure 8: EB binding percentage. After EBs was transferred onto protein coated plate and culture for 2 days, binding EBs was counted compared with total EBs. Statistically significant differences were indicated for $P < 0.005$ (***), not significant (NS).

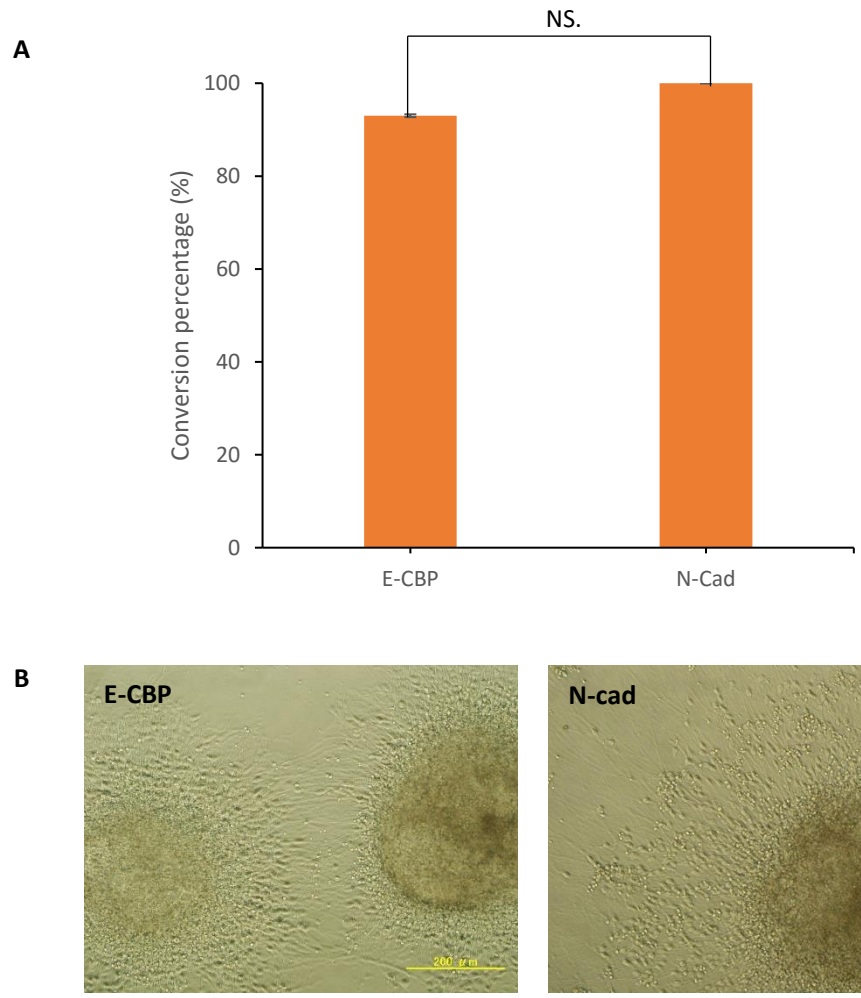

Figure 9: Cell conversion. (A) Cell conversion percentage. After EBs was transferred onto protein coated plate and culture for 3 days, EBs which showed neurite outgrowth was counted compared with total EBs. (B) Bright-field images of neurite outgrowth from EBs cultured on various materials at day 3. Scale bars: 200 μm. Statically significant differences were indicated for $P > 0.05$ (Not significant, NS)

For real-time PCR analysis, total RNA was extracted from EBs after cultured on various material for 10 days. The expression of various neural-related markers were evaluated such as, Nestin (neural progenitor cell marker), β-III tubulin (early neural differentiation marker), MAP-2 (microtubule-associated protein-2; neurons marker), and GAPDH for normalization of amount of cDNA. Nestin expression, EBs on E-CBP was 2 times higher than EBs on N-cadherin, whereas, β-III tubulin expression from EBs on E-CBP was little bit lower than EBs on N-cadherin. MAP-2 expression from E-CBP sample was 2 times higher than N-cadherin sample. Taken together, the ratio of neural-related gene expression from E-CBP was

related to N-cadherin (Fig 10A). Consequently, E-CBP and N-cadherin had neural inductive effect on miPS cells.

For immunostaining, cells were fixed and stained with β-III tubulin and MAP2 antibody after cultured on various materials for 10 days (Fig 10B). Compared to EBs cultured on N-cadherin and laminin, EBs cultured on E-CBP also showed neurite outgrowth morphology in bright-field image and stained with β-III tubulin and MAP2. From the immunostaining results, all neurite outgrowth from EBs which cultured on various materials were stained with β-III tubulin antibody and showed many bundles of neuron. The staining result from MAP2 antibody also showed positive result. Less bundle of MAP2 positive neurons were observed compared to β-III tubulin result. According to real-time PCR result that β-III tubulin expression was higher than expression of MAP2. Therefore, EBs-derived neural cells from this protocol were mostly immature neurons, however, increase in mature neurons can be generated using longer culture period.

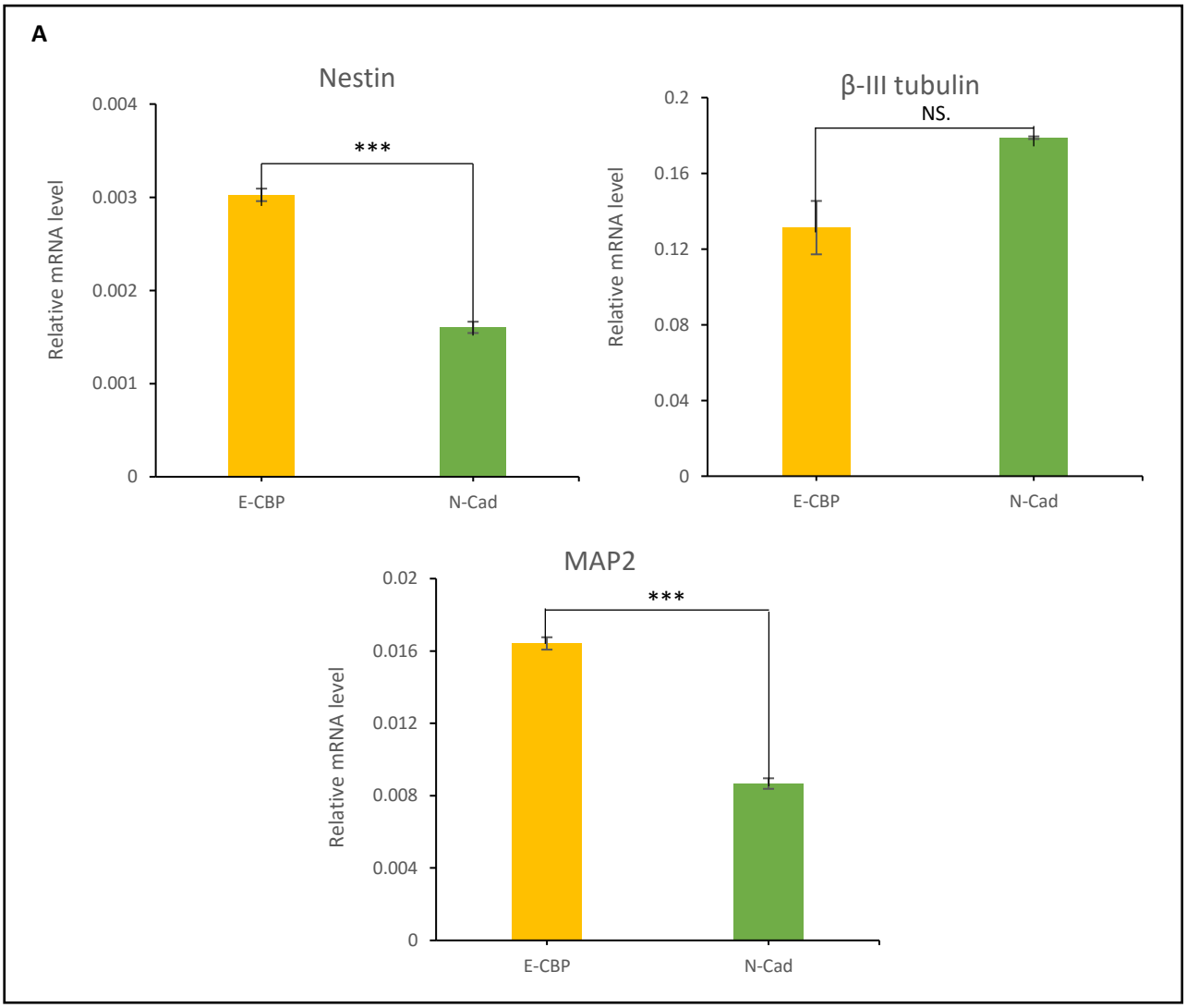

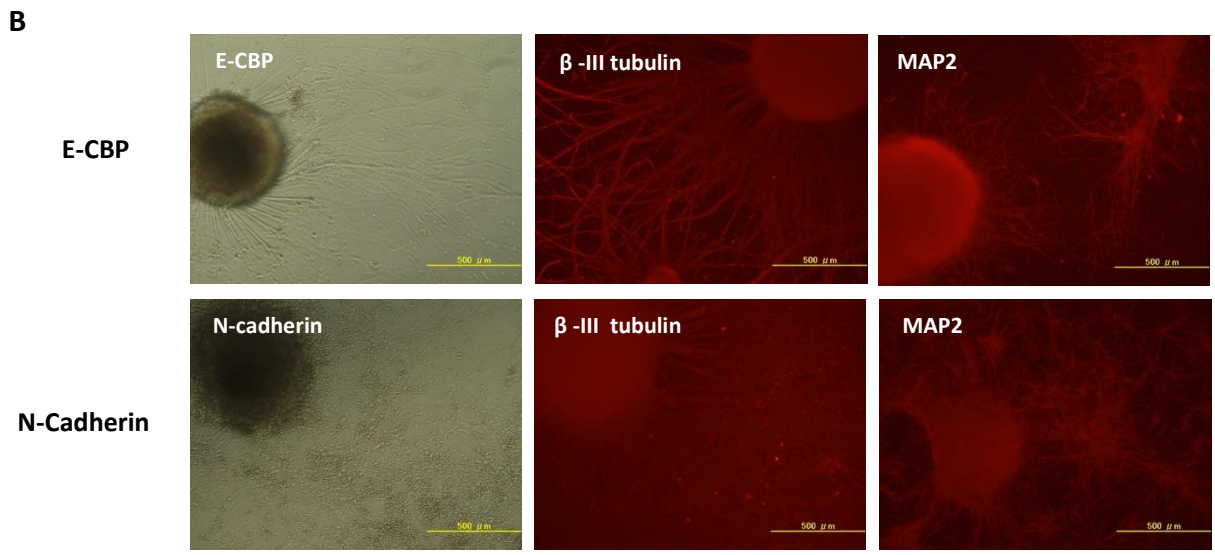

Figure 10: Characterization of neural differentiation. (A) RNA expression from cells which cultured on protein-coated plate was detected using real-time PCR. (B) Immunostaining assay. B-III tubulin and MAP2 were used to detected neural cells. Scale bar 500 µm. Statistically significant differences were indicated for $P < 0.005$ (***), $P > 0.05$ (Not significant, NS).

From the results of real time PCR and immunostaining, it was clarified that E-CBP has the similar effect in cell adhesion activity and neural differentiation as N-cadherin. To further characteristic E-CBP neural-inductive mechanism, E-CBP have to be detected whether induce neural differentiation via signaling pathway as N-cadherin. N-cadherin and Laminin have similar effect in cell adhesion and induction of neural differentiation, while using different mechanism[23]. The function of N-cadherin induced neural differentiation was observed when N-cadherin reduce neural precursor proliferation and induced neural differentiation due to down-regulation of RhoA activity, while Rac1, observed to promoted axonal growth, was activated in cortical cells[24, 25,26]. Whereas, Laminin induced neural differentiation via MAPK/ERK signaling pathway[27, 28]. Despite encouraging data that E-CBP could have cell adhesive activity and neural differentiation on miPS cells, neural-induced signaling pathway had not analyzed yet. One notion was E-CBP is supposed to induce neural differentiation via RhoA suppression and Rac1 activation signaling pathway which can be detected using western blot analysis.

In this study, EB-derived differentiation protocol was used in neural differentiation protocol, however, some undifferentiated miPS cells was retained inside EBs. Therefore, EBs cannot be converted to homogeneous neuron population. To solve this problem, EBs will be dissociated as single cell before

transferred onto E-CBP coated-plate. This is supposed to be better protocol for efficient neural differentiation. Although it is still not completely clear in E-CBP function, SWELYYPLRANL (CBP) sequence shown interesting point in neural differentiation which can be developing to be more effective tools in advance.

3.4 Conclusion

In this study, it was proved that CBP, "SWELYYPLRANL" E-/N-cadherin binding sequence, has neural conversion activity similar to their natural counterpart, N-cadherin. It is suggested that CBP can function as an N-cadherin mimicking peptide for neuro-conversion. The engineered proteins constructed in this study for regulating cellular functions would be useful biomaterials for various applications such as regenerative medicine.

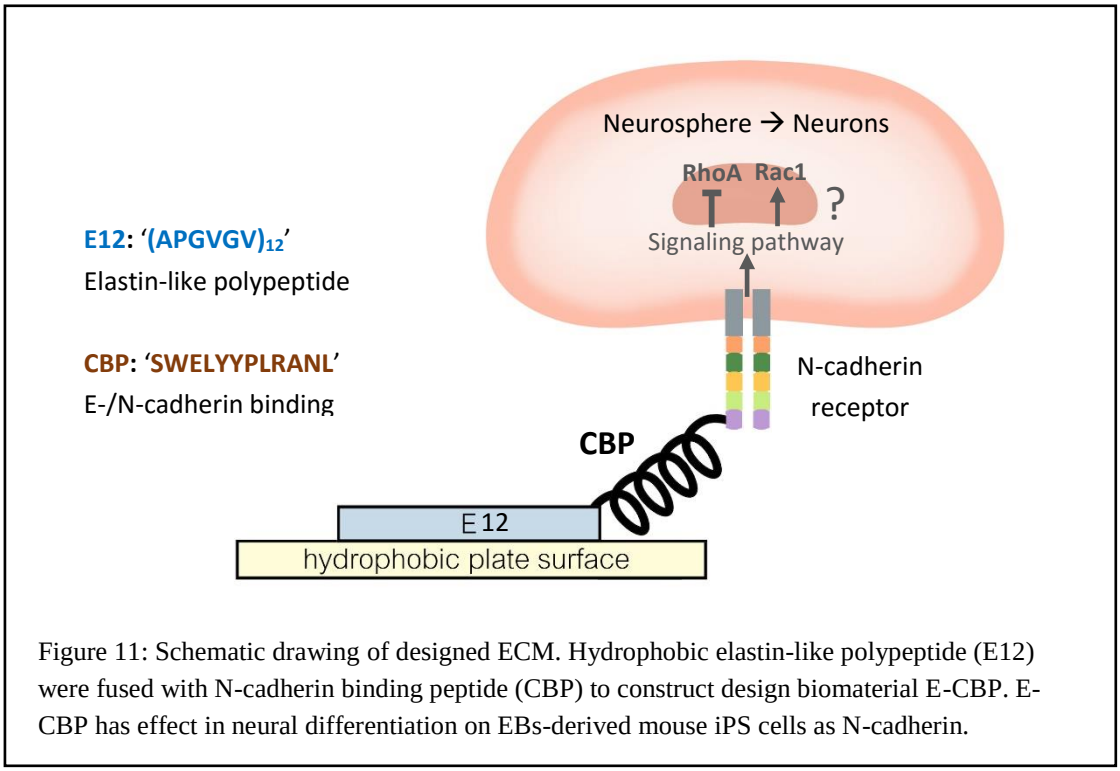

Figure 11: Schematic drawing of designed ECM. Hydrophobic elastin-like polypeptide (E12) were fused with N-cadherin binding peptide (CBP) to construct design biomaterial E-CBP. E-CBP has effect in neural differentiation on EBs-derived mouse iPS cells as N-cadherin.

3.5 References

1. Huebner, E. A., and Strittmatter, S. M. Axon regeneration in the peripheral and central nervous systems. In Cell Biology of the Axon. Springer, 2009, pp. 305–360.
2. Horner, P. J., and Gage, F. H. Regenerating the damaged central nervous system. Nature 407, 6807 (2000), 963–970.
3. Richardson, P., McGuinness, U., and Aguayo, A. Axons from cns neurones regenerate into pns grafts. Nature 284, 5753 (1980), 264–265.
4. Niederost, B., Oertle, T., Fritsche, J., McKinney, R. A., and ¨ Bandtlow, C. E. Nogo-a and myelin-associated glycoprotein mediate neurite growth inhibition by antagonistic regulation of rhoa and rac1. Journal of Neuroscience 22, 23 (2002), 10368–10376.
5. Fournier, A. E., Takizawa, B. T., and Strittmatter, S. M. Rho kinase inhibition enhances axonal regeneration in the injured cns. Journal of Neuroscience 23, 4 (2003), 1416–1423.
6. Gao, X., Bian, W., Yang, J., Tang, K., Kitani, H., Atsumi, T., and Jing, N. A role of n-cadherin in neuronal differentiation of embryonic carcinoma p19 cells. Biochemical and biophysical research communications 284, 5 (2001), 1098–1103.
7. Wang, S., Zhang, Z., Illum, B., Head, B., and Patel, P. Rac1/cdc42-activation enhances expression of total and phosphorylated cav-1 in differentiated human neurons derived from induced pluripotent stem cells (ipscs). The FASEB Journal 31, 1 Supplement (2017), 861–2.
8. Kadowaki, M., Nakamura, S., Machon, O., Krauss, S., Radice, G. L., and Takeichi, M. N-cadherin mediates cortical organization in the mouse brain. Developmental biology 304, 1 (2007), 22–33.
9. Haque, A., Adnan, N., Motazedian, A., Akter, F., Hossain, S., Kutsuzawa, K., Nag, K., Kobatake, E., and Akaike, T. An engineered n-cadherin substrate for differentiation, survival, and selection of pluripotent stem cell-derived neural progenitors. PloS one 10, 8 (2015), e0135170.
10. Matsunaga, M., Hatta, K., and Takeichi, M. Role of n-cadherin cell adhesion molecules in the histogenesis of neural retina. Neuron 1, 4 (1988), 289–295.
11. Miyatani, S., Shimamura, K., Hatta, M., Nagafuchi, A., Nose, A., Matsunaga, M., Hatta, K., and Takeichi, M. Neural cadherin: role in selective cell-cell adhesion. Science 245, 4918 (1989), 631–635.

12. Devemy, E., and Blaschuk, O. W. Identification of a novel dual e-and n-cadherin antagonist. Peptides 30, 8 (2009), 1539–1547.
13. Volk, T., Cohen, O., and Geiger, B. Formation of heterotypic adherens-type junctions between l-cam-containing liver cells and a-camcontaining lens cells. Cell 50, 6 (1987), 987–994.
14. Adnan, N., Mie, M., Haque, A., Hossain, S., Mashimo, Y., Akaike, T., and Kobatake, E. Construction of a defined biomimetic matrix for long-term maintenance of mouse induced pluripotent stem cells. Bioconjugate chemistry 27, 7 (2016), 1599–1605.
15. Schense, J. C., Bloch, J., Aebischer, P., and Hubbell, J. A. Enzymatic incorporation of bioactive peptides into fibrin matrices enhances neurite extension. Nature biotechnology 18, 4 (2000), 415–419.
16. Kobatake, E., Onoda, K., Yanagida, Y., and Aizawa, M. Design and gene engineering synthesis of an extremely thermostable protein with biological activity. Biomacromolecules 1, 3 (2000), 382–386.
17. Kurosawa, H. Methods for inducing embryoid body formation: in vitro differentiation system of embryonic stem cells. Journal of bioscience and bioengineering 103, 5 (2007), 389–398.
18. Desbaillets, I., Ziegler, U., Groscurth, P., and Gassmann, M. Embryoid bodies: an in vitro model of mouse embryogenesis. Experimental physiology 85, 6 (2000), 645–651.
19. Stocker, A. M., and Chenn, A. Differential expression of alphae-catenin and alpha-n-catenin in the developing cerebral cortex. Brain research 1073 (2006), 151–158.
20. Ohnuma, S.-i., Philpott, A., and Harris, W. A. Cell cycle and cell fate in the nervous system. Current opinion in neurobiology 11, 1 (2001), 66–73.
21. Kim, S., Lehtinen, M. K., Sessa, A., Zappaterra, M. W., Cho, S.-H., Gonzalez, D., Boggan, B., Austin, C. A., Wijnholds, J., Gambello, M. J., et al. The apical complex couples cell fate and cell survival to cerebral cortical development. Neuron 66, 1 (2010), 69–84.
22. McConnell, S. K., and Kaznowski, C. E. Cell cycle dependence of laminar determination in developing neocortex. Science 254, 5029 (1991), 282–285.
23. Bixby, J. L., and Zhang, R. Purified n-cadherin is a potent substrate for the rapid induction of neurite outgrowth. The Journal of Cell Biology 110, 4 (1990), 1253–1260.

24. Gao, X., Bian, W., Yang, J., Tang, K., Kitani, H., Atsumi, T., and Jing, N. A role of n-cadherin in neuronal differentiation of embryonic carcinoma p19 cells. Biochemical and biophysical research communications 284, 5 (2001), 1098–1103.
25. Wang, S., Zhang, Z., Illum, B., Head, B., and Patel, P. Rac1/cdc42-activation enhances expression of total and phosphorylated cav-1 in differentiated human neurons derived from induced pluripotent stem cells (ipscs). The FASEB Journal 31, 1 Supplement (2017), 861–2
26. Haque, A., Adnan, N., Motazedian, A., Akter, F., Hossain, S., Kutsuzawa, K., Nag, K., Kobatake, E., and Akaike, T. An engineered n-cadherin substrate for differentiation, survival, and selection of pluripotent stem cell-derived neural progenitors. PloS one 10, 8 (2015), e0135170.
27. Mruthyunjaya, S., Manchanda, R., Godbole, R., Pujari, R., Shiras, A., and Shastry, P. Laminin-1 induces neurite outgrowth in human mesenchymal stem cells in serum/differentiation factors-free conditions through activation of fak–mek/erk signaling pathways. Biochemical and biophysical research communications 391, 1 (2010), 43–48.
28. Campos, L. S., Leone, D. P., Relvas, J. B., Brakebusch, C., Fassler, R., Suter, U., et al. ¨ β1 integrins activate a mapk signalling pathway in neural stem cells that contributes to their maintenance. Development 131, 14 (2004), 3433–3444.

Chapter 4: Construction of Biomimetic ECM for Astrocyte Differentiation from Mouse Induced Pluripotent Stem Cells

4.1 Introduction

In the present, regenerative central nervous system (CNS) is concerned to be challenged and overcome the limited in regeneration after injury in adult[1]. An understanding of factors which influence neurite outgrowth is critical for the development of therapeutics to promote CNS regeneration. In the past, researches were biased in neural, but recently the important role from astrocyte in CNS was shown[2]. Astrocytes are abundant cell types in CNS and play important roles in many essential complex functions, such as maintain cellular homeostasis, supplies energy to neurons, and involving in neural synapse formation, in the healthy CNS[3]. Therefore, understanding the functional roles of astrocyte in CNS in normal and abnormal conditions could be the useful for understating more in brain function, promoting neural regeneration, and modulating disease processes.

In chapter 3, the effects of our designed ECM (E-CBP) for neural differentiation from mouse iPS cells were evaluated compared to N-cadherin and laminin. Addition to these results, we found interesting result from real-time PCR. EBs on laminin showed the similar effects in neural differentiation on N-cadherin, however EBs on laminin showed higher GFAP (astrocyte marker) expression compared to EBs on N-cadherin (Fig 1). Therefore, laminin was expected to be suitable substrate for astrocyte differentiation compared to N-cadherin. Moreover, other research also showed that laminin has ability to enhance neurite outgrowth and migration[4, 5]. However, the bioavailability of laminin is limited according batch-batch composition variation and cause in irreproducible result. Thus, the application of synthetic peptide mimic natural extracellular matrix offers several advantages for construction of biomaterials[6].

Various cell adhesion molecules (CAMs) derived from laminin are known for their ability to bind and induce differentiation of stem cells towards neural lineages[7]. Among these laminin-derived CAMs sequence, pentapeptides, ‘IKVAV’ (Ile-Lys-Val-Ala-Val) found in laminin α-chain[8, 9] and ‘YIGSR’ (Try-Ile-Gly-Ser-Arg)[10] found in laminin β1-chain, were focused because of their activities for cell adhesion via integrin, cell migration and enhancement of neural lineage.

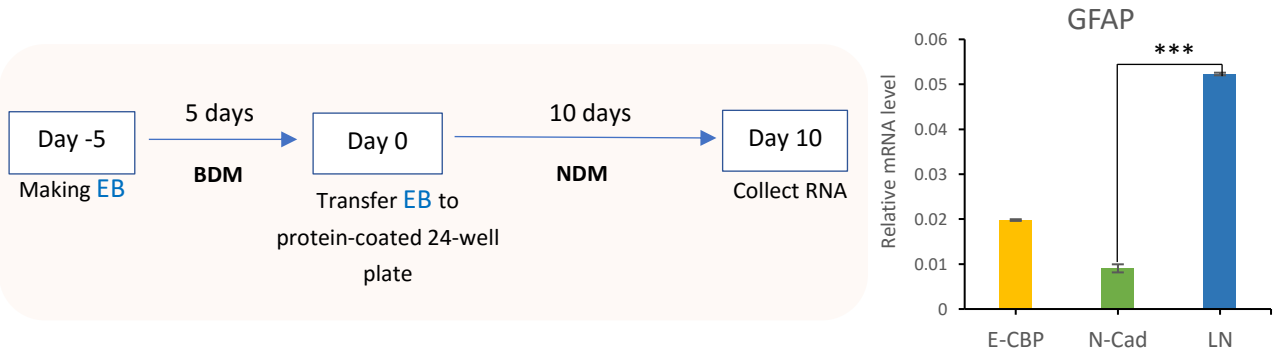

Figure 1: Real-time PCR analysis of differentiation to neural lineage. After 5 days culture in suspension plate for EB formation, EBs were transferred onto material-coated plate. EBs were culture in NDM medium without addition growth factors for 10 days. Then the result was evaluated by real-time PCR using GFAP marker. Statistically significant differences were indicated for $P < 0.005$ (***).

In this study, designed ECM proteins containing laminin-derived CAMs sequences, IKVAV and YIGSR, were constructed for induction of astrocyte differentiation. The designed ECM consisted of functional units; elastin-derived unit, $(APGVGV)_{12}$ (E), as a stable structural unit and laminin-derived CAMs, IKVAV (I) or/and YIGSR (Y) sequence, as active functional units. Therefore, the designed ECM proteins, EI, EY, and EIEY, were hypothesized to recapitulate the complicated biological effects as natural laminin.

Here, the substrate properties in cell adhesive activity of designed ECMs (EI, EY, and EIEY) and effects on astrocyte differentiation from mouse iPS cells were evaluated.

4.2 Materials and Methods

4.2.1 Plasmid construction

Four different plasmids, pET32c-NHis-E12, pET32c-NHis-E12-IKVAV, pET32c-NHis-E12-YIGSR, pET32c-NHis-E12-IKVAV-E12-YIGSR, were used in this experiment. Each plasmids were constructed for expression of designed ECM proteins, E12, EI, EY, and EIEY, respectively. Plasmid construction protocols for pET32c-NHis-E12 and pET32c-NHis-E12-IKVAV have been described elsewhere[11, 12].

For construction of pET32c-NHis -YIGSR, the synthetic oligonucleotide encoding YIGSR (Table 1) was introduced to the 3' end of E12 sequence in pET32c-NHis-E12, by digested with EcoR I (Takara) and Bgl II (Takara). Then YIGSR encoding DNA fragment containing BamH I and EcoR I sites were ligated with digested pET32c-NHis-E12-YIGSR[13].

For construction of pET32c-NHis-E12-IKVAV-E12-YIGSR plasmid, first pET32c-NHis-E12-IKVAV plasmid was digested with EcoR I and Bgl II. Then, the E12-YIGSR insert was digested from pET32c-NHis-E12-YIGSR with BamH I and EcoR I. Finally, the E12-YIGSR fragment was ligated with digested pET32c-NHis-E12-IKVAV plasmid.

Table 1: Oligomer sequences used for construction of EY plasmid

Plasmid		Sequence (5'-3')
EY	Forward oligomer	GATCCTAGATCCTGGCTACATAGGTTCGCGAAAGATCTTGTG
	Reverse oligomer	AATTCACAAGATCTTTCGCGAACCTATGTAGCCAGGATCTAG

4.2.2 Protein expression and purification

The constructed four plasmids, pET32c-NHis-E12, pET32c-NHis-E12-IKVAV, pET32c-NHis-E12-YIGSR, pET32c-NHis-E12-IKVAV-E12-YIGSR were transfected into *E.coli* BL21(DE3) competent cells for expression of proteins. Transformed *E.coli* cells were culture Luria-Bertani (LB) medium containing 50 μg/ml ampicillin and incubated at 37°C until OD reach at 0.6. Protein expression was induced by addition of 1 mM isopropyl β-D-1-thiogalactopyranoside (IPTG). Cells were cultured overnight at 30°C and harvested by centrifugation and resuspended in BugBuster Reagent (Novagen) with Benzonase Nuclease (Sigma-Aldrich). After 30 min rotation at room temperature, the sample was sonicated for 20 min at 4°C. Then, the sample was separated between supernatant (soluble fraction) and inclusion bodies (insoluble fraction) by centrifugation and supernatant was collected. The supernatant was applied to His-Select Nickel Affinity Gel (Sigma-Aldrich) followed by incubation at 4°C for 1 h. After

washing with phosphate buffer (50 mM sodium phosphate, 300 mM NaCl, pH 8.0), proteins were eluted by phosphate buffer with 200 nM imidazole. The resultant protein solution was dialyzed using Slide-A-Lyzer Dialysis Cassettes (Pierce) against phosphate-buffered saline (PBS). The concentrations of the purified proteins were measured using BCA assay (Thermo Scientific) according to the manufacturer's instruction.

4.2.3 Adsorption of constructed proteins on hydrophobic plates

These four types of protein, E12, EI, EY, and EIEY, consisted of E12 motif which had a highly hydrophobic property allowing these targeted proteins adsorb onto the hydrophobic surface of the plate. From this property, these proteins were added to 96-well suspension culture plate (Sumilon, MS-8096R) in varied concentrations from 0 mM to 1000 mM and incubated for 1 h at 37°C. Plates were washed with PBS including 0.05% Tween 20 (PBS-T) followed by addition of Blocking One reagent (Nacalai Tesque, Inc.) overnight at 4°C. After washing with PBS-T, anti-polyhistidine antibody (Sigma-Aldrich) was added to the plate and incubated for 1 h at 37°C followed by washing with PBS-T again. Then, anti-mouse IgG peroxidase conjugate (Sigma-Aldrich) was added and incubated for 1h at 37°C. After washing with PBS-T, TMB peroxidase substrate (KPL, Inc.) was added to the plate. Finally, 1 M HCl was added to stop the reaction and the absorbance at 450 nm was measured by a microplate reader.

4.2.4 mouse iPS cell culture

Standard mouse iPSC line APS0002-iPS-MEF-Ng-178B-5 obtained from RIKEN BRC was used in this experiment. The culture media was composed of DMEM (Wako) supplemented with 15% fetal bovine serum (Hyclone, Thermo Scientific), 1% nonessential amino acids (NEAA, Gibco), 0.1 mM 2-mercaptoethanol (Sigma), 1000 U/mL penicillin and 100 µg/mL streptomycin (Gibco), and 1000 U/mL Leukemia inhibitory factor (LIF) (Wako).

Mouse iPS cells were cultured on MMC treated STO cells as feeder cells. Before culturing miPS cells, MMC treated STO cells were prepared as follows. The SNL76/7 (STO) cells were cultured on

gelatin coated dishes and when cells reached around 90% confluency, cells were treated with 10 µg/mL of mitomycin C contained in DMEM. After treatment for 3-4 h, plates were washed with PBS and the MMC treated STO cells were trypsinized and collected. MMC treated STO cells were cultured on gelatin coated 60 mm dish at a density 10^6 cells/plate. One day after MMC treated STO cells culture, 10^4 cells of miPS cells were seeded to the plates and the medium was changed to the culture medium for miPS cells. Cells were cultured in a humidified incubator with 5% CO_2 at 37°C for 3-4 days on feeder cells before further passage.

4.2.5 Induction of Astrocyte differentiation from miPS cells

miPS cells were cultured in suspension plate with basal differentiation medium (BDM) in the absence of anti-differentiation factors such as LIF and feeder cells to form Embryoid bodies (EBs). EB is the multicellular three-dimension structure which mimic post-implantation embryonic tissues and has the ability to differentiate into all three germ layers; ectoderm, mesoderm, endoderm [14,15]. EBs were formed by culturing miPS cells at $5x10^4$ cells/well in 6-well suspension culture plate using basal differentiation media (BDM). BDM was composed of Glassgow Minimum Essential Medium (GMEM, Wako), supplemented with 10% KSR (Gibco), 1 mM sodium pyruvate (Gibco), 1% nonessential amino acids (Gibco), 0.1 mM 2-mercaptoethanol (Sigma), 1000 U/mL penicillin and 100 µg/mL streptomycin (Gibco) and 0.5 µM Retinoic acid. Suspension plate was shaken with shaker in `T-motion' to control cell shape and size. BDM media was changed at day 3 of EBs formation.

After 5 days of EBs formation, EBs were transferred to non-treated 24-well plate (Iwaki) coated with designed proteins. To prepare protein-coated plate, non-treated 24 well plate was coated with each protein, 1000 nM EI, 1000 nM EY and 1000 nM EIEY (250 µl/well) and incubated at 37°C for 1h. After incubation, protein-coated wells were washed with PBS before addition of cells. EBs were transferred to protein-coated well (approximately 50 EBs per well) and cultured in Astrocyte differentiation medium (ADM) which composed of Neurobasal® medium (NB, Gibco), 1% B-27® supplement minus vitamin A (Gibco)and 1% GlutaMAX^{TM} supplement (Gibco) supplemented with 10 ng/ml bFGF, 10 ng/ml EGF, and

10 ng/ml CNTF. After 10 days of culture, medium was changed to ADM supplemented with only 10 ng/ml CNTF and culture for more 10 days. Medium was changed every 3 days.

4.2.6 Immunostaining

Cells were fixed with 4% paraformaldehyde for 15 min at room temperature and then washed with 1% PBS 3 times followed by incubation with PBS including 0.2% Triton X for 3 min. After washed with PBS 2 times, 1% bovine serum albumin (BSA) was added and incubated for 1 h. Then primary antibody was added to samples. In this experiment, monoclonal GFAP (GA5) antibody produced in mouse (Cell Signaling Technology) for glial fibrillary acidic protein (GFAP) was used. Primary antibody was diluted in PBS including 1% BSA in 1:500 ratio and incubated for 1 h. After washed with PBS 3 times, secondary antibody, Rabbit anti-mouse IgG Alexa Flour 568 (1:500, diluted in PBS including 1% BSA) and Hoechst 33258 solution (1:2000, diluted in PBS including 1 % BSA) were added and incubated for 1 h, then washed with PBS 2 times. Finally, samples were observed by using fluorescence microscopy.

4.2.7 Quantitative PCR Analysis

Total RNA was extracted using the RNeasy Mini kit (Qiagen, Valencia, CA) according to the manufacturer's instruction. Using 2.5 μg of total RNA in 20 μl reaction buffer, cDNA was synthesized by using SuperScript^{TM} III Reverse Transcriptase (Thermo Fisher) primed with oligo-dT according to the manufacturer's instruction. Quantitative real-time PCR was performed with the FastStart essential DNA green master (Roche), which consisted of FastStart Taq DNA polymerase and double-stranded DNA specific SYBR green I dye by using LightCycler® Nano instrument (Roche) and the data were analyzed by its software. The expression of astrocyte-related markers (S100β and GFAP) were normalized against expression of GAPDH in same sample. All reactions were done in duplicate. The primers used in this experiment was listed in Table 2.

Table 2: List of primers using in quantitative PCR.

Primers		Sequence (5'-3')
GAPDH	Forward	ATCTTCTTGTGCAGTGCCAGCCSTCGTCCCG
	Reverse	AGTTGAGGTCAATGAAGGGGTCGTTGATGG
S100β	Forward	CTGGAGAAGGCCATGGTTGC
	Reverse	CTCCAGGAAGTGAGAGAGCT
GFAP	Forward	GGAGAGGGACAACTTTGCAC
	Reverse	GCTCTAGGGACTCGTTCGTG

4.2.8 Statistical Analysis

Values are given as mean value ± standard deviation. Statistical analysis was performed by independent two-sample *t*-test with equal valiances. Values of $P < 0.05$ were considered to be statistically significant.

4.3. Result and discussion

4.3.1. Design and expression of EI, EY, and EIEY

Four different plasmids, pET32c-NHis-E12, pET32c-NHis-E12-IKVAV, pET32c-NHis-E12-YIGSR, and pT32c-NHis-E12-IKVAV-E12-YIGSR, were used for protein expression (Fig 2). Expressed proteins were named E12, EI, EY, and EIEY , respectively.

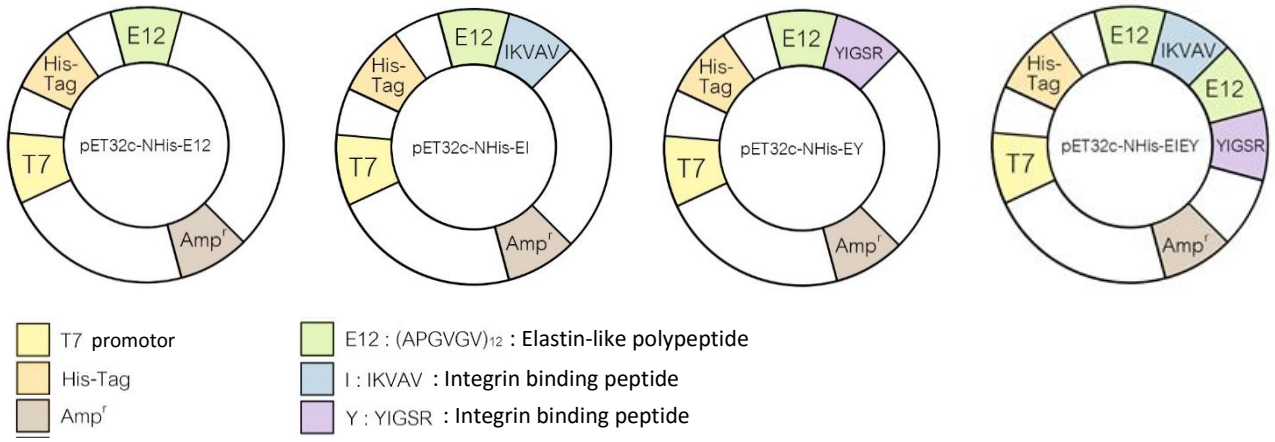

Figure 2: Plasmid construction. pET-32c-NHis-E12, pET32c-NHis-EI, pET32c-NHis-EY, and pET32c-NHis-EIEY. The fusion proteins were under T7 promotor and for purification processes His-Tag region was fused before the position of protein of interest.

Expressed proteins were purified by nickel affinity gel using His-Tag. All proteins were purified from soluble fraction. The size of designed proteins were confirmed by SDS-PAGE (15% acrylamide) which shown in Fig 2. The calculated molecular weight of E12, EI, EY, and EIEY proteins were 8.2 kDa, 9.9 kDa, 9.4 kDa, and 17.3 kDa respectively. However, the band of our design proteins appeared slightly above the expected molecular weight. It is suggested that the physicochemical characteristics of the ELPs presence self assembling hydrophobic region during SDS-PAGE process.

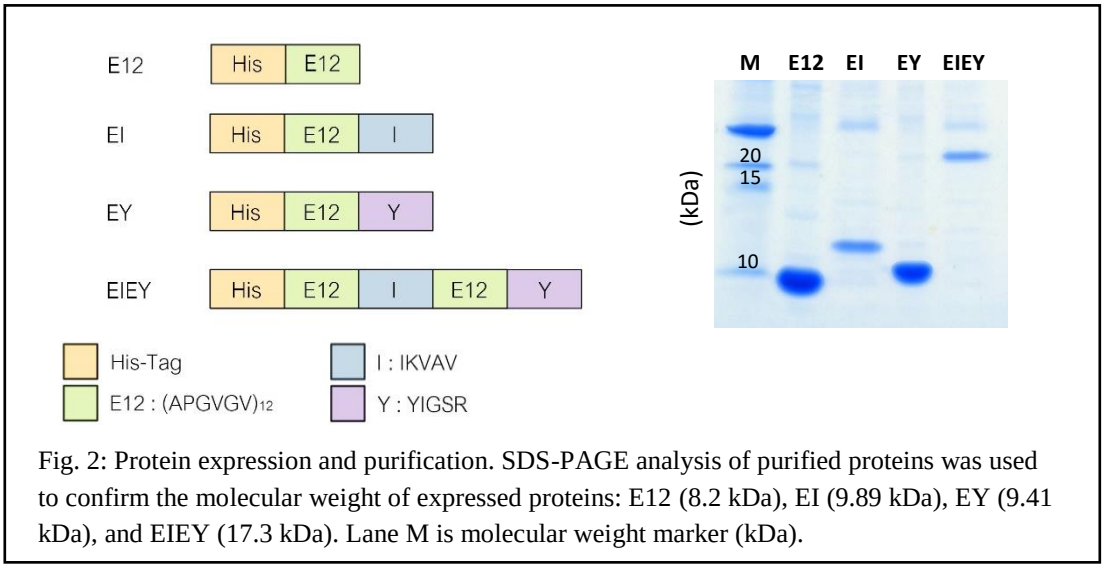

Fig. 2: Protein expression and purification. SDS-PAGE analysis of purified proteins was used to confirm the molecular weight of expressed proteins: E12 (8.2 kDa), EI (9.89 kDa), EY (9.41 kDa), and EIEY (17.3 kDa). Lane M is molecular weight marker (kDa).

4.3.2 Adsorption of constructed protein on the hydrophobic surface of plate

These four-types of protein, E12, EI, EY, and EIEY consisted of E12 (12 repeat of APGVGV sequence) motif which has a highly hydrophobic property allowing these proteins absorbed on hydrophobic surface[11]. These proteins were fused to His-tag at C-terminal of proteins therefore the saturated concentration of each protein adsorbed on hydrophobic surface could be detected by ELISA using anti-polyhistidine antibody. The saturated concentration of each proteins was used for coating hydrophobic plate. As shown in Figure 3, the saturation concentration of EI, EY, and EIEY proteins adsorbed on hydrophobic plate surface were all 1000 nM. These were same as the saturation concentration of E12 protein shown in chapter 2. The result showed the same saturation concentration for all proteins, however each protein showed the different amount of adsorbed proteins. These results could be explained due to the different types of peptide sequences.

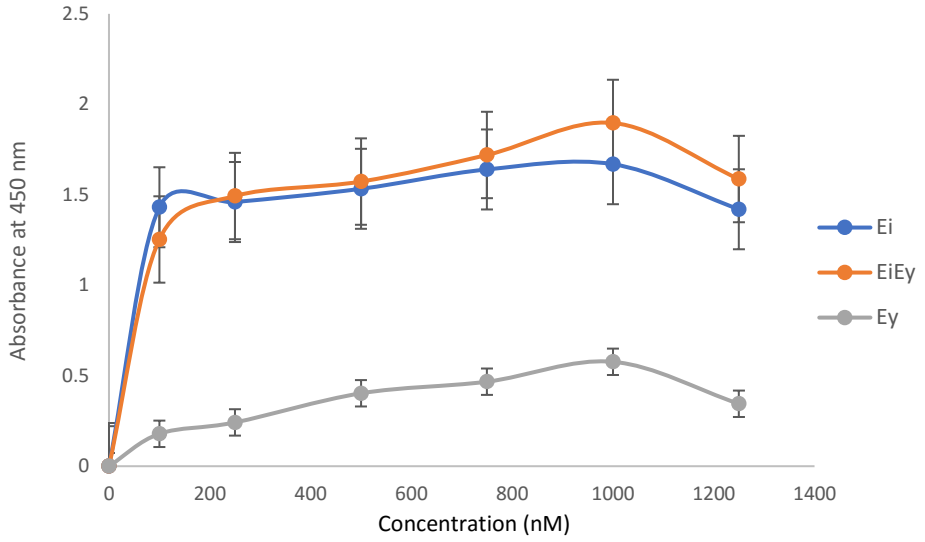

Fig. 3: Adsorption of EI, EY, and EIEY on the hydrophobic surface of plate. Various concentration of proteins were coated on the surface of suspension culture plate, then the saturated-protein adsorbed on surface was detected by ELISA.

4.3.3 Astrocyte differentiation on designed ECMs-coated plate from mouse iPS cells

Next, we tested whether our designed ECM proteins, EI, EY, and EIEY, have same effects on cell binding and differentiation as laminin.

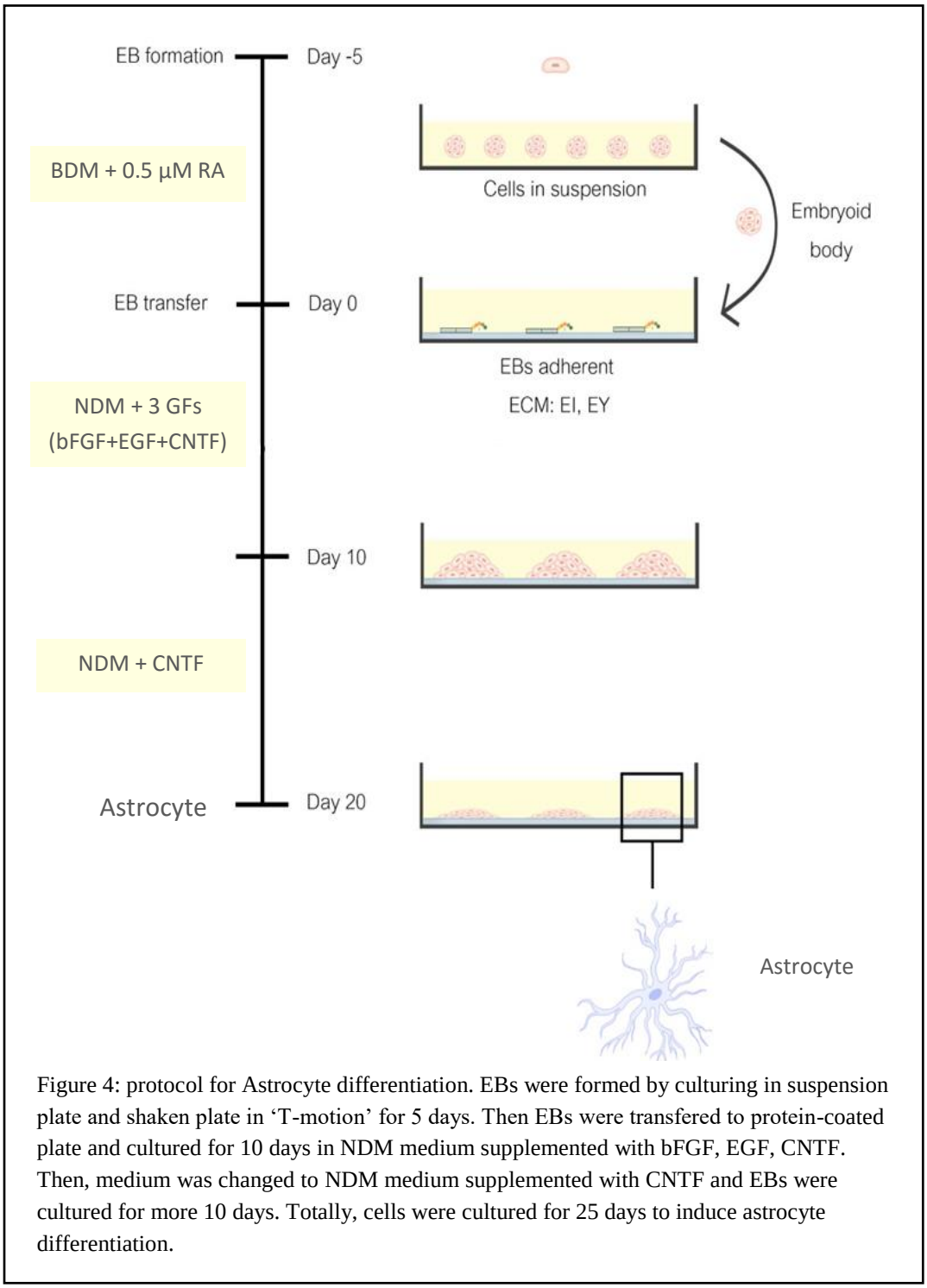

Figure 4: protocol for Astrocyte differentiation. EBs were formed by culturing in suspension plate and shaken plate in 'T-motion' for 5 days. Then EBs were transfered to protein-coated plate and cultured for 10 days in NDM medium supplemented with bFGF, EGF, CNTF. Then, medium was changed to NDM medium supplemented with CNTF and EBs were cultured for more 10 days. Totally, cells were cultured for 25 days to induce astrocyte differentiation.

For astrocyte differentiation from miPS cells, EBs were formed to prepared neural progenitor cells. The size of EBs formed in suspension plate for 5 days were controlled around 150-250 µm (Fig 5). After transfer of EBs onto EI, EY and EIEY-coated 24-well plates, EBs were cultured in NDM medium supplemented with bFGF, EGF, and CNTF. After 10 days, medium was changed to NDM medium

supplemented with only CNTF for more 10 days. Finally, astrocyte differentiation from EBs was evaluated by real-time PCR and immunostaining.

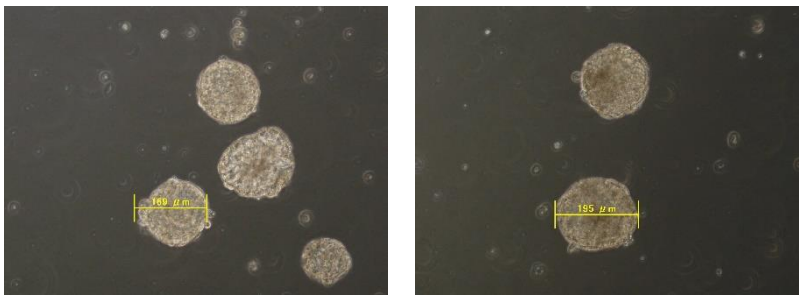

Figure 5: The images of EBs formed by culturing in suspension plate with shake for 5 days. The size of EBs were controlled around 150-250 μm. From these images, 169 μm EB (Left) and 195 μm EB (right).

4.3.3.1 EBs-derived miPS cell adhesion activity on design ECMs-coated plate

After 2 days of EBs transfer onto protein coated-plate, binding EBs on these proteins were evaluated. To calculate the binding EBs ratio, the number of binding EBs and total EBs were counted respectively. E12 and Laminin coated plates were used as negative and positive control. As shown in figure 6, the binding percentage of EBs on E12 showed the lowest binding ratio. The ratio was 5 times smaller than positive control. It was suggested EBs could bind non-specifically on E12, but not significant. Compared to E12, EI showed higher ration of EBs binding and it was almost same as that of Laminin (Fig 5). On the other hand, EBs binding on EY and EIEY showed lower binding ratio than Laminin. From these result, EI is suitable for EBs culture compared to EY or EIEY. Therefore, EI was chosen for next experiment.

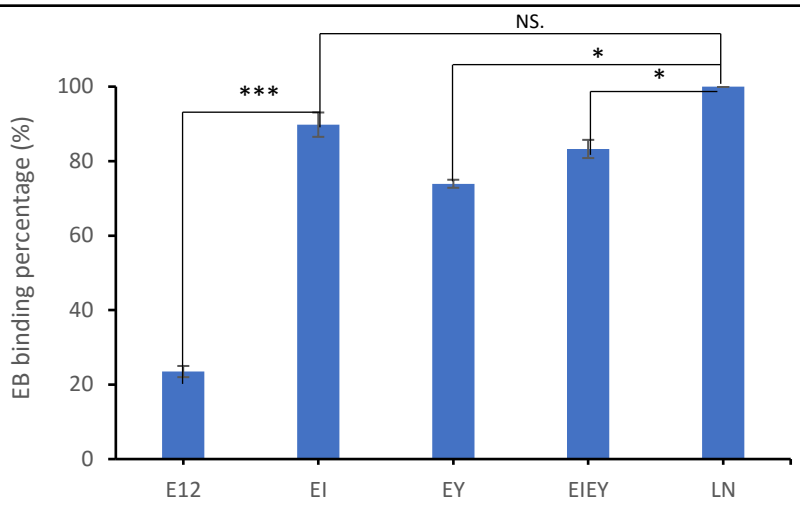

Figure 6: EB binding percentage. After EB was transferred onto protein coated plate (E12, EI, EY, EIEY) and culture for 2 days, binding EBs was counted compared to total EBs. Laminin (LN) coated plate was used as positive control. Statistically significant differences were indicated for $P < 0.05$ (*) and $P < 0.005$ (***).

4.3.3.2 Astrocyte differentiation in various protocol

In the present, various astrocyte differentiation protocols were reported[16, 17, 18], however the effective protocol has been still developed. Our purpose in this study is to test the effect of laminin-derived sequence, IKVAV and YIGSR, in our designed ECM proteins for astrocyte differentiation. In here, three different protocols (Fig 7) were selected from various research and tested whether which protocol was suitable for induction of astrocyte differentiation on the designed ECM proteins.

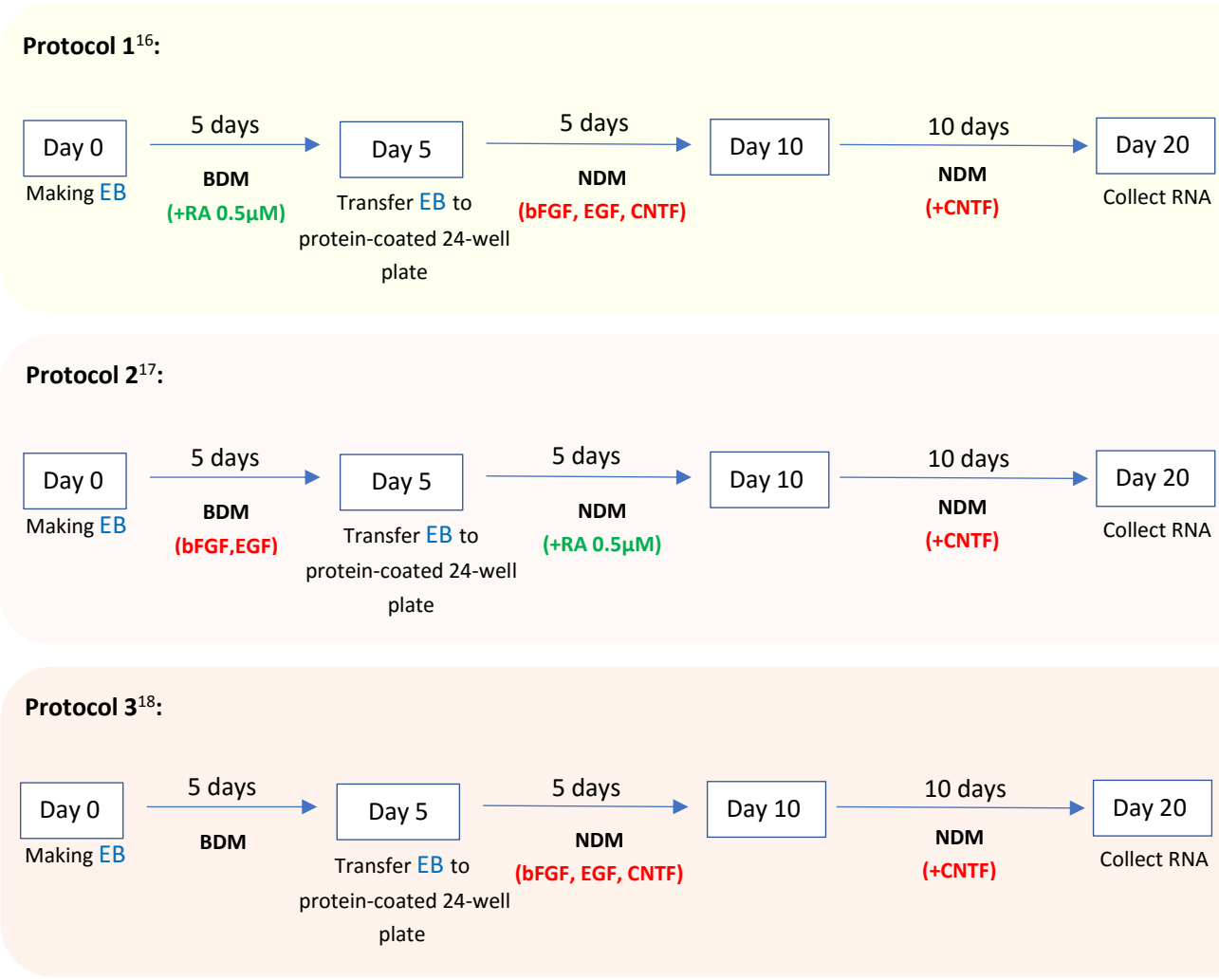

Figure 7: Various astrocyte differentiation protocol was tested with our design ECMs (EI, EY and EIEY).

To clarify the best protocol among three, EBs on EI coated plates were culture in 3 different protocols. After transfer of EBs onto EI coated plate, EBs were cultured in each protocol for 15 days. Astrocyte differentiation was evaluated by real-time PCR. Total RNA was extracted from EBs after cultured on EI in various astrocyte differentiation protocol for 15 days. The expression of various astrocyte-related marker, S100β (astroglial progenitor marker) and GFAP (glail fibrillary acidic protein; astrocyte marker), and GAPDH for normalization of amount of cDNA were evaluated. For S100β expression, EBs on EI cultured in each protocol showed similar expression, however GFAP expression of culture with protocol 1 showed the highest expression among three different protocols. Taken together, protocol 1 was selected as suitable astrocyte differentiation protocol for evaluation of designed ECMs.

4.3.3.3 Astrocyte differentiation on design ECM-coated plate

As mentioned above, protocol 1 was selected for evaluation of astrocyte differentiation from EBs cultured on various designed ECMs. Briefly, mouse iPS cells were cultured in suspension plate for formation of EBs before transfer on designed ECMs-coated plate, EI, EY, EIEY and laminin (as positive control). EBs were culture in NDM medium supplemented with bFGF, EGF and CNTF growth factors for 10 days. Later, NDM medium supplemented with only CNTF was used to cultur for more 10 days (Fig 4). Finally, astrocyte differentiation from EBs was evaluated by real-time PCR.

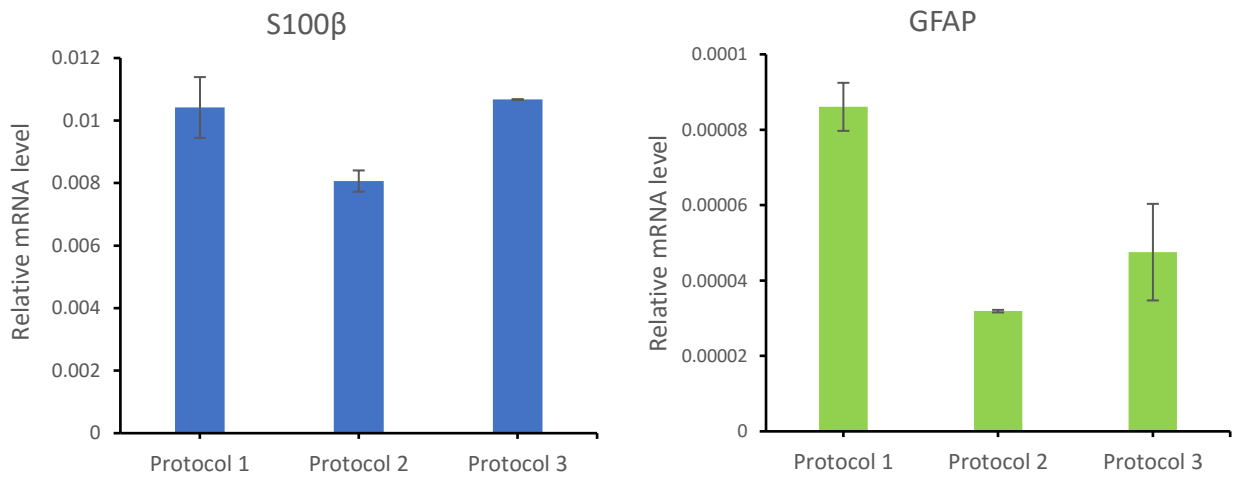

Figure 8: Astrocyte differentiation from various culture protocol. EBs was transferred onto **EI** coated hydrophobic plate and culture in various protocol for 15 days. The result was analyzed using astrocyte-related marker in real-time PCR.

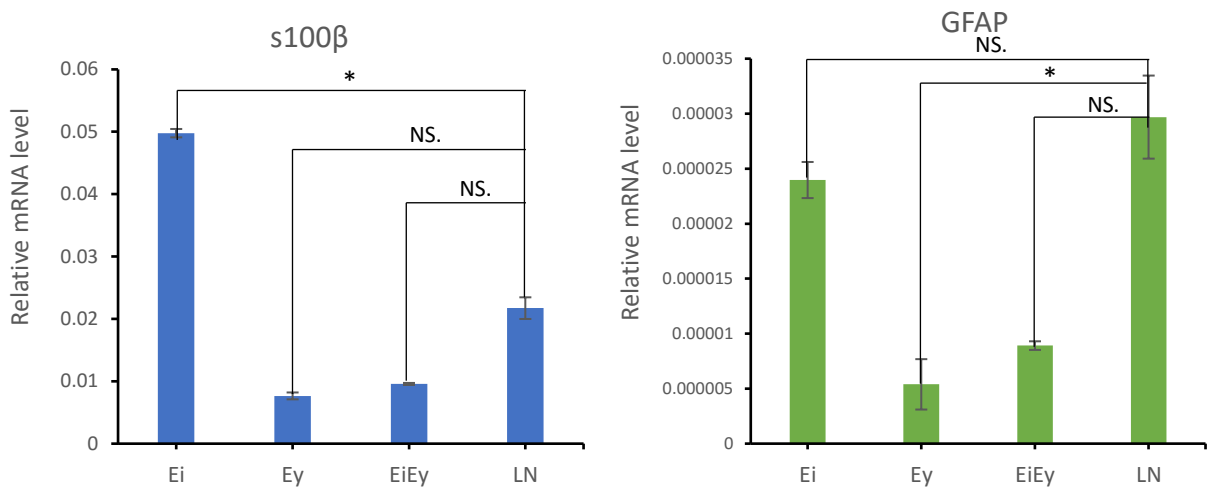

Figure 9: Astrocyte differentiation analysis of EBs cultured on designed ECMs. Real-time PCR analysis of S100β and GFAP expression after 20 days culture on designed ECMs coated plate. Statistically significant differences were indicated for $P < 0.05$ (*) and $P < 0.005$ (***). Not significant (NS).

After transfer of EBs onto various designed ECMs (EI, EY, and EIEY) coated plate, EBs were cultured for 20 days followed by evaluation of the expression of astrocyte-related marker. As shown in figure 9, EBs cultured on EI showed the highest expression in both S100β and GFAP expression, compared to EY and EIEY. However, the GFAP expression from EBs on EI was little bit lower than EBs on laminin. From these results, it was clarified that EI has the particular effects on astrocyte differentiation almost same as laminin.

4.3.3.4 Evaluation the effect of CNTF o astrocyte differentiation

In most of astrocyte differentiation protocols, ciliary neurotrophic factor (CNTF) was added to induce astrocyte differentiation. Therefore, this experiment was done to determine whether the addition of ciliary neurotrophic factor (CNTF) had the effect on astrocyte differentiation from mouse iPS cells, additionally to confirmed the effect in astrocyte differentiation from design ECM (EI).

Experiment design was similar to protocol shown in figure 4, but with and without CNTF was tested. Mouse iPS cells was cultured in suspension plate for formation of EBs before transfer on designed protein-coated plate. After 5 days cultured in suspension plate for EB formation, EBs were transferred onto EI and laminin (as positive control). EBs were cultured in NDM medium supplemented with bFGF, EGF

and with or without CNTF for first 10 days. Then, EBs were cultured in NDM medium supplemented with or without CNTF. Finally, astrocyte differentiation from EBs was evaluated by immunostaining.

For result analysis using immunostaining, cells were fixed and stained with GFAP and β-III tubulin antibody after cultured on EI and laminin using medium with or without CNTF for 20 days (Fig 10). To compared between EBs cultured in medium with CNTF and without CNTF, EBs cultured in medium with CNTF showed higher GFAP positive cells than cultured in medium without CNTF on both EI and laminin coated plate. In contrast to β-III tubulin, EBs cultured in medium with CNTF showed rarely number of β-III tubulin positive cells. From the result of immunostaining, it was clarified that our design protein, EI showed the similar effect as laminin. EI and laminin could induce differentiation to neural lineage from EBs-derived mouse iPS cells, whereas addition of CNTF enhanced astrocyte differentiation. For further characterized of astrocyte differentiation, real-time PCR using astrocyte and neural-related marker have to be analyzed. Looking ahead, it will be interesting to coupled growth factors, bFGF, EGF, and CNTF, into more complex extracellular matrix that may induce astrocyte differentiation spontaneously.

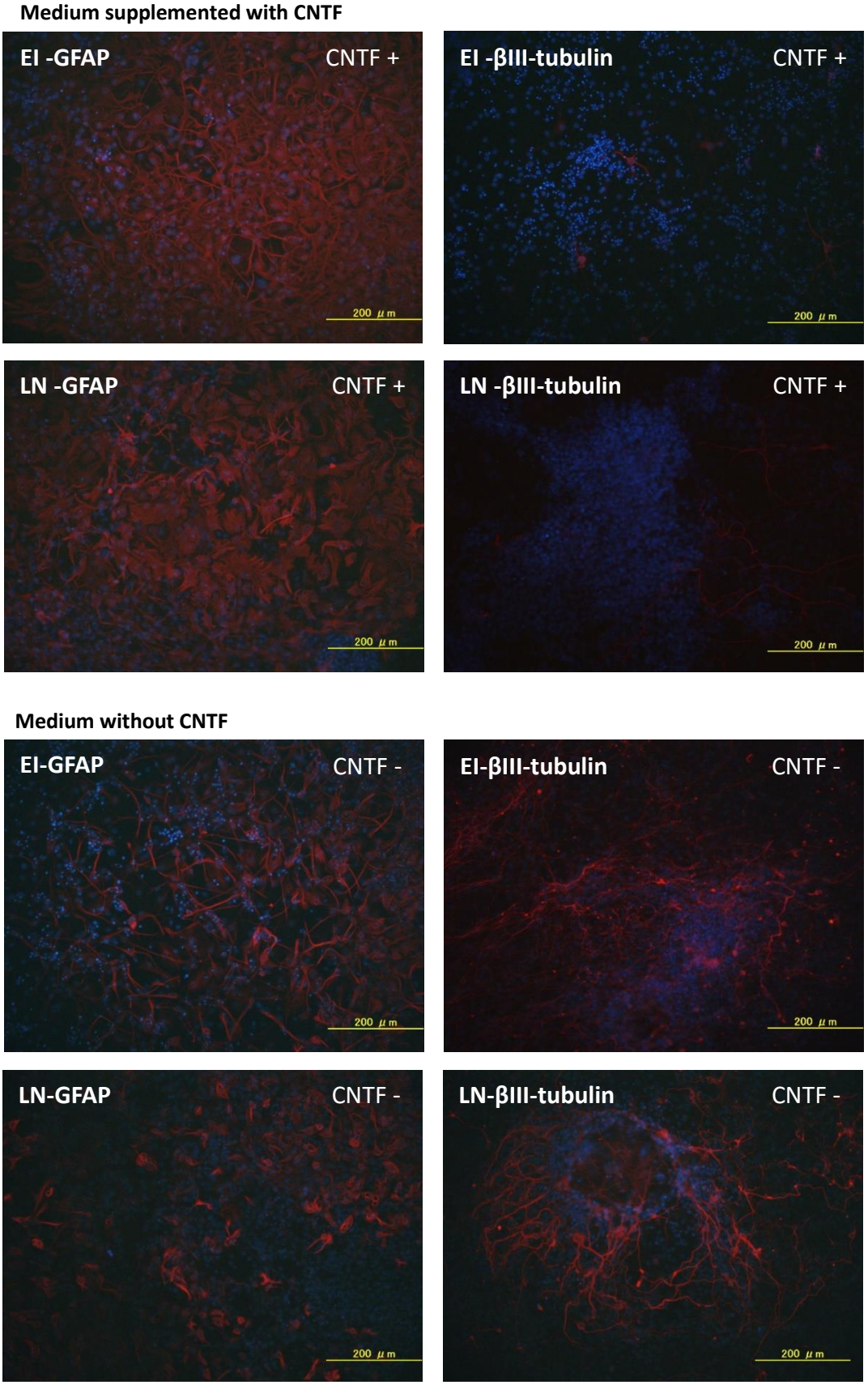

Figure 10: Immunostaining assay. After EBs was cultured for 20 days in medium with or without CNTF, the result was analyzed by immunostaining. GFAP and βIII-tubulin were used to detected astrocyte and neural cells, respectively. Scale bar 200 μm.

4.4 Conclusion

In this study, it was proved that 'IKVAV', laminin α chain-derived CAMs sequence, has EBs adhesion activity and show the effect on cell culture protocol for astrocyte similar as laminin. However, to construct more favorable material outcome is likely to be achieved by combining 'IKVAV' with other laminin-functional domain and coupled with growth factors in order to better recapitulate the multiplicity of biologic information encoded within the natural extracellular matrix. Thus, the concept of biomaterials created from engineered proteins provide various useful applications such as regenerative medicine and tissue engineering.

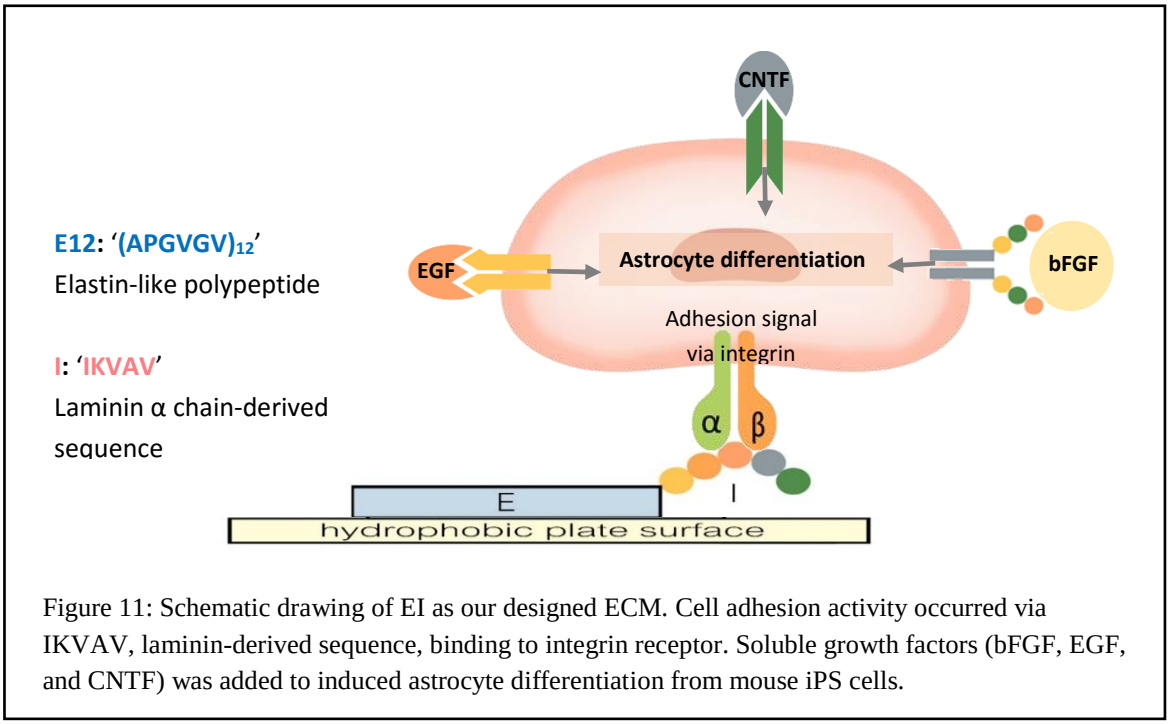

Figure 11: Schematic drawing of EI as our designed ECM. Cell adhesion activity occurred via IKVAV, laminin-derived sequence, binding to integrin receptor. Soluble growth factors (bFGF, EGF, and CNTF) was added to induced astrocyte differentiation from mouse iPS cells.

4.5 Reference

1. Chandrasekaran, A., Avci, H. X., Leist, M., Kobolak, J., and ´ Dinnyes, A. ´ Astrocyte differentiation of human pluripotent stem cells: new tools for neurological disorder research. Frontiers in cellular neuroscience 10 (2016).
2. Crompton, L. A., Cordero-Llana, O., and Caldwell, M. A. Astrocytes in a dish: Using pluripotent stem cells to model neurodegenerative and neurodevelopmental disorders. Brain Pathology 27, 4 (2017), 530–544.
3. Sofroniew, M. V., and Vinters, H. V. Astrocytes: biology and pathology. Acta neuropathologica 119, 1 (2010), 7–35.
4. Laura, M., Leipzig, N. D., and Shoichet, M. S. Promoting neuron adhesion and growth. Materials today 11, 5 (2008), 36–43.
5. Hall, P. E., Lathia, J. D., Caldwell, M. A., et al. Laminin enhances the growth of human neural stem cells in defined culture media. BMC neuroscience 9, 1 (2008), 71.
6. Bellis, S. L. Advantages of rgd peptides for directing cell association with biomaterials. Biomaterials 32, 18 (2011), 4205–4210.
7. Schense, J. C., Bloch, J., Aebischer, P., and Hubbell, J. A. Enzymatic incorporation of bioactive peptides into fibrin matrices enhances neurite extension. Nature biotechnology 18, 4 (2000), 415–419.
8. Sephel, G., Tashiro, K., Sasaki, M., Greatorex, D., Martin, G., Yamada, Y., and Kleinman, H. Laminin a chain synthetic peptide which supports neurite outgrowth. Biochemical and biophysical research communications 162, 2 (1989), 821–829.
9. Sephel, G., Tashiro, K., Sasaki, M., Greatorex, D., Martin, G., Yamada, Y., and Kleinman, H. Laminin a chain synthetic peptide which supports neurite outgrowth. Biochemical and biophysical research communications 162, 2 (1989), 821–829.
10. Graf, J., Iwamoto, Y., Sasaki, M., Martin, G. R., Kleinman, H. K., Robey, F. A., and Yamada, Y. Identification of an amino acid sequence in laminin mediating cell attachment, chemotaxis, and receptor binding. Cell 48, 6 (1987), 989–996.

11. Kobatake, E., Onoda, K., Yanagida, Y., and Aizawa, M. Design and gene engineering synthesis of an extremely thermostable protein with biological activity. Biomacromolecules 1, 3 (2000), 382–386.
12. Nakamura, M., Mie, M., Mihara, H., Nakamura, M., and Kobatake, E. Construction of multi-functional extracellular matrix proteins that promote tube formation of endothelial cells. Biomaterials 29, 20 (2008), 2977–2986.
13. Nakamura, M., Mie, M., Nakamura, M., and Kobatake, E. Construction of multi-functional extracellular matrix proteins that inhibits migration and tube formation of endothelial cells. Biotechnology letters 34, 8 (2012), 1571–1577.
14. Kurosawa, H. Methods for inducing embryoid body formation: in vitro differentiation system of embryonic stem cells. Journal of bioscience and bioengineering 103, 5 (2007), 389–398.
15. Desbaillets, I., Ziegler, U., Groscurth, P., and Gassmann, M. Embryoid bodies: an in vitro model of mouse embryogenesis. Experimental physiology 85, 6 (2000), 645–651.
16.] Krencik, R., and Zhang, S.-C. Directed differentiation of functional astroglial subtypes from human pluripotent stem cells. Nature protocols 6, 11 (2011), 1710–1717.
17. Sareen, D., Gowing, G., Sahabian, A., Staggenborg, K., Paradis, R., Avalos, P., Latter, J., Ornelas, L., Garcia, L., and Svendsen, C. N. Human induced pluripotent stem cells are a novel source of neural progenitor cells (inpcs) that migrate and integrate in the rodent spinal cord. Journal of Comparative Neurology 522, 12 (2014), 2707–2728.
18. Emdad, L., D'Souza, S. L., Kothari, H. P., Qadeer, Z. A., and Germano, I. M. Efficient differentiation of human embryonic and induced pluripotent stem cells into functional astrocytes. Stem cells and development 21, 3 (2011), 404–410.

Chapter 5: Conclusion

Conclusions:

In the present, tissue engineering techniques have been developed and require effective materials. One perspective for constructing biomimetic materials are multi-functional designs to create a natural niche-like cellular microenvironment where cell interact with other cells, extracellular matrix, and signaling molecules. Mimicking these interactions, which is similar to natural extracellular matrix, in designed biomaterials can facilitate the desired regulation.

The aim of this thesis is to generate multi-functional ECMs providing proper environments for cell differentiation and maintenance to be grown and functionalized.

In the present study, designed ECM proteins which have similar abilities in purpose to natural ECMs were developed. The main strategy for designing ECM proteins relies on the combination of 2 units; a stable structural unit and an active functional unit. Elastin-like polypeptide, $(APGVGV)_{12}$, (E), which can bind to hydrophobic surfaces was used as stable structural unit [(1)] in all of my experiments. Various kinds of active functional units that regulate cellular functions were fused to structural units (Fig.1). Furthermore, growth factors were tethered to the ECM proteins for induction of proliferation and differentiation of cells without addition of any soluble growth factors. This combination is expected to be a strategy for the construction of efficient multi-functional ECMs.

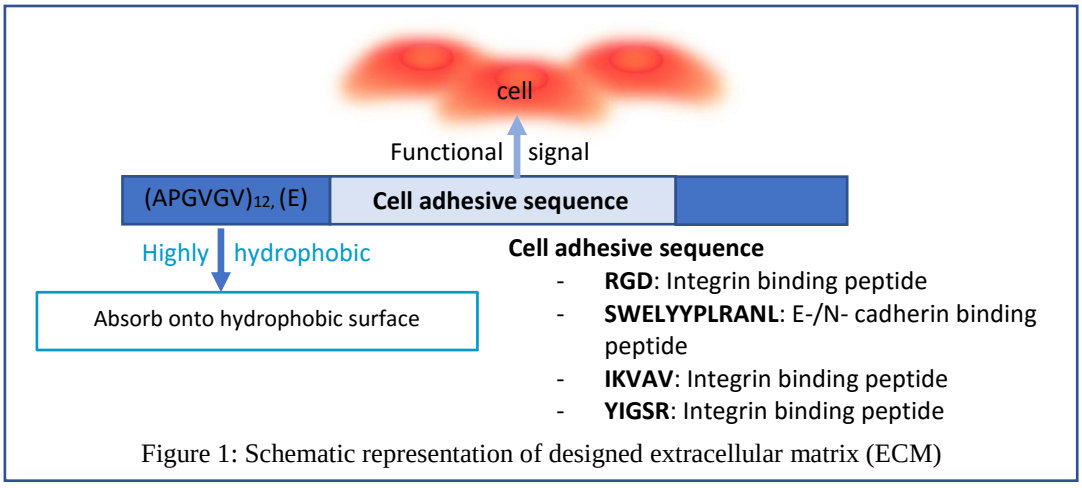

Figure 1: Schematic representation of designed extracellular matrix (ECM)

In chapter 2, immobilized growth factor into ECMs was proposed to achieved multi-functional material and also controllable release of growth factor. Here, bFGF-tethered ECM protein via electrostatic

interaction was constructed. When the soluble growth factors were applied, it was difficult to control their local concentrations due to diffusion, cell uptake, and degradation. To overcome such problems, the strategy of tethering growth factors to designed ECMs was applied. bFGF has a highly basic amino acid domain in its heparin binding region, so I focused on this property of bFGF for tethering to the designed ECM (ERE-D20). For tethering bFGF, a polyaspartic domain (D20), 5 repeats of 4 aspartic acids and serine, was introduced to designed ECM, ERE, which consists of elastin-like polypeptide (E) as a structural unit and cell adhesive RGD sequence as an active functional unit (Fig 2). Cells cultured on bFGF-tethered ERE-D20 were well attached and grown without addition of soluble bFGF. Addition of bFGF inhibitor proved that bFGF tethered to ERE-D20 induced cell proliferation. From these results, bFGF-tethered designed ECM via electrostatic interaction, could be an alternative method to construct efficient multi-functional ECMs.

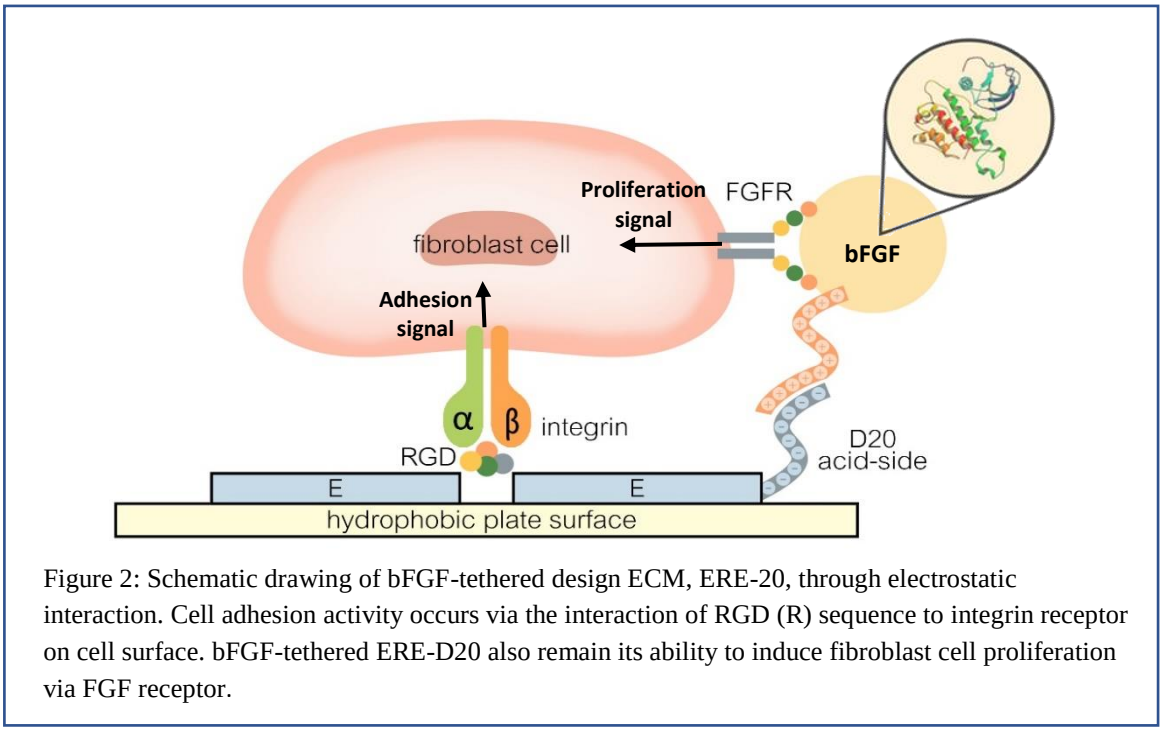

Figure 2: Schematic drawing of bFGF-tethered design ECM, ERE-20, through electrostatic interaction. Cell adhesion activity occurs via the interaction of RGD (R) sequence to integrin receptor on cell surface. bFGF-tethered ERE-D20 also remain its ability to induce fibroblast cell proliferation via FGF receptor.

In chapter 3, N-cadherin which is well studied in neural cell-cell adhesion activity and have ability in induction of neurite outgrowth, was focused for induction of neural differentiation from mouse iPS cells. N-cadherin binding peptide was expected to enhance neural differentiation due to the down regulation of

Rho/ROCK signaling. Due to this property, N-cadherin binding peptide was fused to the structural unit, E12, for construction of neural inductive designed ECM protein.

The designed ECM protein (E-CBP) that contains elastin-derived unit (E), $(APGVGV)_{12}$, as a stable structural unit and E-/N- cadherin binding peptide (CBP), SWELYYPLRANL [(2)], as an active functional unit was developed (Fig 3). As it is known that N-cadherin induces neural differentiation from miPSCs [(3)], here CBPs have been characterized for their capability to mimic N-cadherin in the neural differentiation. The designed ECM protein consisting of E-CBP was shown to promote the neural differentiation of miPSCs without exogenous neuro-inductive signals. Embryoid bodies (EB) of miPSCs were transferred onto E-CBP coated plates and 10 days later the samples were analyzed. From these results, it was proved that CBP has neural conversion activity similar to their natural counterpart, N-cadherin. It is suggested that CBP can function as an N-cadherin mimicking peptide for neuro-conversion

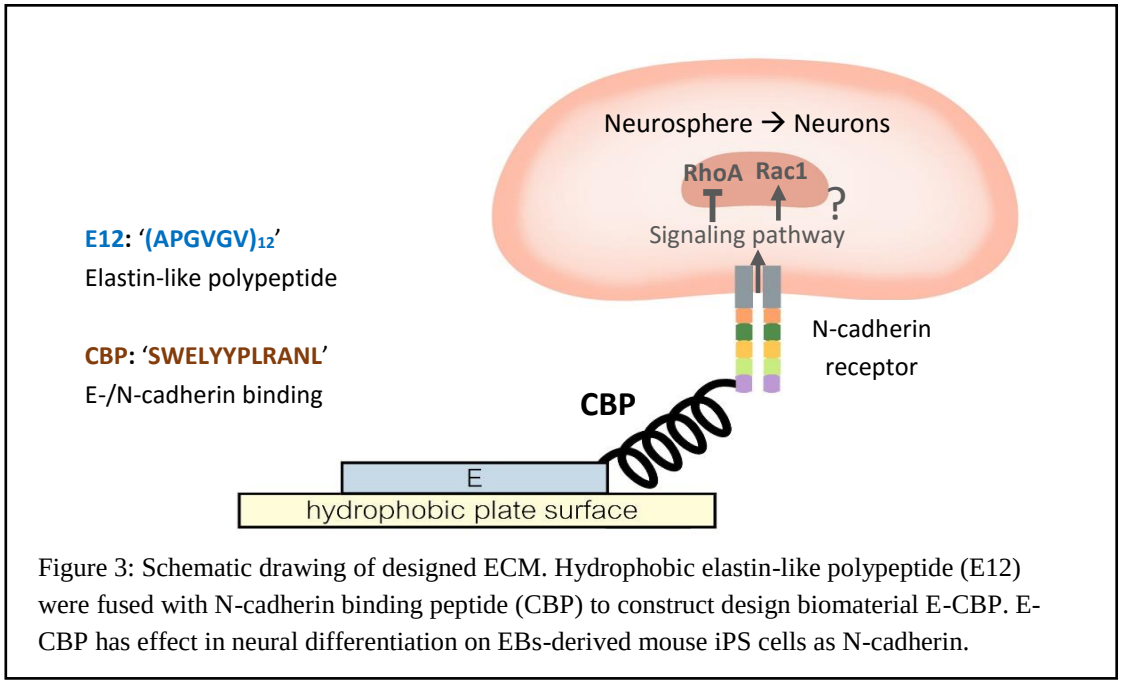

Figure 3: Schematic drawing of designed ECM. Hydrophobic elastin-like polypeptide (E12) were fused with N-cadherin binding peptide (CBP) to construct design biomaterial E-CBP. E-CBP has effect in neural differentiation on EBs-derived mouse iPS cells as N-cadherin.

Finally, the designed ECM proteins for astrocyte differentiation from miPSCs were constructed. The designed ECM proteins (EI, EY, and EIEY) that contain stable structural unit (E) and active functional units, IKVAV (I)[(4)] and YIGSR (Y)[(5)], were constructed. EBs were transferred onto EI, EY, and EIEY coated plates and soluble CNTF and bFGF were added to culture medium. After 20 days culture,

inductions of astrocyte differentiation were evaluated by immunostaining. From these results, combination of the designed ECM protein and CNTF acts instructively for differentiation of miPSCs to an astrocyte fate. Therefore, CNTF-tethered designed ECM protein can be expected to be an efficient multi-functional ECM for astrocyte differentiation.

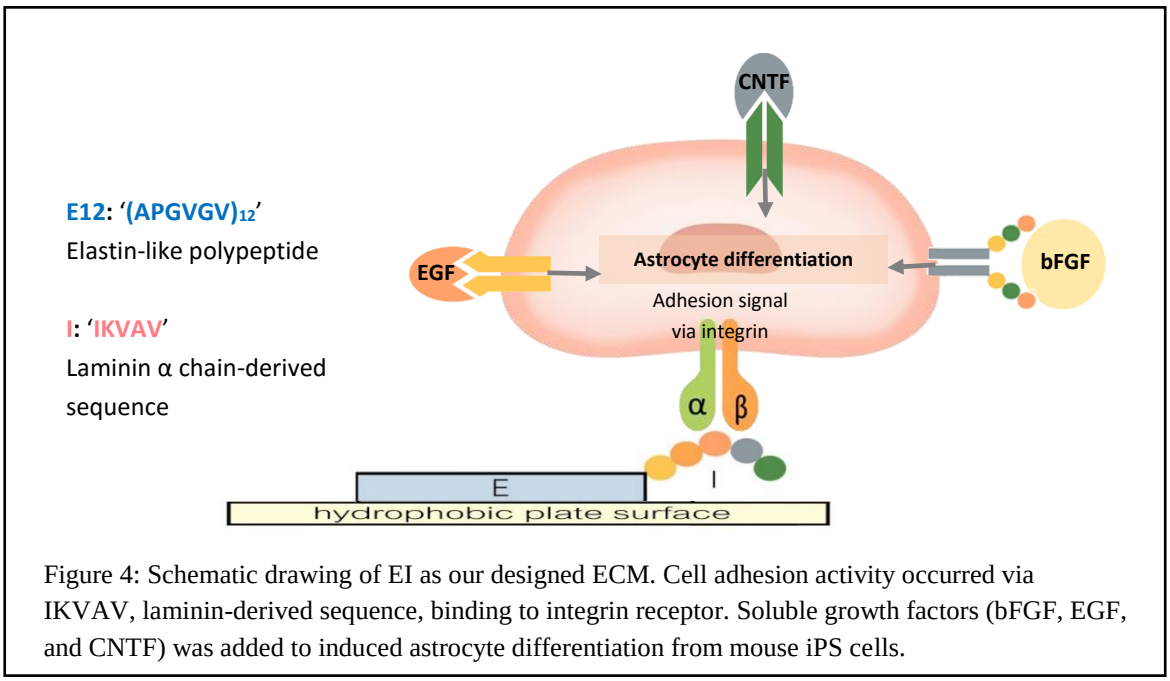

Figure 4: Schematic drawing of EI as our designed ECM. Cell adhesion activity occurred via IKVAV, laminin-derived sequence, binding to integrin receptor. Soluble growth factors (bFGF, EGF, and CNTF) was added to induced astrocyte differentiation from mouse iPS cells.

In conclusion from above experiments, the engineered proteins constructed in this study for regulating cellular functions would be useful biomaterials for various applications such as regenerative medicine.

In the future perspectives, more complex multi-functional ECMs can be developed for example, combining various synthetic CAMs sequence in material construction and also coupling of growth factors. These various combinations of CAMs sequence and growth factors within same ECMS can be proposed the effective materials for tissue engineering (Fig 5).

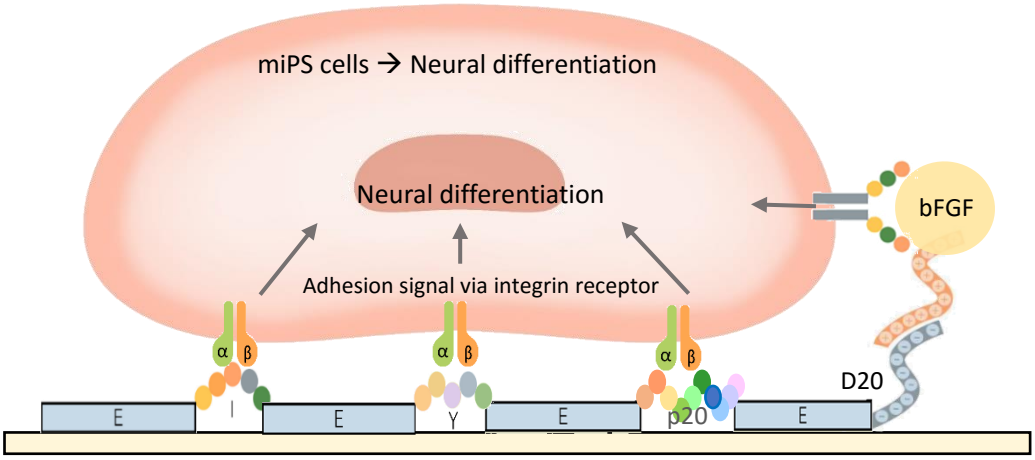

Figure 5: Schematic drawing of complex designed ECMs to construct multi-functional ECM which can recapitulate the multiplicity of biological information mimic natural extracellular

Reference:

1.E. Kobatake, K. Onoda, Y. Yanagida, M. Aizawa, "Design and gene engineering systhesis of an extremely thermostable protein with biological activity," *Biomacromolecules*, 1(3) (2000), pp. 382-386.

2.E. Devemy, OW. Blaschuk. "Identification of a novel dual E- and N-cadherin antagonist," *Peptides*, 30(8) (2009), pp. 1539-1547.

3.A. Haque, X. Shan Yue, A. Motazedian, Y. Tagawa, T. Akaike. "Characterization and neural differentiation of mouse embryonic and induced pluripotent stem cells on cadherin-based substrata," Biomaterials, 33 (2012), pp. 5094-5106.

4.K. Tashiro, G.E. Sephel, B. Weeks, "A synthetic peptide containing the IKVAV sequence from the α chain of laminin mediates cell attachment, migration and neurite outgrowth," *J. Biol. Chem*. 264 (1989), pp. 16174-16182.

5. S.P. Massia, S.S. Rao, J.A. Hubbell, "Covalently immobilized laminin peptide Tyr-Ile-Gly-Ser-Arg (YIGSR) supports cell spreading and colocalization of the 67 kilodalton receptor with alpha-actin and viniculin. *J. Biol. Chem*. 268 (1993), pp. 8053-8059.

List of Abbreviations

Abbreviated form	Elaborated form
APGVGV	Arginine-proline-glycine-valine-glycine-valine
BDM	Basal differentiation medium
bFGF	Basic fibroblast growth factor
CAM	Cell adhesion molecule
CCK	Cell Counting Kit
cDNA	Complementary DNA
CNTF	Ciliary neurotrophic factor
CNS	Central nervous system
D20	5 repeats of 4 aspartic acids and serine
DAPI	4´,6-diamidino-2-phenylindole
DMEM	Dulbecco's Modified Eagle's Medium
DNA	Deoxyribonucleic acid
EB	Embryoid body
ECM	Extracellular matrix
EGF	Epidermal growth factor
ELISA	Enzyme-linked immunosorbent assay
ELP	Elastin-like polypeptide
ESC	Embryonic stem cell
FBS	Fetal bovine serum
FGFR	Fibroblast growth factor receptor
GFAP	Glial fibrillary acidic protein
GMEM	Glasgow Minimum Essential Medium
HRP	Horseradish peroxidase
IKVAV	Isoleucine-lysine-valine-alanine-valine

iPSC	Induced pluripotent stem cell
IPTG	Isopropyl β-D-1-thiogalactopyranoside
kDa	Kilo Dalton
KSR	Knockout serum replacement
LB	Luria-Bertani
LIF	Leukemia inhibitory factor
MAP2	Microtubule-associated protein 2
MEF	Mouse embryonic fibroblast
MMC	Mitomycin C
NCAM	Neural cell adhesion molecule
NEAA	Non-essential amino acid
NPC	Neural progenitor cell
NS	Neurosphere
PBS	Phosphate buffer saline
PCR	Polymerase chain reaction
PNS	Peripheral nervous system
qRT-PCR	Quantitative real time polymerase chain reaction
RA	Retinoic acid
RGD	Arginine-glycine-aspartic acid
RNA	Ribonucleic acid
STO	Sandos inbred mice Thioguanine/Ouabain
S100β	S100 calcium-binding protein β
Tuj	Β-III tubulin
YIGSR	Tyrosine-isoleucine-glycine-serine-arginine

Acknowledgement

My phD. study could never happen without the help of a number of people who has been with me throughout the journey. As my phD. Come close to an end, it is time for me to express my sincere gratitude to a number of people who have support me during the whole journey. I also consider myself the most fortunate student who made a decision to come here without knowing anybody and have many memorable experience.

First, I would like to thank to my supervisor Professor Kobatake Eiry, Department of Environment Chemistry and Engineering, Tokyo institute of technology, for giving me the opportunity to work and complete my Master and phD. Research in his laboratory.

Words cannot express my gratitude for my co-supervisor Associate Prefessor Masayasu Mie for his support during 5 years. I can firmly say that the entire research would never happened without your help and encouragement. I hope one day I will be able to teach and supervise lab's student with patience and understanding just like you do for me.

I sincerely thank Associate professor Ajioka Itsuki and his lab member, Postdoctoral fellow Oshikawa Mio and Research assistant Okada Kei at Ajioka lab, Center for Brain integration Research, Tokyo Medical and Dental University for my precious internship. I learnt a lot of research techniques, experiment planning procedure, working as team work and they are always welcome me. It is my honor to do my internship in this lab.

My special thanks to Ikeda Yusuke, who is my really great supporter. I cannot live in Japan smoothly and get really good job in Japan without his help. Thank you to always support and continue studying until phD together and thank you to his family that always be kind and encourage me.

It is no way that a phD project can be done alone. I would like to thank to Dr. Nihad Adnan, who inspire me to do stem cell work and also some of my work start from his idea. I really enjoy discuss our research with him and it make me have more energy to work hard and try to get our good experiment's result. Thank you so much Adnan to come here and work together.

I would like to thank both past and present members of Kobatake-Mie laboratory. My special thank is also for Shimamura Houri, Osada Sayaka , Omori Yumeko, and Guo Wei, who are good companions with me and always cheer me up. I am really happy to meet you guys and please keep in touch. I really thank to Noyala Jennifer also. She help me correct my English and because of her, I have a confident to present my thesis in English. Thank you to always listen to me and cheer me up, Jennifer.

I would also thank to acknowledgement Grant-in-aid for Scientific Research from the Ministry of Education, Culture, Sports, Science and Technology of Japan. Because of this scholarship, I can study and finish my Master and phD. without the financial problem.

I would like to thank you the most important people in my life, my family. They are the people who always support and beside me in every tough moment. They are my closest confidents and friends in a sense also. Especially my Dad, who have been there through the worst and best days. He never let me pass through the problem alone but hold my hand and pass through it together. I realize that he want me to be happy in whatever I do and always support me. My family have sacrificed, letting me go far away from home to have great experience. I cannot be me today without their support. To be far away from home make me realize the power of unconditional love from family.

Lastly, I have lost my dearest aunt (Aunt Dang) before my final phD presentation and we haven't had chance to meet each other at the last time. I would like to dedicate all the hard work and this thesis to the memory of her. You have been remembered as our wonderful woman and we miss you every day.

Chawapun Suttinont

27/02/2018